AXISYMMETRIC FINITE CYLINDER WITH RIGID ENDS AND A CIRCUMFERENTIAL EDGE CRACK

A THESIS SUBMITTED TO
THE GRADUATE SCHOOL OF NATURAL AND APPLIED SCIENCES
OF
MIDDLE EAST TECHNICAL UNIVERSITY

BY

AYŞE RUŞEN DURUCAN

IN PARTIAL FULFILLMENT OF THE REQUIREMENTS
FOR
THE DEGREE OF MASTER OF SCIENCE
IN
ENGINEERING SCIENCES

AUGUST 2010

Approval of the thesis:

AXISYMMETRIC FINITE CYLINDER WITH RIGID ENDS AND A CIRCUMFERENTIAL EDGE CRACK

submitted by **AYŞE RUŞEN DURUCAN** in partial fulfillment of the requirements for the degree of **Master of Science in Engineering Sciences Department, Middle East Technical University** by,

Prof. Dr. Canan Özgen
Dean, **Graduate School of Natural and Applied Sciences** _____________

Prof. Dr. Turgut Tokdemir
Head of Department, **Engineering Sciences** _____________

Prof. Dr. M. Ruşen Geçit
Supervisor, **Engineering Sciences Dept., METU** _____________

Examining Committee Members

Prof. Dr. Murat Dicleli _____________________
Engineering Sciences Dept., METU

Prof. Dr. M. Ruşen Geçit _____________________
Engineering Sciences Dept., METU

Prof. Dr. Ahmet N. Eraslan _____________________
Engineering Sciences Dept., METU

Prof. Dr. M. Polat Saka _____________________
Civil Engineering Dept., Univ. of Bahrain

Assist. Prof. Dr. Ferhat Akgül _____________________
Engineering Sciences Dept., METU

Date: 25.08.20010

I hereby declare that all information in this document has been obtained and presented in accordance with academic rules and ethical conduct. I also declare that, as required by these rules and conduct, I have fully cited and referenced all material and results that are not original to this work.

Name, Last name : Ayşe Ruşen Durucan

Signature :

ABSTRACT

AXISYMMETRIC FINITE CYLINDER WITH RIGID ENDS AND A CIRCUMFERENTIAL EDGE CRACK

Durucan, Ayşe Ruşen
M.S., Department of Engineering Sciences
Supervisor: Prof. Dr. M. Ruşen Geçit

August 2010, 158 pages

An axisymmetric finite cylinder with rigid ends and a circumferential edge crack is considered in this study. The finite cylinder is under the action of uniformly distributed loads of intensity p_0 at two rigid ends. Material of the finite cylinder is assumed to be linearly elastic and isotropic. This finite cylinder problem is solved by considering an infinite cylinder containing an internal ring-shaped crack located at $z = 0$ plane and two penny-shaped rigid inclusions located at $z = \pm L$ planes. General expressions of the infinite cylinder problem are obtained by solving Navier equations with Fourier and Hankel transforms. This infinite cylinder problem is then converted to the target problem by letting the radius of the rigid inclusions approach the radius of the cylinder and letting the outer edge of the crack approach the surface of the cylinder. Consequently, these rigid inclusions form the rigid ends and internal crack form the circumferential edge crack resulting in the problem of a finite cylinder with rigid ends having an edge crack. The problem is reduced to a set of three singular integral equations. These singular integral equations are converted to a system of linear algebraic equations with the aid of Gauss-Lobatto and Gauss-Jacobi integration formulas and are solved numerically.

Keywords: Edge crack. Finite cylinder. Stress intensity factor. Rigid inclusion.

ÖZ

ÇEVRESEL KENAR ÇATLAĞI İÇEREN
UÇLARI RİJİT EKSENEL SİMETRİK SONLU SİLİNDİR

Durucan, Ayşe Ruşen
Yüksek Lisans, Mühendislik Bilimleri Bölümü
Tez Yöneticisi: Prof. Dr. M. Ruşen Geçit

Ağustos 2010, 158 sayfa

Bu çalışmada dairesel kenar çatlağı içeren, uçları rijit eksenel simetrik sonlu silindir problemi incelenmektedir. İncelenen sonlu silindir iki rijit ucundan p_0 şiddetindeki düzgün yayılı çekme yüküne maruz kalmaktadır. Malzemenin izotrop ve doğrusal elastik olduğu kabul edilmektedir. Bu sonlu silindir problemi, $z = \pm L$ düzlemlerinde disk şeklinde iki rijit enklüzyon ve $z = 0$ düzleminde halka şeklinde bir iç çatlak içeren sonsuz silindir kullanılarak çözülmektedir. Sonsuz silindir probleminin genel ifadeleri, Navier denklemlerinin, Fourier ve Hankel dönüşümlerinin kullanılarak çözülmesiyle elde edilmektedir. Bu sonsuz silindir problemi rijit enklüzyonların yarıçaplarının silindir yarıçapına ulaşmasıyla oluşan rijit uçlar ve halka şeklindeki iç çatlağın dış kenarının silindir yüzeyine ulaşmasıyla oluşan kenar çatlağı içeren sonlu silindir problemine dönüştürülmektedir. Problem, üç tekil integral denklemine indirgenmekte, daha sonra Gauss-Lobatto ve Gauss-Jacobi integrasyon formülleri kullanılarak lineer cebrik denklemlere dönüştürülüp ve sayısal olarak çözülmektedir.

Anahtar kelimeler: Kenar çatlağı. Sonlu silindir. Gerilme şiddeti katsayısı. Rijit enklüzyon.

To My Mother, Mediha ÜNSAL

ACKNOWLEDGEMENT

I would like to express my sincere thanks to my advisor Prof. Dr. M. Ruşen Geçit for his inspiring supervision, continuous encouragement, precious help and patience during this thesis.

I would like to give my deepest thanks to my husband Cengizhan Durucan for his understanding and support during my thesis.

I wish to express special thanks to my family for their emotional support and encouragement during my thesis.

TABLE OF CONTENTS

LIST OF FIGURES

FIGURES

LIST OF TABLES

TABLES

NOMENCLATURE

a, b	Radii of ring-shaped crack
A	Radius of cylinder
B_i, M_i, P_i	Bounded functions
c	Radii of penny-shaped inclusions
c_i	Arbitrary integration constants
C_i	Weighting constants of the Gauss-Lobatto polynomials
d_i	Coefficient functions
E_1, E_2	Functions used as abbreviations
I_0, I_1	Modified Bessel functions of the 1st kind of order zero and one
J_0, J_1	Bessel functions of the 1st kind of order zero and one
k_{1a}, k_{1b}	Mode I stress intensity factors at the edges of crack
k_{1A}, k_{2A}	Mode I and II stress intensity factors at the corner of the finite cylinder
k_{1c}, k_{2c}	Mode I and II stress intensity factors at the edges of inclusion
$\bar{k}_{1a}, \bar{k}_{2b}$	Normalized Mode I stress intensity factors at the edges of crack
$\bar{k}_{1A}, \bar{k}_{2A}$	Normalized Mode I and II stress intensity factors at the corner of the finite cylinder
$\bar{k}_{1c}, \bar{k}_{2c}$	Normalized Mode I and II stress intensity factors at the edge of inclusions
K, E	Complete elliptic integrals of the 1st and the 2nd kinds
K_0, K_1	Modified Bessel functions of the 2nd kind of order zero and one
L_{ij}	Integrands of the kernels N_{ij}
$L_{ij\infty}$, $L_{ij\infty 0}$	Dominants parts of L_{ij} as $\alpha \to \infty$ and $\alpha \to 0$

L	Distance between crack and inclusions
$m(r)$	Crack surface displacement derivative
$m(r,t)$, $m^*(r,t)$	Kernels
m_i, M_i, T_i	Kernels
$m^*(r)$	Hölder-continuous functions on crack
$\overline{m}(\phi)$	Normalized bounded function on crack
$M(\rho)$	Hankel transforms of $m(r)$
N_{ij}	Kernels of the integral equations
N_{ijb}, N_{ijs}	Bounded and singular parts of N_{ij} as $\alpha\rightarrow\infty$
N_{ijs0}	Singular parts of N_{ij} as $\alpha\rightarrow 0$
p_0	Intensity of the axial tensile load
$p_1(r)$, $p_2(r)$	Normal and shear stress jump on rigid inclusions
$p_1^*(r)$, $p_2^*(r)$	Hölder-continuous functions on inclusions
$\bar{p}_1(\eta)$, $\bar{p}_2(\eta)$	Normalized bounded functions on inclusions
$P_1(\rho)$, $P_2(\rho)$	Hankel transform of $p_1(r)$ and $p_2(r)$
$P_n(\alpha,\beta)$	Jacobi polynomials
q_i, s_i, y_i,	Coefficients
r, z	Cylindrical coordinates
t	Integration variable
u, w	Displacement components in r- and z-directions
U, W	Hankel transforms *of* u, w
$U_c(r,\alpha)$	Fourier cosine transform of $u(r,z)$
W_i	Weighting constants of the Jacobi polynomials
$W_s(r,\alpha)$	Fourier sine transform of $w(r,z)$

α	Fourier transform variable
β	Power of singularity at the edge of the crack
γ	Power of singularity at the edge of the inclusion
Δ	4^{th} order linear ordinary differential operator
Δ_i	2^{nd} order linear ordinary differential operators
η, ε	Normalized variables on inclusions
θ	Power of singularity at the edge of the edge crack
κ	$3 - 4\nu$
μ	Shear modulus of elasticity
ν	Poisson's ratio
ξ	Hankel transform variable
σ, τ	Normal and shearing stresses
σ_{zb}, σ_{zs}	Bounded and singular parts of σ_z at the edges of the crack and inclusions
ϕ, ψ	Normalized variables on cracks

CHAPTER 1

INTRODUCTION

Various engineering branches use machine elements which have numerous discontinuities. These discontinuities may occur in the form of voids, notches, cracks or inclusions. They are major factors affecting the load carrying capacities and influencing the stress distributions in the bodies. They must be carefully examined, because of the stated reasons. Stress distributions become infinity in the vicinity of the inclusions and cracks as well as the corners of the elements. In these regions, stress distributions can be calculated in terms of the stress intensity factors.

Stress intensity factors are related to the loading conditions and geometric properties of the bodies. Loading conditions which affect the stress intensity factors may be treated in three modes: (i) Mode I, loading normal to the crack plane, (ii) Mode II, in plane shear loading and (iii) Mode III, out of plane shear loading. Geometry and the locations of the corresponding cracks, inclusions, notches and holes as well as geometry of the body are some of the geometric properties affecting the related stress intensity factors.

Machine elements with large probability of containing singularities are very important in fracture mechanics. Finite cylinders are among these elements. Stresses in the vicinity of the crack and inclusion tips alternate with singularity, regardless of the configuration of the cracked element. In general, these sorts of problems may be studied by numerical and analytical methods based on the solution of corresponding partial differential equations. The assumption of linear elastic material allows to the superposition of the stress and displacements. This superposition principle provides the solution for complex finite cylinder arrangements analytically by using the combination of simple cases.

In the light of the above discussions, several solutions for finite cylinder problems containing edge cracks and penny-shaped inclusions can be found in the literature. However, problem of the finite cylinder containing an edge crack has not been solved by the method used in this research study.

1.1 Literature Review

Erdöl and Erdoğan (1978) considered the problem of a long thick walled hollow cylinder containing ring shaped internal or edge crack which is subjected to uniform axial load and steady-state thermal stress. The problem was reduced to an integral equation having a simple Cauchy kernel for the internal crack and a generalized Cauchy kernel for the edge crack. Solutions were obtained for the stated loading conditions in terms of stress intensity factors.

Chang (1985) obtained the general solution of the stress intensity factor of a finite cylinder containing a concentric penny-shaped crack under torsion. The general solution has been obtained by using Hankel transform and Fourier series. It has been proved that the solutions of a penny-shaped crack in an infinite long cylinder and in a circular plate of infinite radius may be derived from the general solution presented in this work.

Zhang (1988) considered the problem of concentric penny-shaped crack in a finite orthotropic cylinder under torsion. The general solution in terms of stress intensity factors were obtained by using the Hankel transform and Fourier series. Results of the study for mixed boundary value problem have been represented with the aid of a Fredholm integral equation of the second kind. Also it was concluded that the solutions of a concentric penny-shaped crack in an infinite long orthotropic cylinder and circular plate of infinite radius may be derived from the general solution obtained in this study.

Liang and Zang (1992) considered the problem of a concentric penny-shaped crack of Mode III in a finite cylinder. Solution of the problem was obtained by using the Hankel transform and the Fourier series. Results were obtained in terms of stress intensity factors. Furthermore, it was proven that the concentric penny-shaped cracks in an infinite cylinder and infinite circular plate are special cases of the problem of a concentric penny-shaped crack in a finite cylinder.

Meshii and Watanabe (2001) studied the development of a practical method to calculate the Mode I stress intensity factor for an inner surface circumferential crack in a finite length cylinder. Thin shell theory formed the bases underlying the developed method in this study. The proposed method has been valid for relatively short cracks and for a wide range of mean radius to wall thickness ratio.

Wu and Dzenis (2002) obtained a closed-form solution for the problem of a Mode III edge crack between two bonded elastic strips. The stress intensity factors for the edge crack have been calculated. It was observed that, for the limiting particular cases, the obtained results coincide with the results available in the literature.

Lee (2002) considered the problem of stress distribution in a circular cylinder with a circumferential edge crack subjected to uniform shearing stresses. The crack was located on a plane perpendicular to the axis of cylinder and the lateral surface of the cylinder is free of stress. The problem was reduced to the solution of a couple of singular integral equations by using a suitable stress function. These singular integral equations were solved numerically and the stress intensity factors were obtained.

Lee (2002) considered the singular stress problem of a peripheral edge crack in a long circular cylinder under torsion. Considered problem is solved by using Fourier integral transform and reduced to the solution of two integral equations. The solution of these two integral equations was obtained numerically by using the method given in Erdoğan et al. (1973). Finally, the stress intensity factors and crack opening displacements are presented graphically. In addition to that, Lee (2002 & 2003) considered the same problem for torsional and tensile loadings, respectively.

Kadıoğlu (2005) obtained an analytical solution for the linear elastic, axisymmetric problem of edge cracks in an infinite hollow cylinder. The cylinder has been subjected to uniform crack surface pressure. Considered problem has been reduced to a singular integral equation with the unknown crack surface displacement derivative. An asymptotic analysis was performed in order to derive the generalized Cauchy kernel related to edge cracks. The resulting singular integral equation has been solved numerically and the related stress intensity factors are presented for different values of material and geometric properties.

Guo et al. (2005) studied the orthotropic strip with an edge crack. Varying material properties have been assumed for the strip. The solution for the problem has been obtained by using the Laplace and Fourier integral transforms. These integral transforms have been used to reduce the problem to a singular integral equation. Finally, numerical results of the stress intensity factors have been presented.

Toygar and Geçit (2006) considered the problem of an axisymmetric infinite cylinder of linearly elastic and isotropic material containing a ring shaped crack and two ring-shaped rigid inclusions. The problem has been reduced to three singular integral equations. Then, these equations are converted to a system of linear algebraic equations and solved numerically. Solutions have been presented in terms of stress intensity factors.

Freese and Baratta (2006) obtained solutions for some linear elastic single edge-crack configurations in terms of stress intensity factors. Solutions for various loading conditions have been extracted from the solution of uniformly loaded single edge cracked finite strip configurations. Results for the asymptotic behavior and a common expression for the full range of crack length to strip width ratio has been presented.

Kaman and Geçit (2006) considered the problem of a cracked semi-infinite cylinder and a finite cylinder of linearly elastic and isotropic material. Solution for the complex problem has been obtained by the superposition of simpler problems. Then, the problem has been reduced to a system of singular integral equations. Next, Gauss–Lobatto and Gauss–Jacobi integration formulas have been used to convert these integral equations to a system of linear algebraic equations. Finally, this system of linear algebraic equations has been solved numerically.

Yan (2007) considered the problem of a rectangular tensile plate containing an edge crack. A boundary element method proposed by the author has been used to present the stress intensity factors for the considered problem. Furthermore, stress intensity factors of a crack emanating from an edge half-circular hole were calculated. Results obtained in terms of stress intensity factors for two cases have been discussed and it was found that the boundary element method used for the solution was accurate for obtaining the stress intensity factors of crack problems in finite plates.

Kaman and Geçit (2008) considered the problem of an axisymmetric finite cylinder of linearly elastic and isotropic material containing a penny-shaped transverse crack. Solution of the complex problem was obtained by the superposition of simpler problems. Moreover, the problem has been reduced to a system of singular integral equations. Then, Gauss–Lobatto and Gauss–Jacobi integration formulas have been used to convert these integral equations to a system of linear algebraic equations. The system of linear algebraic equations has been solved numerically and the results were presented in terms of stress intensity factors at the edges of the rigid support and the crack.

1.2 A Brief Introduction and the Solution Method of the Problem

An axisymmetric finite cylinder with rigid ends containing an edge crack subjected to a tensile axial load of uniform intensity p_0 at both ends is considered in this research study. Material of the cylinder is assumed to be linearly elastic and isotropic. Lateral surface of the cylinder, considered in this research study, is free of stresses.

Formulation of the finite cylinder problem is obtained by a procedure starting with considering an infinite cylinder, containing a ring-shaped crack located at $z = 0$ plane and two rigid penny-shaped inclusions located at $z = \pm L$ planes, subjected to tensile axial loads of uniform intensity p_0 at infinity, and then letting the radius of the inclusions approach the radius of the cylinder.

Solution for the infinite cylinder loaded at infinity having a ring-shaped crack and two penny-shaped rigid inclusions is obtained by superposition of the following two problems: (I) An infinite cylinder loaded at infinity with no crack or inclusion, (II) an infinite cylinder with a ring-shaped crack and two penny-shaped rigid inclusions with no load at infinity.

General expressions for the solution of the problem must contain sufficient number of unknowns in order to satisfy all of the necessary boundary conditions. For this purpose, the perturbation problem (II) is separated into three main subproblems in terms of three infinite media; (II-i) an infinite medium containing a ring-shaped crack located at $z = 0$ plane, (II-ii) an infinite medium containing two penny-shaped rigid inclusions located at $z = \pm L$ planes and (II-iii) an infinite medium with no crack or inclusion. Solution of these subproblems are obtained by applying Hankel transforms to the first and the second media, in r-direction, as well as applying Fourier transform to the third medium, in z-direction, on Navier equations.

With the combined general expressions for the stresses and the displacements, the boundary conditions at the lateral surface of the infinite cylinder and the boundary conditions on the crack and inclusion surfaces are satisfied. As a result, three singular integral equations are obtained.

The infinite cylinder problem is then converted to the target problem, by letting the radius of the rigid inclusions approach the radius of the cylinder and letting the outer edge of the ring-shaped crack approach the lateral surface of the cylinder. As a result, these rigid inclusions form the rigid ends of the cylinder and a finite cylinder with rigid ends containing an edge crack is obtained.

Finally, these singular integral equations are converted to linear algebraic equations by using Gauss-Lobatto and Gauss-Jacobi integration formulas. Then, these linear algebraic equations are solved numerically to obtain the stress intensity factors at the edges of the internal crack, at the root of the edge crack in infinite and finite cylinders and at the edge of the rigid inclusions in infinite cylinder as well as at the corners of the finite cylinder.

CHAPTER II

INFINITE CYLINDER PROBLEM

2.1 General Equations

An axisymmetric infinite cylinder of radius A with a transverse ring-shaped crack of width $(b-a)$ located at $z=0$ plane and two penny shaped inclusions of radius c located at $z=\pm L$ planes is considered. This cylinder is under the action of uniformly distributed tensile loads of intensity p_0 at infinity (Fig. 2.1). Material of the cylinder is assumed to be linearly elastic and isotropic.

Stress-displacement relations (2.1a-c) and Navier equations (2.2a,b), Geçit (1986), used for this type of problems, can be listed as follows,

$$\sigma_r = \frac{\mu}{\kappa-1}\left[(\kappa+1)\frac{\partial u}{\partial r} + (3-\kappa)\left(\frac{u}{r}+\frac{\partial w}{\partial z}\right)\right],$$

$$\sigma_z = \frac{\mu}{\kappa-1}\left[(\kappa+1)\frac{\partial w}{\partial z} + (3-\kappa)\left(\frac{\partial u}{\partial r}+\frac{u}{r}\right)\right],$$

$$\tau_{rz} = \mu\left(\frac{\partial u}{\partial z}+\frac{\partial w}{\partial r}\right). \qquad (2.1\mathrm{a}-\mathrm{c})$$

where σ and τ are normal and shearing stresses, μ is the shear modulus.

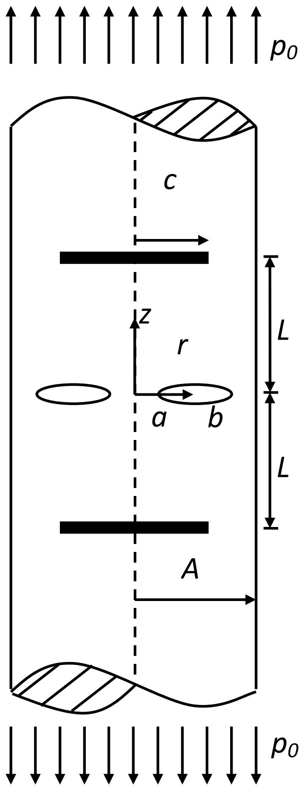

Figure 2.1 Geometry and loading of the infinite cylinder.

$$(\kappa+1)\left(\frac{\partial^2 u}{\partial r^2}+\frac{1}{r}\frac{\partial u}{\partial r}-\frac{u}{r^2}\right)+(\kappa-1)\frac{\partial^2 u}{\partial z^2}+\frac{\partial^2 w}{\partial r \partial z}=0,$$

$$2\left(\frac{\partial^2 u}{\partial r \partial z}+\frac{1}{r}\frac{\partial u}{\partial z}\right)+(\kappa-1)\left(\frac{\partial^2 w}{\partial r^2}+\frac{1}{r}\frac{\partial w}{\partial r}\right)+(\kappa+1)\frac{\partial^2 w}{\partial z^2}=0. \qquad (2.2\mathrm{a,b})$$

where u and w are displacements in *r*- and *z*-directions in cylindrical coordinate system, $\kappa = 3-4\nu$ and ν is the Poisson's ratio.

2.2 Formulation of the Problem

The complex problem of an axisymmetric infinite cylinder, containing a transverse ring shaped crack and two rigid inclusions, under axial loading at infinity is solved by the superposition of the following two simpler problems: (i) problem of an infinite cylinder, without crack or inclusion, under axial tensile loading of uniform intensity

p_0 at infinity and (ii) problem of an infinite cylinder with a crack and two inclusions subjected to the negative of the stresses at the location of the crack and displacements at the location of the inclusions calculated from the solution of problem (i) (Fig. 2.2).

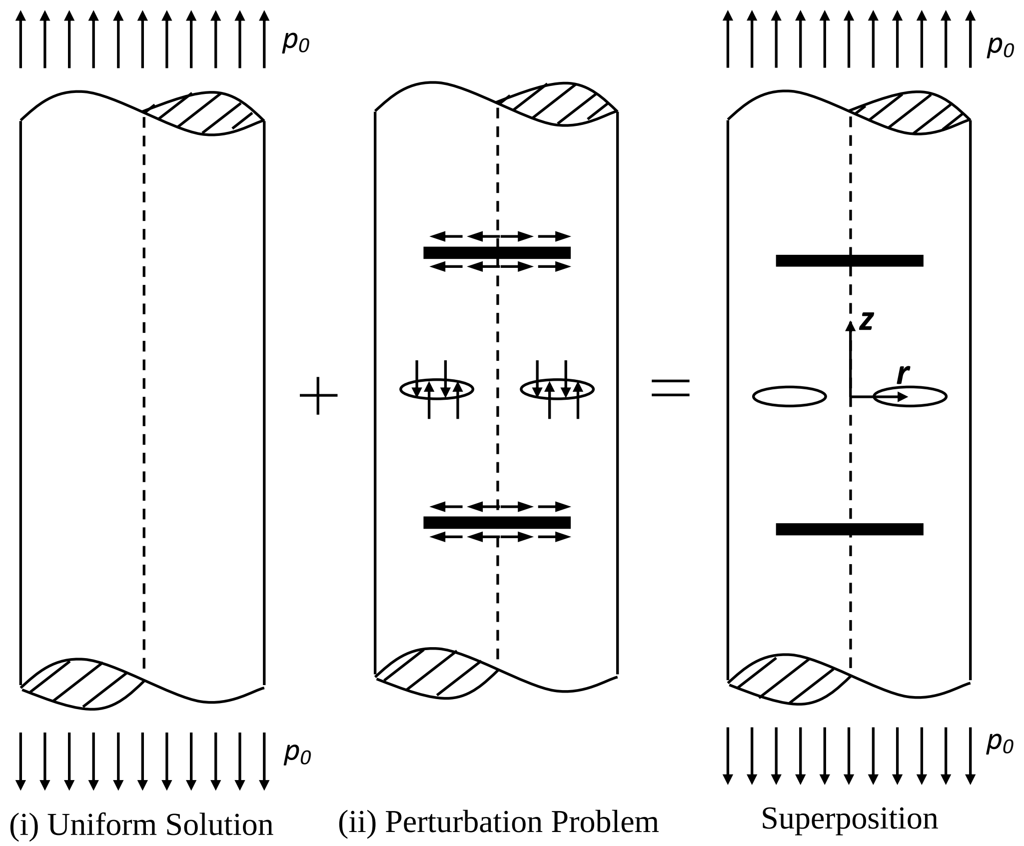

Figure 2.2 Superposition scheme for the solution of the infinite cylinder problem.

2.2.1 Uniform Solution

The problem of an infinite axisymmetric cylinder of radius A loaded at infinity with an axial tension of uniform intensity p_0 is considered. For this type of problems, it may be expected that u and w is independent of z and r, respectively.

$$u(r,z) = u(r),$$

$$w(r,z) = w(z). \tag{2.3a, b}$$

In case of uniform axial loading, Eqs. (2.2a, b) are uncoupled and turn into

$$\frac{d^2u}{dr^2} + \frac{1}{r}\frac{du}{dr} - \frac{u}{r^2} = 0,$$

$$\frac{d^2w}{dz^2} = 0. \tag{2.4a, b}$$

Eqs. (2.4a, b) are solved with the following conditions

$$u(0) = 0,$$

$$w(0) = 0,$$

$$\sigma_r(A, z) = 0,$$

$$\tau_{rz}(A, z) = 0,$$

$$\sigma_z(r, \infty) = p_0. \tag{2.5a – e}$$

The solution can be easily obtained in the following form

$$u_{uniform}(r) = -\frac{(\kappa - 3)p_0}{2\mu(\kappa - 7)}r,$$

$$w_{uniform}(z) = -\frac{2p_0}{\mu(\kappa - 7)}z,$$

$$\sigma_{r_{uniform}}(r, z) = 0,$$

$$\sigma_{z_{uniform}}(r, z) = p_0,$$

$$\tau_{rz_{uniform}}(r,z) = 0. \qquad (2.6\text{a} - \text{e})$$

2.2.2 Perturbation Problem

The displacement expressions and the stress components for perturbation problem of an axisymmetric infinite cylinder, containing a transverse ring shaped crack and two rigid inclusions, with no loads at infinity can be obtained by adding the general expressions of (II-i) an infinite cylinder containing a transverse ring-shaped crack of width $(b-a)$ located at the symmetry plane of $z=0$, (II-ii) an infinite cylinder having two penny-shaped rigid inclusions of radius c located at $z=\pm L$ planes and (II-iii) an infinite cylinder without crack or inclusion under the action of arbitrary axisymmetric loading (Fig. 2.3). This procedure is implemented to have sufficient number of unknowns in order to satisfy all of the boundary conditions that are required.

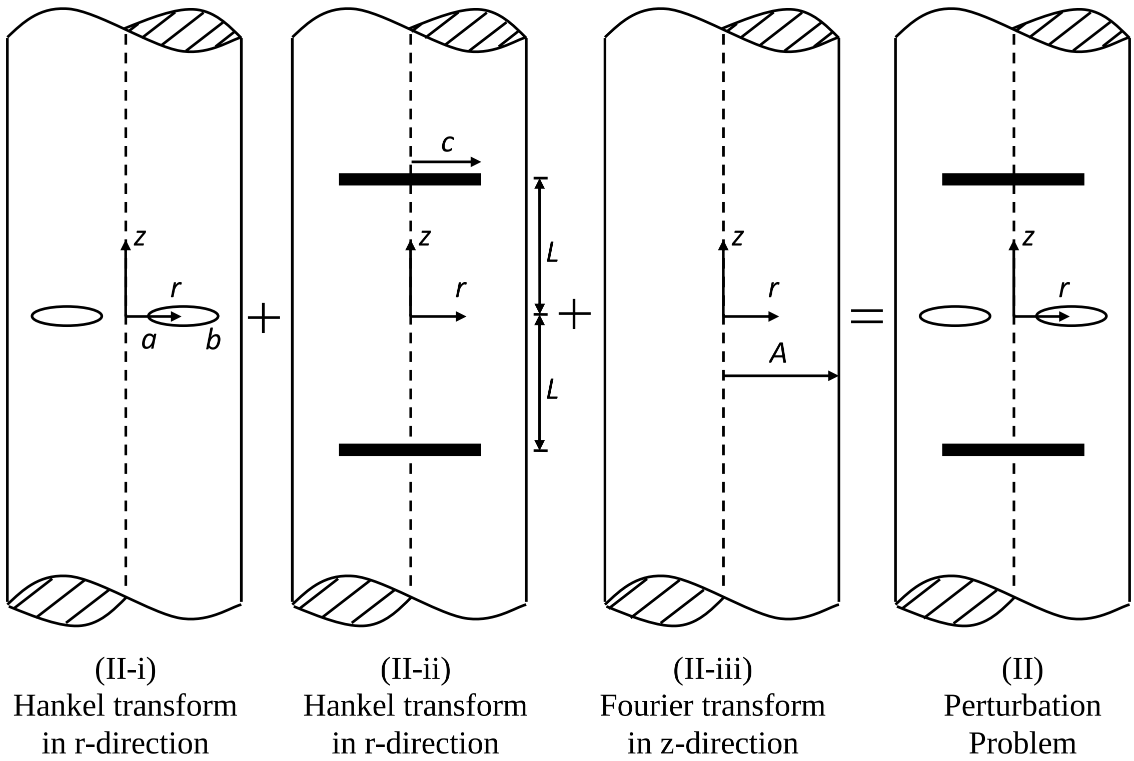

Figure 2.3 Addition of solutions for the perturbation problem.

Solution for the infinite medium $(0 \le r \le \infty)$ gives general expressions for the infinite cylinder $(0 \le r \le A)$ by imposing appropriate boundary conditions at $r = A$.

Symmetry about $z = 0$ plane allows to consider the problem only in the upper half plane$(z \ge 0)$.

2.2.2.1 Infinite Medium Having a Ring Shaped Crack

In this case, a ring-shaped transverse crack of width $(b - a)$ is located at the symmetry plane of $z = 0$ in an infinite medium. Considering an infinite medium with Region i-1 $(0 \le r < \infty, 0 \le z < \infty)$ and Region i-2 $(0 \le r < \infty, 0 \le z < -\infty)$, using integral transforms, H_0 Hankel transform, Sneddon (1972), of Eq. (2.2b) and H_1 transform of Eq.(2.2a), in r-direction (Fig. 2.4) and combining the resulting equations, gives,

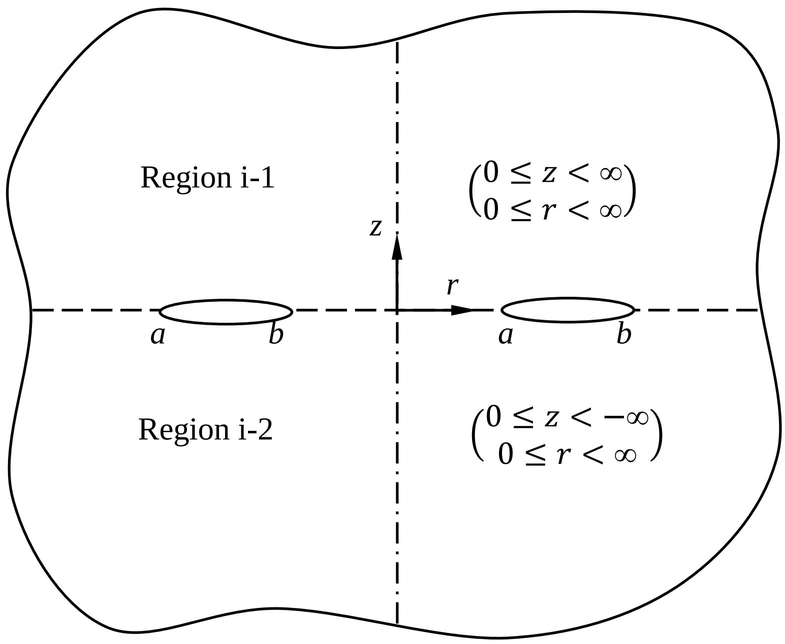

Figure 2.4 Infinite medium having a ring-shaped crack.

$$\frac{d^4U}{dz^4} - 2\rho^2 \frac{d^2U}{dz^2} + \rho^4 = 0, \tag{2.7}$$

where ρ is the Hankel transform variable, $U(\rho,z)$ is H_1 Hankel transform of $u(r,z)$ and $W(\rho,z)$ is H_0 Hankel transform of $w(r,z)$ in *r*-direction

$$U(\rho,z)=\int_0^\infty u(r,z)rJ_1(\rho r)dr,$$

$$W(\rho,z)=\int_0^\infty w(r,z)rJ_0(\rho r)dr, \tag{2.8a, b}$$

where J_0 and J_1 are the Bessel functions of the first kind of order zero and one, respectively.

Solution of Eq. (2.7) for the Region i-1 $(0\le r<\infty, 0\le z<\infty)$ (Fig. 2.4) gives

$$U_{i-1}(\rho,z)=(c_1+c_2 z)e^{-\rho z}+(c_3+c_4 z)e^{\rho z}, \tag{2.9}$$

where c_1, c_2, c_3 and c_4 are arbitrary unknown constants. Back substitution to the transformed ordinary differential equations gives

$$W_{i-1}(\rho,z)=\left[c_1+\left(z+\frac{\kappa}{\rho}\right)c_2\right]e^{-\rho z}-\left[c_3+\left(z-\frac{\kappa}{\rho}\right)c_4\right]e^{\rho z}. \tag{2.10}$$

The unknown constants c_3 and c_4 must be zero in order to have finite displacements in the upper semi-infinite domain$(z\to\infty)$. Consequently,

$$U_{i-1}(\rho,z)=(c_1+c_2 z)e^{-\rho z},$$

$$W_{i-1}(\rho,z)=\left[c_1+\left(z+\frac{\kappa}{\rho}\right)c_2\right]e^{-\rho z}\ . \tag{2.11a, b}$$

Displacement components can be obtained by taking the inverse transforms of Eqs. (2.11a, b)

$$u_{i-1}(\rho, z) = \int_0^\infty (c_1 + c_2 z)e^{-\rho z}\rho J_1(\rho r)d\rho,$$

$$w_{i-1}(\rho, z) = \int_0^\infty \left[c_1 + \left(z + \frac{\kappa}{\rho}\right)c_2\right] e^{-\rho z}\rho J_0(\rho r)d\rho. \qquad (2.12\mathrm{a, b})$$

Substituting Eqs. (2.12a,b) in Eqs.(2.1a-c), the following expressions can be obtained for the stress components in the Region i-1 $(0 \leq r < \infty, 0 \leq z < \infty)$

$$\sigma_{r_{i-1}}(r, z) = \mu \int_0^\infty -2(c_1 + c_2 z)e^{-\rho z}\frac{\rho}{r}J_1(\rho r)d\rho$$

$$+\mu \int_0^\infty [2\rho(c_1 + c_2 z) + (\kappa - 3)c_2]\, e^{-\rho z}\rho J_0(\rho r)d\rho,$$

$$\sigma_{z_{i-1}}(r, z) = \mu \int_0^\infty [-2\rho(c_1 + c_2 z) - (\kappa + 1)c_2]e^{-\rho z}\rho J_0(\rho r)d\rho,$$

$$\tau_{rz_{i-1}}(r, z) = \mu \int_0^\infty [-2\rho(c_1 + c_2 z) - (\kappa - 1)c_2]e^{-\rho z}\rho J_1(\rho r)d\rho. \qquad (2.13\mathrm{a} - \mathrm{c})$$

A similar procedure is implemented for Region i-2 $(0 \leq r < \infty, 0 \leq z < -\infty)$ to obtain the displacement and stress expressions,

$$U_{i-2}(\rho, z) = (c_5 + c_6 z)e^{\rho z},$$

$$W_{i-2}(\rho, z) = \left[-c_5 - \left(z - \frac{\kappa}{\rho}\right)c_6\right] e^{\rho z}. \qquad (2.14\mathrm{a, b})$$

Displacement components can be obtained by taking the inverse transforms of Eqs. (2.14a, b)

$$u_{i-2}(\rho, z) = \int_0^\infty (c_5 + c_6 z)e^{\rho z}\rho J_1(\rho r)d\rho,$$

$$w_{i-2}(\rho,z) = \int_0^\infty \left[-c_5 - \left(z - \frac{\kappa}{\rho}\right)c_6\right] e^{\rho z}\rho J_0(\rho r)d\rho. \qquad (2.15\text{a, b})$$

Substituting Eqs. (15a,b) in Eqs. (2.1a-c), the following expressions can be obtained for the stress components in the Region i-2 $(0 \le r < \infty, 0 \le z < -\infty)$

$$\sigma_{r_{i-2}}(r,z) = \mu\int_0^\infty -2(c_5 + c_6 z)e^{\rho z}\frac{\rho}{r}J_1(\rho r)d\rho$$
$$+\mu\int_0^\infty [2\rho(c_5 + c_6 z) - (\kappa - 3)c_6]\, e^{\rho z}\rho J_0(\rho r)d\rho,$$

$$\sigma_{z_{i-2}}(r,z) = \mu\int_0^\infty [-2\rho(c_5 + c_6 z) + (\kappa + 1)c_6]e^{\rho z}\rho J_0(\rho r)d\rho,$$

$$\tau_{rz_{i-2}}(r,z) = \mu\int_0^\infty [2\rho(c_5 + c_6 z) - (\kappa - 1)c_6]e^{\rho z}\rho J_1(\rho r)d\rho. \qquad (2.16\text{a} - \text{c})$$

General expressions given in Eqs. (2.12a,b) and (2.13a-c) for Region i-1 $(0 \le r < \infty, 0 \le z < \infty)$ and Eqs. (2.15a,b) and (2.16a-c) for Region i-2 $(0 \le r < \infty, 0 \le z < -\infty)$ must satisfy the following conditions:

$$\sigma_{z_{i-1}}(r,0^+) = \sigma_{z_{i-2}}(r,0^-), \qquad (0 \le r < \infty)$$

$$\tau_{rz_{i-1}}(r,0^+) = \tau_{rz_{i-2}}(r,0^-), \qquad (0 \le r < \infty)$$

$$u_{i-1}(r,0^+) = u_{i-2}(r,0^-), \qquad (0 \le r < \infty)$$

$$w_{i-1}(r,0^+) = w_{i-2}(r,0^-). \qquad (0 \le r < a, b < r < \infty) \qquad (2.17\text{a} - \text{d})$$

It should be noted that, Eqs. (2.17a, b) are stress type continuity conditions while Eqs. (2.17c, d) are displacement type. Eq. (2.17d) may be replaced with Eq.(2.18) in order to have the same type of continuity conditions,

$$\frac{\partial}{\partial r}[w_1(r,0^+)] - \frac{\partial}{\partial r}[w_2(r,0^-)] = 2m(r), \qquad (a < r < b) \tag{2.18}$$

where $m(r)$, is the new unknown function such that $m(r) = 0$ when $(0 < r < a,\ b < r < \infty)$. The constant unknowns c_1, c_2, c_5 and c_6 can be expressed in terms of $M(\rho)$ as;

$$c_1 = \frac{\kappa - 1}{\kappa + 1}\frac{M(\rho)}{\rho},$$

$$c_2 = -\frac{2}{\kappa + 1}M(\rho),$$

$$c_5 = \frac{\kappa - 1}{\kappa + 1}\frac{M(\rho)}{\rho},$$

$$c_6 = \frac{2}{\kappa + 1}M(\rho), \tag{2.19a - d}$$

using the boundary conditions given in Eqs.(2.17a-c) and Eqs.(2.18) , where

$$M(\rho) = \int_a^b m(r) r J_1(\rho r) dr. \tag{2.20}$$

Subsequently, the displacement and the stress expressions for Region i-1 $(0 \le r < \infty,\ 0 \le z < \infty)$, shown in Fig. (2.4) turns into;

$$u_{i-1}(\rho, z) = \frac{1}{\kappa + 1}\int_0^\infty [\kappa - 1 - 2\rho z] M(\rho) e^{-\rho z} \rho J_1(\rho r) d\rho,$$

$$w_{i-1}(\rho, z) = \frac{1}{\kappa + 1}\int_0^\infty [-\kappa - 1 - 2\rho z] M(\rho) e^{-\rho z} \rho J_0(\rho r) d\rho,$$

$$\sigma_{r_{i-1}}(r, z) = \frac{2\mu}{\kappa + 1}\int_0^\infty \left[(2\rho z - \kappa + 1)\frac{1}{r}J_1(\rho r) + 2(1 - \rho z)\rho J_0(\rho r)\right] M(\rho) e^{-\rho z} d\rho,$$

$$\sigma_{z_{i-1}}(r,z) = \frac{4\mu}{\kappa+1}\int_0^\infty [\rho z + 1]M(\rho)e^{-\rho z}\rho J_0(\rho r)d\rho,$$

$$\tau_{rz_{i-1}}(r,z) = \frac{4\mu}{\kappa+1}\int_0^\infty \rho z M(\rho)e^{-\rho z}\rho J_1(\rho r)d\rho. \qquad (2.21\mathrm{a}-\mathrm{e})$$

2.2.2.2 The Infinite Medium Having two Inclusions

In this case, two penny-shaped rigid inclusions of radius c are located at the $z = \pm L$ planes in an infinite medium. Considering an infinite medium with Region ii-1 $(0 \le r < \infty, -L < z < L)$, Region ii-2 $(0 \le r < \infty, L \le z < \infty)$ and Region ii-3 $(0 \le r < \infty, -L \le z < -\infty)$, using integral transforms, H_0 Hankel transforms of Eq.(2.2b) and H_1 transform of Eq.(2.2a) in r-direction (Fig. 2.5), solution of Eq.(2.7) for the Region ii-1 $(0 \le r < \infty, -L < z < L)$ is obtained as

$$U(\rho,z) = (c_7 + c_8 z)e^{-\rho z} + (c_9 + c_{10}z)e^{\rho z}, \qquad (2.22)$$

where c_7, c_8, c_9 and c_{10} are arbitrary unknown constants. Back substitution to the transformed ordinary differential equations gives

$$W(\rho,z) = \left[c_7 + \left(z + \frac{\kappa}{\rho}\right)c_8\right]e^{-\rho z} - \left[c_9 + \left(z - \frac{\kappa}{\rho}\right)c_{10}\right]e^{\rho z}. \qquad (2.23)$$

Displacement components in the Region ii-1 $(0 \le r < \infty, -L < z < L)$ *can* be obtained by taking the inverse transforms of Eqs.(2.22) and (2.23)

$$u_{ii-1}(\rho,z) = \int_0^\infty [(c_9 - c_{10}z)e^{-\rho z} + (c_9 + c_{10}z)e^{\rho z}]\rho J_1(\rho r)d\rho,$$

$$w_{ii-1}(\rho,z) = \int_0^\infty \left\{\left[c_9 - \left(z + \frac{\kappa}{\rho}\right)c_{10}\right]e^{-\rho z} + \left[-c_9 - \left(z - \frac{\kappa}{\rho}\right)c_{10}\right]e^{\rho z}\right\}\rho J_0(\rho r)d\rho\,. \qquad (2.24\mathrm{a,b})$$

Substituting Eqs. (2.24a,b) in Eqs.(2.1a-c), expressions for the stress components can be obtained in the Region ii-1 $(0 \leq r < \infty, -L < z < L)$ as

$$\sigma_{r_{i-1}}(r,z) = \mu \int_0^\infty [2(-c_9 + c_{10}z)e^{-\rho z} - 2(c_9 + c_{10}z)e^{\rho z}] \frac{\rho}{r} J_1(\rho r)$$
$$+ \mu \int_0^\infty \{[2\rho(c_9 - c_{10}z) - (\kappa - 3)c_{10}]\, e^{-\rho z}$$
$$+ [2\rho(c_9 + c_{10}z) - (\kappa - 3)c_{10}]\, e^{\rho z}\} \rho J_0(\rho r) d\rho,$$

$$\sigma_{z_{i-1}}(r,z) = \mu \int_0^\infty \{[-2(c_9 - c_{10}z) + (\kappa + 1)c_{10}]e^{-\rho z}$$
$$+ [-2(c_9 + c_{10}z) + (\kappa + 1)c_{10}]e^{\rho z}\} \rho J_0(\rho r) d\rho,$$

$$\tau_{rz_{i-1}}(r,z) = \mu \int_0^\infty [-2\rho(c_9 - c_{10}z) + (\kappa - 1)c_{10}]e^{-\rho z}$$
$$+ [2\rho(c_9 + c_{10}z) - (\kappa - 1)c_{10}]e^{\rho z} \rho J_1(\rho r) d\rho. \qquad (2.25\text{a} - \text{c})$$

Expressions for the Region ii-2 $(0 \leq r < \infty, L \leq z < \infty)$ are obtained similarly in the form,

$$u_{ii-2}(\rho,z) = \int_0^\infty (c_7 + c_8 z) e^{-\rho z} \rho J_1(\rho r) d\rho,$$

$$w_{ii-2}(\rho,z) = \int_0^\infty \left[c_7 + \left(z + \frac{\kappa}{\rho}\right) c_8\right] e^{-\rho z} \rho J_0(\rho r) d\rho, \qquad (2.26\text{a, b})$$

$$\sigma_{r_{ii-2}}(r,z) = \mu \int_0^\infty -2(c_7 + c_8 z)e^{-\rho z} \frac{\rho}{r} J_1(\rho r) d\rho$$
$$+ \mu \int_0^\infty [2\rho(c_7 + c_8 z) + (\kappa - 3)c_8]\, e^{-\rho z} \rho J_0(\rho r) d\rho,$$

$$\sigma_{z_{ii-2}}(r,z) = \mu \int_0^\infty [-2\rho(c_7 + c_8 z) - (\kappa + 1)c_8]e^{-\rho z} \rho J_0(\rho r) d\rho,$$

$$\tau_{rz_{ii-2}}(r,z) = \mu \int_0^\infty [-2\rho(c_7 + c_8 z) - (\kappa - 1)c_8] e^{-\rho z} \rho J_1(\rho r) d\rho. \qquad (2.27\text{a} - \text{c})$$

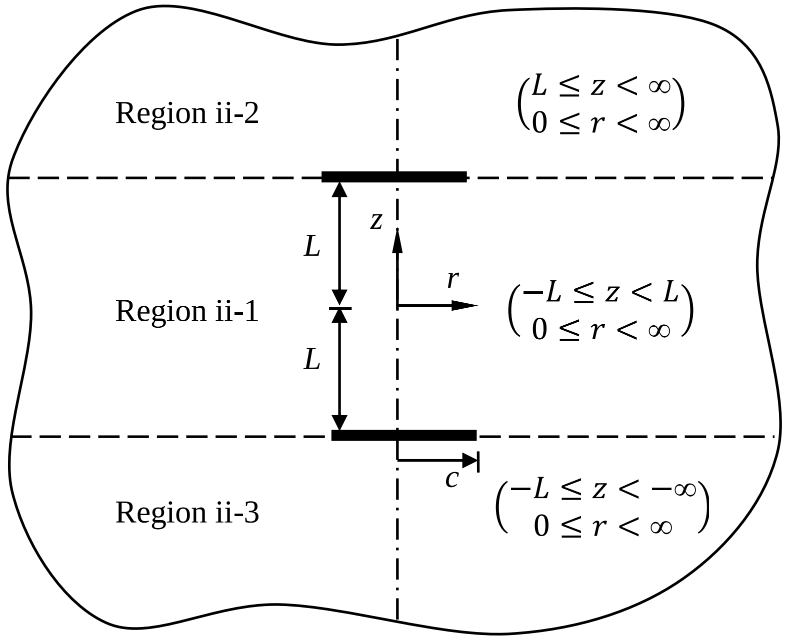

Figure 2.5 Infinite medium having two penny-shaped rigid inclusions.

General expressions given in Eqs. (2.24a,b) and (2.25a-c) for Region ii-1 $(0 \leq r < \infty, -L < z < L)$ and Eqs. (2.26a,b) and (2.27a-c) for Region ii-2 $(0 \leq r < \infty, L \leq z < \infty)$ must satisfy the following conditions.

$$\sigma_{z_{ii-1}}(r, L^-) = \sigma_{z_{ii-2}}(r, L^+), \qquad (c < r < \infty)$$

$$\tau_{rz_{ii-1}}(r, L^-) = \tau_{rz_{ii-2}}(r, L^+), \qquad (c < r < \infty)$$

$$u_{ii-1}(r, L^-) = u_{ii-2}(r, L^+), \qquad (0 \leq r < \infty)$$

$$w_{ii-1}(r, L^-) = w_{ii-2}(r, L^+), \qquad (0 \leq r < \infty) \qquad (2.28\text{a} - \text{d})$$

$$\tau_{z_{ii-2}}(r, L^+) - \tau_{z_{ii-1}}(r, L^-) = p_1(r), \qquad (0 \leq r < c)$$

$$\sigma_{z_{ii-2}}(r, L^+) - \sigma_{z_{ii-1}}(r, L^-) = p_2(r), \qquad (0 \le r < c) \qquad (2.29\text{a, b})$$

where $p_1(r)$ is jump in the shearing stress τ_{rz} and $p_2(r)$ is jump in the normal stress σ_{rz} through the rigid inclusion. The unknown constants can be calculated from Eqs.(2.28) and (2.29):

$$c_7 = \frac{1}{2\mu(\kappa+1)\rho}\{[-(\rho L+\kappa)P_1(\rho) + \rho L P_2(\rho)]e^{\rho L} + [\rho L P_2(\rho) + (\rho L - \kappa)P_1(\rho)]e^{-\rho L}\},$$

$$c_8 = \frac{1}{\mu(\kappa+1)}[P_1(\rho)\cosh(\rho L) - P_2(\rho)\sinh(\rho L)],$$

$$c_9 = \frac{1}{2\mu(\kappa+1)\rho}\{\rho L[P_1(\rho) + P_2(\rho)] - \kappa P_1(\rho)\}e^{-\rho L},$$

$$c_{10} = -\frac{1}{2\mu(\kappa+1)}[P_1(\rho) + P_2(\rho)]e^{-\rho L}, \qquad (2.30\text{a} - \text{d})$$

where

$$P_1(\rho) = \int_0^c p_1(r) r J_1(\rho r) dr,$$

$$P_2(\rho) = \int_0^c p_1(r) r J_0(\rho r) dr. \qquad (2.31\text{a, b})$$

The displacements and the stresses for Region ii-1 ($0 \le r < \infty, -L < z < L$) are written as;

$$u_{ii-1}(\rho, z) = \frac{1}{2\mu(\kappa+1)}\int_0^\infty \langle\{[\rho(z+L) - \kappa]P_1(\rho) + \rho(z+L)P_2(\rho)\}e^{-\rho(z+L)} + \{[-\rho(z-L) - \kappa]P_1(\rho) - \rho(z-L)P_2(\rho)\}e^{\rho(z-L)}\rangle J_1(\rho r) d\rho,$$

$$w_{ii-1}(\rho,z)=\frac{1}{2\mu(\kappa+1)}\int_0^{\infty}\langle\{\rho(z+L)P_1(\rho)+[\rho(z+L)+\kappa]P_2(\rho)\}e^{-\rho(z+L)}$$
$$+\{\rho(z-L)P_1(\rho)+[\rho(z-L)-\kappa]P_2(\rho)\}e^{\rho(z-L)}\rangle J_0(\rho r)d\rho,$$

$$\sigma_{r_{ii-1}}(r,z)=\frac{1}{2(\kappa+1)}\int_0^{\infty}\langle\{[2\rho(z+L)-(\kappa+3)]P_1(\rho)$$
$$+[2\rho(z+L)+(\kappa-3)]P_2(\rho)\}e^{-\rho(z+L)}$$
$$+\{[-2\rho(z-L)-(\kappa+3)]P_1(\rho)$$
$$+[-2\rho(z-L)+(\kappa-3)]P_2(\rho)\}e^{\rho(z-L)}\rangle\rho J_0(\rho r)d\rho$$
$$+\frac{1}{2(\kappa+1)}\int_0^{\infty}\langle\{[-2\rho(z+L)+2\kappa]P_1(\rho)$$
$$-2\rho(z+L)P_2(\rho)\}e^{-\rho(z+L)}$$
$$+\{[2\rho(z-L)+2\kappa]P_1(\rho)+2\rho(z-L)P_2(\rho)\}e^{\rho(z-L)}\rangle\frac{1}{r}J_1(\rho r)d\rho,$$

$$\sigma_{z_{ii-1}}(r,z)=\frac{1}{2(\kappa+1)}\int_0^{\infty}\langle\{[-2\rho(z+L)+(\kappa-1)]P_1(\rho)$$
$$+[-2\rho(z+L)-(\kappa+1)]P_2(\rho)\}e^{-\rho(z+L)}$$
$$+\{[2\rho(z-L)+(\kappa-1)]P_1(\rho)$$
$$+[2\rho(z-L)-(\kappa+1)]P_2(\rho)\}e^{\rho(z-L)}\rangle\rho J_0(\rho r)d\rho,$$

$$\tau_{rz_{ii-1}}(r,z)=\frac{1}{2(\kappa+1)}\int_0^{\infty}\langle\{[-2\rho(z+L)+(\kappa+1)]P_1(\rho)$$
$$+[-2\rho(z+L)-(\kappa-1)]P_2(\rho)\}e^{-\rho(z+L)}$$
$$+\{[-2\rho(z-L)-(\kappa+1)]P_1(\rho)$$
$$+[-2\rho(z-L)+(\kappa-1)]P_2(\rho)\}e^{\rho(z-L)}\rangle\rho J_1(\rho r)d\rho. \quad (2.32\mathrm{a-e})$$

The displacements and the stresses for Region ii-2 ($0\le r<\infty, L\le z<\infty$) are written as;

$$u_{ii-2}(\rho,z)=\frac{1}{2\mu(\kappa+1)}\int_0^{\infty}\langle\{[\rho(z+L)-\kappa]P_1(\rho)+\rho(z+L)P_2(\rho)\}e^{-\rho(z+L)}$$
$$+\{[+\rho(z-L)-\kappa]P_1(\rho)-\rho(z-L)P_2(\rho)\}e^{-\rho(z-L)}\rangle J_1(\rho r)d\rho,$$

$$w_{ii-2}(\rho,z)=\frac{1}{2\mu(\kappa+1)}\int_0^\infty \langle\{\rho(z+L)P_1(\rho)+[\rho(z+L)+\kappa]P_2(\rho)\}e^{-\rho(z+L)}$$
$$+\{\rho(z-L)P_1(\rho)+[-\rho(z-L)-\kappa]P_2(\rho)\}e^{-\rho(z-L)}\rangle J_0(\rho r)d\rho,$$

$$\sigma_{r_{ii-2}}(r,z)=\frac{1}{2(\kappa+1)}\int_0^\infty \langle\{[2\rho(z+L)-(\kappa+3)]P_1(\rho)$$
$$+[2\rho(z+L)+(\kappa-3)]P_2(\rho)\}e^{-\rho(z+L)}$$
$$+\{[2\rho(z-L)-(\kappa+3)]P_1(\rho)$$
$$+[-2\rho(z-L)-(\kappa-3)]P_2(\rho)\}e^{-\rho(z-L)}\rangle\rho J_0(\rho r)d\rho$$
$$+\frac{1}{2(\kappa+1)}\int_0^\infty \langle\{[-2\rho(z+L)+2\kappa]P_1(\rho)$$
$$-2\rho(z+L)P_2(\rho)\}e^{-\rho(z+L)}$$
$$+\{[-2\rho(z-L)+2\kappa]P_1(\rho)$$
$$+2\rho(z-L)P_2(\rho)\}e^{-\rho(z-L)}\rangle\frac{1}{r}J_1(\rho r)d\rho,$$

$$\sigma_{z_{ii-2}}(r,z)=\frac{1}{2(\kappa+1)}\int_0^\infty \langle\{[-2\rho(z+L)+(\kappa-1)]P_1(\rho)$$
$$+[-2\rho(z+L)-(\kappa+1)]P_2(\rho)\}e^{-\rho(z+L)}$$
$$+\{[-2\rho(z-L)+(\kappa-1)]P_1(\rho)$$
$$+[2\rho(z-L)+(\kappa+1)]P_2(\rho)\}e^{-\rho(z-L)}\rangle\rho J_0(\rho r)d\rho,$$

$$\tau_{rz_{ii-2}}(r,z)=\frac{1}{2(\kappa+1)}\int_0^\infty \langle\{[-2\rho(z+L)+(\kappa+1)]P_1(\rho)$$
$$+[-2\rho(z+L)-(\kappa-1)]P_2(\rho)\}e^{-\rho(z+L)}$$
$$+\{[-2\rho(z-L)+(\kappa+1)]P_1(\rho)$$
$$+[2\rho(z-L)+(\kappa-1)]P_2(\rho)\}e^{-\rho(z-L)}\rangle\rho J_1(\rho r)d\rho. \qquad (2.33\text{a}-\text{e})$$

2.2.2.3 Infinite Medium under the Action of Arbitrary Axisymmetric Loading

The infinite medium problem without cracks or inclusions is considered in this section. Solution of this problem may be obtained by taking the Fourier cosine transform, Sneddon(1951), of the first Navier equation, Eq.(2.2a), and the Fourier cosine transform of the second Navier equation, Eq.(2.2b), in the z-direction and combining the resulting equation. Finally, the following equation can be obtained;

$$x^4 \frac{d^4U_c}{dx^4} + 2x\frac{d^3U_c}{dx^3} - (2x^4 + 3x^2)\frac{d^2U_c}{dx^2} - (2x^3 - 3x)\frac{dU_c}{dx} + (x^4 + 2x^2 - 3)U_c = 0, \tag{2.34}$$

where U_c is the Fourier cosine transform of $u(r, z)$.

$$U_c(r, \alpha) = \int_0^\infty u(r, z) \cos(\alpha, z) dz, \tag{2.35}$$

$x = \alpha r$ and α is the Fourier transform variable. Notinging that Eq. (2.34) may be written in the form, McLachlan(1934),

$$\Delta_1(\Delta_2 U_c) + \Delta_3(\Delta_4 U_c) = 0, \tag{2.37}$$

where $\Delta_1, \Delta_2, \Delta_3$ and Δ_4 are second order linear ordinary differential operators with variable coefficients in x:

$$\Delta_1 = x^2 \frac{d^2}{dx^2} - 3x\frac{d}{dx} - x^2 + 3,$$

$$\Delta_2 = x^2 \frac{d^2}{dx^2} + x\frac{d}{dx} - x^2 - 1,$$

$$\Delta_3 = x^3 \frac{d^2}{dx^2} + x^2\frac{d}{dx} - x^3 - 4x,$$

$$\Delta_4 = x\frac{d^2}{dx^2} - \frac{d}{dx} - x + \frac{1}{x}, \tag{2.37}$$

solution of Eq. (2.34) may be obtained from the second order ordinary differential equations

$\Delta_2 U_c = 0, \Delta_4 U_c$=0, (2.38)

in the form of

$$U_c(r,\alpha) = -\frac{1}{2}c_{11}I_1(\alpha r) + \frac{1}{2}c_{12}K_1(\alpha r) + c_{13}\alpha r I_0(\alpha r) + c_{14}\alpha r K_0(\alpha r), \quad (2.39)$$

where c_{11}, c_{12}, c_{13} and c_{14} are arbitrary constants and I_0, K_0, I_1 and K_1 are the modified Bessel functions of the first and second kinds of order zero and one, respectively. Due to symmetry about *z*-axis, c_{12} and c_{14} must be zero (Fig. 2.6).

Similarly,

$$W_s(r,\alpha) = \frac{1}{2}c_{11}I_0(\alpha r) - c_{13}[(\kappa+1)I_0(\alpha r) + \alpha r I_1(\alpha r)], \quad (2.40)$$

is obtained where $W_s(r,\alpha)$ is the Fourier sine transform of $w(r,z)$,

$$W_s(r,\alpha) = \int_0^\infty w(r,z)\sin(\alpha,z)dz. \quad (2.41)$$

By taking the inverse transforms of Eqs.(2.39) and Eqs.(2.40), the displacement components are obtained as

$$u_{fourier}(r,z) = \frac{2}{\pi}\int_0^\infty \left[-\frac{1}{2}c_{11}I_1(\alpha r) + c_{13}\alpha r I_0(\alpha r)\right]\cos(\alpha z)\,d\alpha,$$

$$w_{fourier}(r,z) = \frac{2}{\pi}\int_0^\infty \left[\frac{1}{2}c_{11}I_0(\alpha r) - c_{13}[(\kappa+1)I_0(\alpha r) + \alpha r I_1(\alpha r)]\right]\sin(\alpha z)\,d\alpha. \quad (2.42\mathrm{a,b})$$

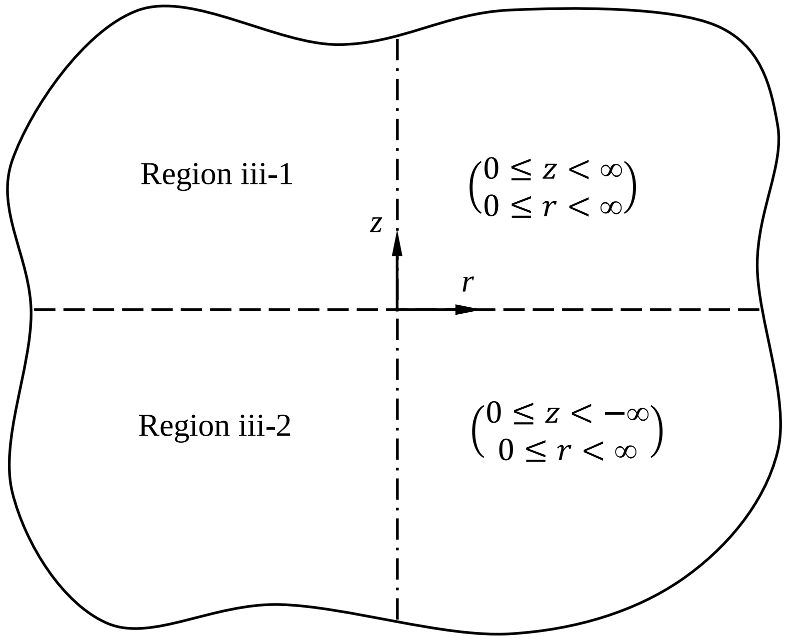

Figure 2.6 Infinite axisymmetric medium with no crack or inclusion.

By substituting Eq.(2.42) in Eq.(2.1), expressions for the stress components can be obtained as

$$\sigma_{r_{fourier}}(r,z) = \frac{2\mu}{\pi}\int_0^\infty \left\{ c_{11}\left[\frac{I_1(\alpha r)}{r} - \alpha I_0(\alpha r)\right] \right.$$
$$\left. + c_{13}[(\kappa-1)\alpha I_0(\alpha r) + 2\alpha^2 r I_1(\alpha r)] \right\} \cos(\alpha z)\, d\alpha,$$

$$\sigma_{z_{fourier}}(r,z) = \frac{2\mu}{\pi}\int_0^\infty \{c_{11}\alpha I_0(\alpha r)$$
$$- c_{13}[(\kappa+5)\alpha I_0(\alpha r) + 2\alpha^2 r I_1(\alpha r)]\} \cos(\alpha z)\, d\alpha,$$

$$\tau_{rz_{fourier}}(r,z) = \frac{2\mu}{\pi}\int_0^\infty \{c_{11}\alpha I_1(\alpha r)$$
$$- c_{13}[(\kappa+1)\alpha I_1(\alpha r) + 2\alpha^2 r I_0(\alpha r)]\} \sin(\alpha z)\, d\alpha. \qquad (2.43\text{a} - \text{c})$$

General expressions for the infinite medium with two penny shaped inclusions, a ring shaped crack, subjected to arbitrary axisymmetric loads, can be obtained by adding the individual expressions:

$$u_{perturbation} = u_{crack} + u_{inclusions} + u_{fourier},$$

$$w_{perturbation} = w_{crack} + w_{inclusions} + w_{fourier},$$

$$\sigma_{r_{perturbation}} = \sigma_{r_{crack}} + \sigma_{r_{inclusions}} + \sigma_{r_{fourier}},$$

$$\sigma_{z_{perturbation}} = \sigma_{z_{crack}} + \sigma_{z_{inclusions}} + \sigma_{z_{fourier}},$$

$$\tau_{rz_{perturbation}} = \tau_{rz_{crack}} + \tau_{rz_{inclusions}} + \tau_{rz_{fourier}}. \qquad (2.44\text{a} - \text{e})$$

These expressions can be used as the expressions of the perturbation problem, for an infinite cylinder with a surface free of stress, providing that they satisfy the homogeneous boundary conditions given below:

$$\sigma_{r_{perturbation}}(A, z) = 0, \qquad (0 \leq z < \infty)$$

$$\tau_{rz_{perturbation}}(A, z) = 0, \qquad (0 \leq z < \infty) \qquad (2.45\text{a}, \text{b})$$

Eqs.(2.45) with (2.12), (2.13), (2.24),(2.25), (2.26), (2.27) and (2.44) give

$$c_{11}\alpha I_1(\alpha A) - c_{13}[(\kappa+1)\alpha I_1(\alpha A) + 2A\alpha^2 I_0(\alpha A)]$$
$$= \frac{1}{\kappa+1}\int_0^\infty \left[\frac{-8\alpha\rho^3}{(\alpha^2+\rho^2)^2}\right] J_1(\rho A)M(\rho)d\rho$$
$$+ \frac{\sin(\alpha L)}{\mu(\kappa+1)}\int_0^\infty \left[\frac{-(\kappa-1)(\alpha^2+\rho^2)\rho^2 - 2(\rho^2-\alpha^2)\rho^2}{(\alpha^2+\rho^2)^2}\right] J_1(\rho A)P_2(\rho)d\rho$$
$$+ \frac{\cos(\alpha L)}{\mu(\kappa+1)}\int_0^\infty \left[\frac{-\alpha(\kappa+1)(\alpha^2+\rho^2)\rho + 4\alpha\rho^3}{(\alpha^2+\rho^2)^2}\right] J_1(\rho A)P_1(\rho)d\rho,$$

$$c_{11}\alpha I_1(\alpha A) - c_{13}[(\kappa+1)\alpha I_1(\alpha A) + 2A\alpha^2 I_0(\alpha A)]$$
$$= \frac{1}{\kappa+1}\int_0^\infty \left[\frac{-8\alpha\rho^3}{(\alpha^2+\rho^2)^2}\right] J_1(\rho A)M(\rho)d\rho$$
$$+ \frac{\sin(\alpha L)}{\mu(\kappa+1)}\int_0^\infty \left[\frac{-2(\rho^2-\alpha^2)\rho^2}{(\alpha^2+\rho^2)^2} - \frac{(\kappa-1)\rho^2}{\alpha^2+\rho^2}\right] J_1(\rho A)P_2(\rho)d\rho$$
$$+ \frac{\cos(\alpha L)}{\mu(\kappa+1)}\int_0^\infty \left[\frac{4\alpha\rho^3}{(\alpha^2+\rho^2)^2}\right.$$
$$\left. + \frac{-(\kappa+1)\alpha\rho}{\alpha^2+\rho^2}\right] J_1(\rho A)P_1(\rho)d\rho. \qquad (2.46\text{a, b})$$

Solution of Eqs. (2.46) give

$$c_{11} = \frac{[(\kappa-1)\alpha A I_0(\alpha A) + 2\alpha^2A^2 I_1(\alpha A)]E_1 + [(\kappa+1)\alpha A I_1(\alpha A) + 2\alpha^2 A^2 I_0(\alpha A)]E_2}{2\alpha^3A^3\left[{I_1}^2(\alpha A) - {I_0}^2(\alpha A)\right] + (\kappa+1)\alpha A {I_1}^2(\alpha A)},$$

$$c_{13} = \frac{\alpha A I_1(\alpha A)E_2 - [I_1(\alpha A) - \alpha A I_0(\alpha A)]E_1}{2\alpha^3A^3\left[{I_1}^2(\alpha A) - {I_0}^2(\alpha A)\right] + (\kappa+1)\alpha A {I_1}^2(\alpha A)}, \qquad (2.47\text{a, b})$$

By using the integral formulas in given Appendix A, it may be shown that

$$E_1 = \frac{1}{\kappa+1}\int_a^b m(t)t\{4\alpha^2 A[AK_0(\alpha A)I_1(\alpha t) - tK_1(\alpha A)I_0(\alpha t)]\}\,dt$$
$$+ \frac{\cos(\alpha L)}{2\mu(\kappa+1)}\int_0^c p_1(t)t\{2\alpha A[-(\kappa+1)K_1(\alpha A)I_1(\alpha t)$$
$$+ 2\alpha t K_1(\alpha A)I_0(\alpha t) - 2\alpha A K_0(\alpha A)I_1(\alpha t)]\}dt$$
$$+ \frac{\sin(\alpha L)}{2\mu(\kappa+1)}\int_0^c p_2(t)t\{2\alpha A[-(\kappa+1)K_1(\alpha A)I_0(\alpha t)$$
$$- 2\alpha t K_1(\alpha A)I_1(\alpha t) + 2\alpha A K_0(\alpha A)I_0(\alpha t)]\}dt,$$

$$E_2 = \frac{1}{\kappa+1}\int_a^b 2m(t)t\{(\kappa+1)K_1(\alpha A)I_1(\alpha t) - 2\alpha t K_1(\alpha A)I_0(\alpha t)$$
$$+ 2\alpha A K_0(\alpha A)I_1(\alpha t) + 2\alpha^2 A[AK_1(\alpha A)I_1(\alpha t) - tK_0(\alpha A)I_0(\alpha t)]\}\,dt$$
$$+ \frac{\cos(\alpha L)}{2\mu(\kappa+1)}\int_0^c p_1(t)t[4\alpha^2 AtK_0(\alpha A)I_0(\alpha t) + 4\alpha t K_1(\alpha A)I_0(\alpha t)$$
$$- 4(\alpha^2A^2 + \kappa + 1)K_1(\alpha A)I_1(\alpha t) - 2(\kappa+3)\alpha A K_0(\alpha A)I_1(\alpha t)]dt$$
$$+ \frac{\sin(\alpha L)}{2\mu(\kappa+1)}\int_0^c p_2(t)t[-4\alpha^2 AtK_0(\alpha A)I_1(\alpha t)$$
$$+ 4\alpha^2A^2K_1(\alpha A)I_0(\alpha t) - 4\alpha t K_1(\alpha A)I_1(\alpha t)$$
$$- 2(\kappa$$
$$- 1)\alpha A K_0(\alpha A)I_0(\alpha t)]dt. \qquad (2.48\text{a, b})$$

The general displacement expressions and stress components for the perturbation problem of an infinite cylinder with a crack, two inclusions and a stress-free surface turn into:

$$
\begin{aligned}
u_{cyl\,.per.}(r,z) = {} & \frac{1}{\kappa+1}\int_a^b m(t)t\,\langle\int_0^\infty [\kappa-1-2\rho z]e^{-\rho z}J_1(\rho t)\,J_1(\rho r)d\rho \\
& + \frac{2}{\pi}\int_0^\infty \frac{1}{d_0}\big\{\{2\alpha t[\kappa+1+d_2+d_1d_3]\alpha A I_0(\alpha t) \\
& - [2d_1+(\kappa+1)(d_2+d_1d_3)]\alpha A I_1(\alpha t)\}I_1(\alpha r) \\
& - 2[2\alpha^2 AtI_0(\alpha t)-(d_2+d_1d_3)\alpha A I_1(\alpha t)]\alpha r I_0(\alpha r)\big\}\cos\alpha z d\alpha\rangle\, dt \\
& + \frac{1}{2\mu(\kappa+1)}\int_0^c p_1(t)t\,\langle\int_0^\infty \big\{[\rho(z+L)-\kappa]e^{-\rho(z+L)} \\
& - [\rho(z-L)+\kappa]e^{\rho(z-L)}\big\}J_1(\rho t)J_1(\rho r)d\rho \\
& - \frac{2}{\pi}\int_0^\infty \frac{1}{d_0}\big\{\{2\alpha t[\kappa+1+d_2+d_1d_3]\alpha A I_0(\alpha t) \\
& - [2d_1+(\kappa+1)^2+2(\kappa+1)(d_2+d_1d_3)]\alpha A I_1(\alpha t)\}I_1(\alpha r) \\
& + 2[-2\alpha^2 AtI_0(\alpha t) \\
& + (\kappa+1+d_2+d_1d_3)\alpha A I_1(\alpha t)]\alpha r I_0(\alpha r)\big\}\cos\alpha L\cos\alpha z d\alpha\rangle\, dt \\
& + \frac{1}{2\mu(\kappa+1)}\int_0^c p_2(t)\,t\,\langle\int_0^\infty \big\{\rho(z+L)e^{-\rho(z+L)} \\
& - \rho(z-L)e^{\rho(z-L)}\big\}J_0(\rho t)J_1(\rho r)d\rho \\
& - \frac{2}{\pi}\int_0^\infty \frac{1}{d_0}\big\{\{[2d_1-(\kappa+1)^2]\alpha A I_0(\alpha t) \\
& - 2\alpha t(\kappa+1+d_2+d_1d_3)\alpha A I_1(\alpha t)\}I_1(\alpha r) \\
& + [2(\kappa+1-d_2-d_1d_3)\alpha A I_0(\alpha t) \\
& + 4\alpha^2 AtI_1(\alpha t)]\alpha r I_0(\alpha r)\big\}\sin\alpha L\cos\alpha z d\alpha\rangle\, dt,
\end{aligned}
$$

$$
\begin{aligned}
w_{cyl.per.}(r,z) = {} & \frac{1}{\kappa+1}\int_a^b m(t)t\,\langle\int_0^\infty [-\kappa-1-2\rho z]e^{-\rho z}J_1(\rho t)\,J_0(\rho r)d\rho \\
& + \frac{2}{\pi}\int_0^\infty \frac{1}{d_0}\big\{\{2\alpha t[\kappa+1-d_2-d_1d_3]\alpha A I_0(\alpha t) \\
& + [2d_1-(\kappa+1)(d_2+d_1d_3)]\alpha A I_1(\alpha t)\}I_0(\alpha r) \\
& + 2[2\alpha^2 A t I_0(\alpha t)-(d_2+d_1d_3)\alpha A I_1(\alpha t)]\alpha r I_1(\alpha r)\big\}\sin\alpha z d\alpha\rangle\,dt \\
& + \frac{1}{2\mu(\kappa+1)}\int_0^c p_1(t)t\,\langle\int_0^\infty \big\{\rho(z+L)e^{-\rho(z+L)} \\
& + \rho(z-L)e^{\rho(z-L)}\big\}J_1(\rho t)J_0(\rho r)d\rho \\
& - \frac{2}{\pi}\int_0^\infty \frac{1}{d_0}\big\{\{2\alpha t[\kappa+1-d_2-d_1d_3]\alpha A I_0(\alpha t) \\
& + [2d_1-(\kappa+1)^2]\alpha A I_1(\alpha t)\}I_0(\alpha r) \\
& + 2[2\alpha^2 A t I_0(\alpha t) \\
& - (\kappa+1+d_2+d_1d_3)\alpha A I_1(\alpha t)]\alpha r I_1(\alpha r)\big\}\cos\alpha L\sin\alpha z d\alpha\rangle\,dt \\
& + \frac{1}{2\mu(\kappa+1)}\int_0^c p_2(t)t\,\langle\int_0^\infty \big\{[\rho(z+L)+\kappa]e^{-\rho(z+L)} \\
& + [\rho(z-L)-\kappa]e^{\rho(z-L)}\big\}J_0(\rho t)J_0(\rho r)d\rho \\
& - \frac{2}{\pi}\int_0^\infty \frac{1}{d_0}\big\{\{-[2d_1+(\kappa+1)^2-2(\kappa+1)(d_2+d_1d_3)]\alpha A I_0(\alpha t) \\
& - 2\alpha t(\kappa+1-d_2-d_1d_3)\alpha A I_1(\alpha t)\}I_0(\alpha r) \\
& + [-2(\kappa+1-d_2-d_1d_3)\alpha A I_0(\alpha t) \\
& - 4\alpha^2 A t I_1(\alpha t)]\alpha r I_1(\alpha r)\big\}\sin\alpha L\sin\alpha z d\alpha\rangle\,dt,
\end{aligned}
$$

$$\sigma_{r_{cyl.per.}}(r,z) = \frac{2\mu}{\kappa+1}\int_a^b m(t)t\,\langle 2\int_0^\infty \rho(1-\rho z)e^{-\rho z}J_1(\rho t)\,J_0(\rho r)d\rho$$

$$+\int_0^\infty (2\rho z-\kappa+1)\,e^{-\rho z}J_1(\rho t)\frac{J_1(\rho r)}{r}d\rho$$

$$-\frac{2}{\pi}\int_0^\infty \frac{1}{d_0}\Big\{\{-2\alpha t[2+d_2+d_1d_3]\alpha AI_0(\alpha t)$$

$$+2(d_1+d_2+d_1d_3)\alpha AI_1(\alpha t)\}\alpha I_0(\alpha r)$$

$$+\{2\alpha t(\kappa+1+d_2+d_1d_3)\alpha AI_0(\alpha t)$$

$$-[2d_1+(\kappa+1)(d_2+d_1d_3)]\alpha AI_1(\alpha t)\}\frac{I_1(\alpha r)}{r}$$

$$+[2\alpha^2 AtI_0(\alpha t)-(d_2+d_1d_3)\alpha AI_1(\alpha t)]2\alpha^2 rI_1(\alpha r)\Big\}\cos\alpha z d\alpha\rangle\,dt$$

$$-\frac{1}{2(\kappa+1)}\int_0^c p_1(t)t\,\langle\int_0^\infty\{[-2\rho(z+L)+\kappa+3]e^{-\rho(z+L)}$$

$$+[2\rho(z-L)+\kappa+3]e^{\rho(z-L)}\}\rho J_1(\rho t)J_0(\rho r)d\rho$$

$$+\int_0^\infty\{[2\rho(z+L)-2\kappa]e^{-\rho(z+L)}$$

$$+[-2\rho(z-L)-2\kappa]e^{\rho(z-L)}\}\frac{J_1(\rho r)}{r}J_1(\rho t)d\rho$$

$$+\frac{2}{\pi}\int_0^\infty\frac{1}{d_0}\Big\{\{4\alpha t[2+d_2+d_1d_3]\alpha AI_0(\alpha t)$$

$$-[4d_1+4(\kappa+1)+2(\kappa+3)(d_2+d_1d_3)]\alpha AI_1(\alpha t)\}\alpha I_0(\alpha r)$$

$$+2[-2\alpha^2 AtI_0(\alpha t)+(\kappa+1+d_2+d_1d_3)\alpha AI_1(\alpha t)]2\alpha^2 rI_1(\alpha r)$$

$$+\{-4\alpha t[\kappa+1+d_2+d_1d_3]\alpha AI_0(\alpha t)$$

$$+2[2d_1+\kappa^2-1$$

$$+2(\kappa+1)(d_2+d_1d_3)]\alpha AI_1(\alpha t)\}\frac{I_1(\alpha r)}{r}\Big\}\cos\alpha L\cos\alpha z d\alpha\rangle\,dt$$

$$-\frac{1}{2(\kappa+1)}\int_0^c p_2(t)t\,\langle\int_0^\infty\{[-2\rho(z+L)-\kappa+3]e^{-\rho(z+L)}$$

$$+[2\rho(z-L)-\kappa+3]e^{\rho(z-L)}\}\rho J_0(\rho t)J_0(\rho r)d\rho$$

$$+\int_0^\infty\{2\rho(z+L)e^{-\rho(z+L)}-2\rho(z-L)e^{\rho(z-L)}\}\frac{J_1(\rho r)}{r}J_0(\rho t)d\rho$$

$$+\frac{2}{\pi}\int_0^\infty \frac{1}{d_0}\Big\{\{-4\alpha t[2+d_2+d_1d_3]\alpha A I_1(\alpha t)$$

$$+[4d_1-4(\kappa+1)-2(\kappa-1)(d_2+d_1d_3)]\alpha A I_0(\alpha t)\}\alpha I_0(\alpha r)$$

$$+\{2\,[-2d_1+(\kappa+1)^2]\alpha A I_0(\alpha t)$$

$$+4\alpha t[\kappa+1+d_2+d_1d_3]\alpha A I_1(\alpha t)\}\frac{I_1(\alpha r)}{r}$$

$$+\{2(\kappa+1-d_2-d_1d_3)\alpha A I_0(\alpha t)$$

$$+4\alpha^2 A t I_1(\alpha t)\}2\alpha^2 r I_1(\alpha r)\}\sin\alpha L\cos\alpha z d\alpha\rangle\, dt,$$

$$\sigma_{z_{cyl.per.}}(r,z)=\frac{4\mu}{\kappa+1}\int_a^b m(t)t\,\langle\int_0^\infty \rho(\rho z+1)\,e^{-\rho z}J_1(\rho t)J_0(\rho r)d\rho$$

$$-\frac{1}{\pi}\int_0^\infty \frac{1}{d_0}\big\{\{2\alpha t(-4+d_2+d_1d_3)\alpha A I_0(\alpha t)$$

$$+[-2d_1+4(d_2+d_1d_3)]\alpha A I_1(\alpha t)\}\alpha I_0(\alpha r)$$

$$+\{-2\alpha^2 A t I_0(\alpha t)$$

$$+(d_2+d_1d_3)\alpha A I_1(\alpha t)\}2\alpha^2 r I_1(\alpha r)\big\}\cos\alpha z d\alpha\rangle\, dt$$

$$-\frac{1}{2(\kappa+1)}\int_0^c p_1(t)t\,\langle\int_0^\infty \big\{[2\rho(z+L)-(\kappa-1)]e^{-\rho(z+L)}$$

$$+[-2\rho(z-L)-(\kappa-1)]e^{\rho(z-L)}\big\}\rho J_1(\rho t)J_0(\rho r)d\rho$$

$$+\frac{2}{\pi}\int_0^\infty \frac{1}{d_0}\big\{\{-4\alpha t(-4+d_2+d_1d_3)\alpha A I_0(\alpha t)$$

$$+2[2d_1-4(\kappa+1)+(\kappa-3)(d_2+d_1d_3)]\alpha A I_1(\alpha t)\}\alpha I_0(\alpha r)$$

$$+\{4\alpha^2 A t I_0(\alpha t)$$

$$-2(1+\kappa+d_2+d_1d_3)\alpha A I_1(\alpha t)\}2\alpha^2 r I_1(\alpha r)\big\}\cos\alpha L\cos\alpha z d\alpha\rangle\, dt$$

$$-\frac{1}{2(\kappa+1)}\int_0^c p_2(t)t\,\langle\int_0^\infty \big\{[2\rho(z+L)+(\kappa+1)]e^{-\rho(z+L)}$$

$$+[-2\rho(z-L)+(\kappa+1)]e^{\rho(z-L)}\big\}\rho J_0(\rho t)J_0(\rho r)d\rho$$

$$+\frac{2}{\pi}\int_0^\infty \frac{1}{d_0}\big\{\{-2[2d_1+4(\kappa+1)-(\kappa+5)(d_2+d_1d_3)]\alpha A I_0(\alpha t)$$

$$+4\alpha t(-4+d_2+d_1d_3)\alpha A I_1(\alpha t)\}\alpha I_0(\alpha r)$$

$$+\{-2(1+\kappa-d_2-d_1d_3)\alpha A I_0(\alpha t)$$

$$-4\alpha^2 A t I_1(\alpha t)\}2\alpha^2 r I_1(\alpha r)\big\}\sin\alpha L\cos\alpha z d\alpha\rangle\, dt,$$

$$
\begin{aligned}
&\tau_{rz_{cyl\,.per.}}(r,z) \\
&= \frac{4\mu}{\kappa+1}\int_a^b m(t)t\left\langle\int_0^\infty \rho^2 z\, e^{-\rho z} J_1(\rho t)J_1(\rho r)d\rho\right. \\
&- \frac{1}{\pi}\int_0^\infty \frac{1}{d_0}\big\{\{2\alpha t(d_2+d_1d_3)\alpha A I_0(\alpha t) - 2d_1\alpha A I_1(\alpha t)\}\alpha I_1(\alpha r) \\
&+ \{-4\alpha^2 A t I_0(\alpha t) \\
&\left. + 2\alpha(d_2+d_1d_3)\alpha A I_1(\alpha t)\}\alpha r I_0(\alpha r)\big\}\sin\alpha z d\alpha\right\rangle dt \\
&- \frac{1}{2(\kappa+1)}\int_0^c p_1(t)t\left\langle\int_0^\infty \big\{[2\rho(z+L)-(\kappa+1)]e^{-\rho(z+L)}\right. \\
&+ [2\rho(z-L)+(\kappa+1)]e^{\rho(z-L)}\big\}\rho J_1(\rho t)J_1(\rho r)d\rho \\
&+ \frac{2}{\pi}\int_0^\infty \frac{1}{d_0}\big\{\{-4\alpha t(d_2+d_1d_3)\alpha A I_0(\alpha t) \\
&+ 2[2d_1+(\kappa+1)(d_2+d_1d_3)]\alpha A I_1(\alpha t)\}\alpha I_1(\alpha r) \\
&+ 2\{4\alpha^2 A t I_0(\alpha t) \\
&\left. - 2\alpha(1+\kappa+d_2+d_1d_3)\alpha A I_1(\alpha t)\}\alpha r I_0(\alpha r)\big\}\cos\alpha L\sin\alpha z d\alpha\right\rangle dt \\
&- \frac{1}{2(\kappa+1)}\int_0^c p_2(t)t\left\langle\int_0^\infty \big\{[2\rho(z+L)+(\kappa-1)]e^{-\rho(z+L)}\right. \\
&+ [2\rho(z-L)-(\kappa-1)]e^{\rho(z-L)}\big\}\rho J_0(\rho t)J_1(\rho r)d\rho \\
&+ \frac{2}{\pi}\int_0^\infty \frac{1}{d_0}\big\{\{2[-2d_1+(\kappa+1)(d_2+d_1d_3)]\alpha A I_0(\alpha t) \\
&+ 4\alpha t(d_2+d_1d_3)\alpha A I_1(\alpha t)\}\alpha I_1(\alpha r) \\
&+ 2\{-2\alpha(1+\kappa-d_2-d_1d_3)\alpha A I_0(\alpha t) \\
&\left. - 4\alpha^2 A t I_1(\alpha t)\}\alpha r I_0(\alpha r)\big\}\sin\alpha L\sin\alpha z d\alpha\right\rangle dt, \qquad (2.49\text{a} - \text{e})
\end{aligned}
$$

where

$$d_0 = [2\alpha^3A^3 + \alpha A(\kappa+1)]I_1^2(\alpha A) - 2\alpha^3A^3 I_0^2(\alpha A),$$

$$d_1 = 1+\kappa+2\alpha^2A^2,$$

$$d_2 = 2\alpha^2A^2 I_0(\alpha A)K_0(\alpha A),$$

$$d_3 = I_1(\alpha A)K_1(\alpha A), \qquad (2.50\text{a} - \text{d})$$

integrals of Bessel functions are given in terms of the complete elliptic integrals K and E in Appendix B.

2.2.3 Superposition

The displacement and the stress expressions for the infinite cylinder containing a ring shaped crack located at $z = 0$ plane, two penny shaped inclusions located at $z = \pm L$ planes and subjected to axial tension of uniform intensity p_0 at $z = \pm\infty$ are obtained by the superposition of the uniform solution and the general expressions for the perturbation problem:

$$u = u_{cyl.per.} + u_{uniform},$$

$$w = w_{cyl.per.} + w_{uniform},$$

$$\sigma_r = \sigma_{r_{cyl.per.}} + \sigma_{r_{uniform}},$$

$$\sigma_z = \sigma_{z_{cyl.per.}} + \sigma_{z_{uniform}},$$

$$\tau_{rz} = \tau_{rz_{cyl.per.}} + \tau_{rz_{uniform}}. \qquad (2.51a-e)$$

CHAPTER III

INTEGRAL EQUATIONS

3.1. Derivation of Integral Equations

The unknown functions $m(r)$, $p_1(r)$ and $p_2(r)$ are used in stress and displacement expressions given in Eqs.(2.49) or (2.51). The unknown function $m(r)$ is the crack surface displacement derivative in z-direction while $p_1(r)$ and $p_2(r)$ are the jumps in the shearing and normal stresses through the rigid inclusion, respectively. Since the surface of the crack located at $z = 0$ plane is free of stress and the rigid inclusions located at $z = \pm L$ planes are perfectly bonded to the cylinder, the stress and the displacement expressions, Eqs.(2.51), must satisfy the following conditions

$$\sigma_z(r, 0) = 0, \qquad (a < r < b) \qquad (3.1a)$$

on the crack and

$$u(r, L) = 0\,, \qquad (0 < r < c)$$

$$w(r, L) = \text{constant}, \qquad (0 < r < c) \qquad (3.1b, c)$$

on the rigid inclusion. Displacement type boundary conditions, Eqs.(3.1b,c), are satisfied if the following equations

$$\frac{1}{r}\frac{\partial}{\partial r}[ru(r, L)] = 0, \qquad (0 < r < c)$$

$$\frac{\partial}{\partial r} w(r,L) = 0, \qquad (0 < r < c) \qquad (3.2\text{a, b})$$

are satisfied. Eqs.(3.1a) and (3.2a,b) are all stress type conditions. Substituting Eqs.(2.49d) in Eqs.(3.1a) and Eq.(2.49a,b) in Eq.(3.2a,b) gives the following singular integral equations

$$\begin{aligned}
&\frac{1}{\pi}\int_a^b m(t)[4m_1(r,t) + tN_{11}(r,t)]\,dt \\
&\qquad + \frac{1}{2\mu}\int_0^c \left\{p_1(t)\left[T_1(r,t) + \frac{2}{\pi}N_{12}(r,t)\right]\right. \\
&\qquad \left. + p_2(t)\left[T_2(r,t) + \frac{2}{\pi}N_{13}(r,t)\right]\right\} t\,dt \\
&\qquad = -\frac{(\kappa + 1)}{2\mu}p_0\,, \qquad (a < r < b)
\end{aligned}$$

$$\begin{aligned}
&\int_a^b m(t)\left[T_3(r,t) + \frac{2}{\pi}N_{21}(r,t)\right] t\,dt \\
&\qquad + \frac{1}{2\mu}\int_0^c p_1(t)\left[tT_4(r,t) - \frac{2\kappa}{\pi}m_1(r,t) + \frac{2}{\pi}tN_{22}(r,t)\right] dt \\
&\qquad + \frac{1}{2\mu}\int_0^c p_2(t)\left[T_5(r,t) + \frac{2}{\pi}N_{23}(r,t)\right] t\,dt \\
&\qquad = \frac{(\kappa - 3)(\kappa + 1)}{\mu(\kappa - 7)}p_0, \qquad (0 \le r < c)
\end{aligned}$$

$$\begin{aligned}
&\int_a^b m(t)\left[T_6(r,t) + \frac{2}{\pi}N_{31}(r,t)\right] t\,dt \\
&\qquad + \frac{1}{2\mu}\int_0^c p_1(t)\left[T_7(r,t) + \frac{2}{\pi}N_{32}(r,t)\right] t\,dt \\
&\qquad + \frac{1}{2\mu}\int_0^c p_2(t)\left[tT_8(r,t) - \frac{2\kappa}{\pi}m_2(r,t) + \frac{2}{\pi}tN_{33}(r,t)\right] t\,dt \\
&\qquad = 0, \qquad (0 \le r < c) \qquad (3.3\text{a} - \text{c})
\end{aligned}$$

where

$$m_1(r,t) = \frac{t}{t^2-r^2}\begin{cases} \dfrac{t^2-r^2}{tr}K\left(\dfrac{t}{r}\right)+\dfrac{r}{t}E\left(\dfrac{t}{r}\right), & t<r \\ E\left(\dfrac{r}{t}\right), & t>r \end{cases}$$

$$m_2(r,t) = \frac{r}{t^2-r^2}\begin{cases} \dfrac{t}{r}E\left(\dfrac{t}{r}\right), & t<r \\ \dfrac{t^2}{r^2}E\left(\dfrac{r}{t}\right)-\dfrac{t^2-r^2}{r^2}K\left(\dfrac{r}{t}\right), & t>r \end{cases} \tag{3.4a, b}$$

K and E are the complete elliptic integrals of the first and the second kinds. It should be noted that $m(r)$ and $p_1(r)$ are odd, $p_2(r)$ is even, integrals from 0 to c in Eqs.(3.3) may be converted to integrals from $-c$ to c and Eqs.(3.3) may be rewritten in the form

$$\begin{aligned} &\frac{1}{\pi}\int_a^b m(t)\left[\frac{2}{t-r}+2M_3(r,t)+tN_{11}(r,t)\right]dt \\ &\qquad +\frac{1}{4\mu}\int_{-c}^{c}\left\{p_1(t)\left[tT_1(r,|t|)+\frac{2}{\pi}|t|N_{12}(r,t)\right]\right. \\ &\qquad \left.+p_2(t)|t|\left[T_2(r,|t|)+\frac{2}{\pi}N_{13}(r,t)\right]\right\}dt \\ &\qquad =-\frac{(\kappa+1)}{2\mu}p_0, \qquad (a<r<b) \end{aligned}$$

$$\begin{aligned} &\int_a^b m(t)\left[T_3(r,t)+\frac{2}{\pi}N_{21}(r,t)\right]tdt \\ &\qquad +\frac{1}{4\mu}\int_{-c}^{c}p_1(t)\left[tT_4(r,|t|)-\frac{2\kappa}{\pi}\frac{1}{t-r}-\frac{2\kappa}{\pi}M_4(r,t)\right. \\ &\qquad \left.+\frac{2}{\pi}|t|N_{22}(r,t)\right]dt+\frac{1}{4\mu}\int_{-c}^{c}p_2(t)\left[T_5(r,|t|)+\frac{2}{\pi}N_{23}(r,t)\right]|t|dt \\ &\qquad =\frac{(\kappa-3)(\kappa+1)}{\mu(\kappa-7)}p_0, \qquad (-c<r<c) \end{aligned}$$

$$\int_a^b m(t)\left[T_6(r,t)+\frac{2}{\pi}N_{31}(r,t)\right]tdt$$
$$+\frac{1}{4\mu}\int_{-c}^{c}p_1(t)\left[tT_7(r,|t|)+\frac{2}{\pi}|t|N_{32}(r,t)\right]dt$$
$$+\frac{1}{4\mu}\int_{-c}^{c}p_2(t)\left[|t|T_8(r,|t|)-\frac{2\kappa}{\pi}\frac{1}{t-r}-\frac{2\kappa}{\pi}M_5(r,t)\right.$$
$$\left.+\frac{2}{\pi}|t|N_{33}(r,t)\right]tdt, \qquad (-c<r<c) \quad (3.5\text{a}-\text{c})$$

where

$$M_3(r,t)=\frac{m_3(r,t)-1}{t-r},$$

$$M_4(r,t)=\frac{m_4(r,t)-1}{t-r},$$

$$M_5(r,t)=\frac{m_5(r,t)-1}{t-r}, \qquad (3.6\text{a}-\text{c})$$

and

$$m_3(r,t)=2\begin{cases}\dfrac{t-r}{r}K\left(\dfrac{t}{r}\right)+\dfrac{r}{t+r}E\left(\dfrac{t}{r}\right) & t<r\\ \dfrac{t}{t+r}E\left(\dfrac{r}{t}\right) & t>r\end{cases},$$

$$m_4(r,t)=\begin{cases}\dfrac{t^2-r^2}{|tr|}K\left(\left|\dfrac{t}{r}\right|\right)+\left|\dfrac{r}{t}\right|E\left(\left|\dfrac{t}{r}\right|\right) & |t|<|r|\\ E\left(\left|\dfrac{r}{t}\right|\right) & |t|>|r|\end{cases},$$

$$m_5(r,t)=\begin{cases}\left|\dfrac{t}{r}\right|E\left(\left|\dfrac{t}{r}\right|\right) & |t|<|r|\\ -\dfrac{t^2-r^2}{r^2}K\left(\left|\dfrac{r}{t}\right|\right)+\dfrac{t^2}{r^2}E\left(\left|\dfrac{r}{t}\right|\right) & |t|>|r|\end{cases}, \qquad (3.7\text{a}-\text{c})$$

The kernels $N_{ij}(r,t)(i,j=1-3)$ in Eqs.(3.3) are in the form of improper integrals

$$N_{ij}(r,t)=\int_0^{\infty} L_{ij}(r,t,\alpha)d\alpha, \qquad (i,j=1-3) \qquad (3.8)$$

The integrands $T_i(r,t)(i=1-8)$ and $L_{ij}(r,t,\alpha)(i,j=1-3)$ containing the complete elliptic integrals K and E are given in Appendix C and Appendix D, respectively.

The single-valuedness condition, Eq.(3.9a), for the crack and the equilibrium equations, Eqs.(3.9b,c) for the rigid inclusions

$$\int_a^b m(t)dt=0,$$

$$\int_{-c}^{c} p_i(t)tdt=0, \qquad (i=1,2) \qquad (3.9a-b)$$

have to be satisfied in the solution of three singular integral equations, given in Eqs.(3.5).

In the singular integral equations, given in Eqs.(3.5), the simple Cauchy kernel, Muskhelisvili(1953), $1/(t-r)$ becomes unbounded when $t=r$. Additionally, the kernels $N_{ij}(r,t)(i,j=1-3)$ may contain unbounded parts. Consequently, the improper integrals resulting in $N_{ij}(r,t)(i,j=1-3)$ have to be considered closely and such expressions in $L_{ij}(r,t,\alpha)(i,j=1-3)$ causing probable singular expressions in $N_{ij}(r,t)(i,j=1-3)$ have to be examined separately. Unbounded terms may rise because of the behavior of $L_{ij}(r,t,\alpha)(i,j=1-3)$ when $\alpha\to\infty$.

When $L_{ij}(r,t,\alpha)(i,j=1-3)$ are examined as $\alpha\to\infty$,

$$L_{ij\infty}(r,t,\alpha)=\lim_{\alpha\to\infty} L_{ij}(r,t,\alpha), \qquad (i,j=1-3) \qquad (3.10)$$

L_{11} , L_{22} and L_{33} are the only integrands containing unbounded terms given in Eq.(3.10) and these unbounded terms can be written in the form

$$L_{11\infty}(r,t,\alpha) = \frac{e^{-\alpha(2A-t-r)}}{\sqrt{tr}}\{-4(A-r)(A-t)\alpha^2 + [2(A-r) + 6(A-t)]\alpha - 4\},$$

$$L_{22\infty}(r,t,\alpha) = \frac{\cos^2(\alpha L)\, e^{-\alpha(2A-t-r)}}{\sqrt{tr}}\Big\{-2(A-r)(A-t)\alpha^2 + [-\kappa(A-r) - (\kappa-2)(A-t)]\alpha - \frac{1}{2}(\kappa-1)^2\Big\},$$

$$L_{33\infty}(r,t,\alpha) = \frac{\sin^2(\alpha L)\, e^{-\alpha(2A-t-r)}}{\sqrt{tr}}\Big\{-2(A-r)(A-t)\alpha^2 + [\kappa(A-r) + (\kappa+2)(A-t)]\alpha - \frac{1}{2}(\kappa+1)^2\Big\}. \qquad (3.11\mathrm{a-c})$$

By the integration of $L_{ij}(r,t,\alpha)(i,j = 1-3)$, the probable singular parts of the kernels $N_{ij}(r,t)(i,j = 1-3)$,

$$N_{iis}(r,t) = \int_0^\infty L_{ii\infty}(r,t,\alpha)d\alpha, \qquad (i = 1-3) \qquad (3.12)$$

may calculated to be

$$N_{11s}(r,t) = \frac{1}{\sqrt{tr}}\left[-4(A-r)^2\frac{\partial^2}{\partial r^2} + 12(A-r)\frac{\partial}{\partial r} - 2\right]\frac{1}{t+r-2A},$$

$$N_{22s}(r,t) = \frac{1}{2\sqrt{tr}}\left\{\left[-2(A-r)^2\frac{\partial^2}{\partial r^2} + 6(A-r)\frac{\partial}{\partial r} + \frac{1}{2}(\kappa^2-3)\right]\left[\frac{1}{t+r-2A} + \frac{1}{t-r+2A}\right] + \left[-2(A+r)^2\frac{\partial^2}{\partial r^2} - 6(A+r)\frac{\partial}{\partial r} + \frac{1}{2}(\kappa^2-3)\right]\left[\frac{1}{t-r-2A} + \frac{1}{t+r+2A}\right]\right\},$$

$$N_{33s}(r,t) = \frac{1}{2\sqrt{tr}}\left\{\left[-2(A-r)^2\frac{\partial^2}{\partial r^2} + 6(A-r)\frac{\partial}{\partial r} + \frac{1}{2}(\kappa^2-3)\right]\left[\frac{1}{t+r-2A} + \frac{1}{t-r+2A}\right] + \left[-2(A+r)^2\frac{\partial^2}{\partial r^2} - 6(A+r)\frac{\partial}{\partial r} + \frac{1}{2}(\kappa^2-3)\right]\left[\frac{1}{t-r-2A} + \frac{1}{t+r+2A}\right]\right\}. \qquad (3.13\mathrm{a}-\mathrm{c})$$

Bounded parts of kernels $N_{ij}(r,t)(i,j=1-3)$ are then calculated from

$$N_{iib}(r,t) = \int_0^\infty [L_{ii}(r,t,\alpha) - L_{ii\infty}(r,t,\alpha)]d\alpha, \qquad (i=1-3) \qquad (3.14)$$

in which the subscript b denotes the bounded parts and

$$N_{ii}(r,t) = N_{iib}(r,t) + N_{iis}(r,t), \qquad (i=1-3) \qquad (3.15)$$

it is noteworthy that $N_{ii}(r,t)(i=1-3)$ are singular if $r,t \to A$.

3.2 Characteristic Equations

The crack surface displacement derivative $m(r)$ and the stress jumps $p_1(r)$ and $p_2(r)$ through the rigid inclusions may have singularities at the ends $r=a,b$ and $r=\pm c$, respectively. Their singular behavior may be determined by examining the singular integral equations Eqs(3.5) around these end points using the complex function technique given in Muskhelishvili(1953). The singular behavior of $m(r)$, $p_1(r)$ and $p_2(r)$ can be determined by writing

$$m(r) = \begin{cases} \dfrac{m^*(r)}{[(r-a)(b-r)]^\beta}\ \text{, for internal crack} \\ \dfrac{m^*(r)}{(r-a)^\beta(A-r)^\theta}\ \text{, for edge crack} \end{cases} \qquad (0 < \mathrm{Re}(\beta,\theta) < 1)$$

$$p_1(r) = \frac{p_1{}^*(r)}{(c^2 - r^2)^\gamma}, \qquad (0 < \mathrm{Re}(\gamma) < 1)$$

$$p_2(r) = \frac{p_2{}^*(r)}{(c^2 - r^2)^\gamma}, \qquad (0 < \mathrm{Re}(\gamma) < 1) \quad (3.16\mathrm{a} - \mathrm{c})$$

where β and γ are unknown constants and $m^*(t)$, $p_1{}^*(t)$ and $p_2{}^*(t)$ are Hölder-continuous functions in the respective intervals (a, b) and $(-c, c)$.

Eqs.(3.5), together with Eqs.(3.16) may be written in the form

$$\frac{1}{\pi}\int_a^b \frac{m^*(t)}{[(t-a)(b-t)]^\beta}\left[\frac{2}{t-r} + tN_{11s}(r,t)\right]dt$$
$$= B_1(r), \qquad (a < r < b), (\text{internal crack})$$

or

$$\frac{1}{\pi}\int_a^A \frac{m^*(t)}{(t-a)^\beta (A-t)^\theta}\left[\frac{2}{t-r} + tN_{11s}(r,t)\right]dt = B_1(r), (a < r < A), (\text{edge crack})$$

$$\frac{1}{\pi}\int_{-c}^c \frac{p_1{}^*(t)}{(c^2 - t^2)^\gamma}\left[-\frac{2\kappa}{t-r} + 2|t|N_{22s}(r,t)\right]dt = B_2(r), \quad (-c < r < c)$$

$$\frac{1}{\pi}\int_{-c}^c \frac{p_2{}^*(t)}{(c^2 - t^2)^\gamma}\left[-\frac{2\kappa}{t-r} + 2|t|N_{33s}(r,t)\right]dt$$
$$= B_3(r), \qquad (-c < r < c) \quad (3.17\mathrm{a} - \mathrm{c})$$

where all other and bounded terms are collected in $B_i(r)\ (i = 1 - 3)$. Muskhelishvili's (1953) technique is applied for evaluating the integrals containing singular terms near the end points:

$$\frac{1}{\pi}\int_a^b \frac{m^*(t)}{[(t-a)(b-t)]^\beta (t-r)}dt$$
$$= \frac{m^*(a)\cot(\pi\beta)}{(b-a)^\beta (r-a)^\beta} - \frac{m^*(b)\cot(\pi\beta)}{(b-a)^\beta (b-r)^\beta} + M_1(r),$$

$$\frac{1}{\pi}\int_{-c}^{c} \frac{{p_1}^*(t)}{(c^2-t^2)^\gamma (t-r)}dt = \frac{{p_1}^*(-c)\cot(\pi\gamma)}{(2c)^\gamma (c+r)^\gamma} - \frac{{p_1}^*(c)\cot(\pi\gamma)}{(2c)^\gamma (c-r)^\gamma} + P_3(r),$$

$$\frac{1}{\pi}\int_{-c}^{c} \frac{{p_2}^*(t)}{(c^2-t^2)^\gamma (t-r)}dt$$
$$= \frac{{p_2}^*(-c)\cot(\pi\gamma)}{(2c)^\gamma (c+r)^\gamma} - \frac{{p_2}^*(c)\cot(\pi\gamma)}{(2c)^\gamma (c-r)^\gamma} + P_4(r), \qquad (3.18a-c)$$

$$\frac{1}{\pi}\int_a^A \frac{m^*(t)}{(t-a)^\beta (A-t)^\theta (t+r-2A)}dt$$
$$= -\frac{m^*(A)}{(A-a)^\beta (A-r)^\theta \sin\pi\theta} + M_2(r),$$

$$\frac{1}{\pi}\int_{-A}^{A} \frac{{p_1}^*(t)}{(A^2-t^2)^\gamma (t+r-2A)}dt = -\frac{{p_1}^*(A)}{(2A)^\gamma (A-r)^\gamma \sin\pi\gamma} + P_5(r),$$

$$\frac{1}{\pi}\int_{-A}^{A} \frac{{p_1}^*(t)}{(A^2-t^2)^\gamma (t-r+2A)}dt = -\frac{{p_1}^*(A)}{(2A)^\gamma (A-r)^\gamma \sin\pi\gamma} + P_6(r),$$

$$\frac{1}{\pi}\int_{-A}^{A} \frac{{p_1}^*(t)}{(A^2-t^2)^\gamma (t-r-2A)}dt = -\frac{{p_1}^*(A)}{(2A)^\gamma (A+r)^\gamma \sin\pi\gamma} + P_7(r),$$

$$\frac{1}{\pi}\int_{-A}^{A} \frac{{p_1}^*(t)}{(A^2-t^2)^\gamma (t+r+2A)}dt = -\frac{{p_1}^*(A)}{(2A)^\gamma (A+r)^\gamma \sin\pi\gamma} + P_8(r),$$

$$\frac{1}{\pi}\int_{-A}^{A} \frac{{p_2}^*(t)}{(A^2-t^2)^\gamma (t+r-2A)}dt = -\frac{{p_2}^*(A)}{(2A)^\gamma (A-r)^\gamma \sin\pi\gamma} + P_9(r),$$

$$\frac{1}{\pi}\int_{-A}^{A}\frac{p_2{}^*(t)}{(A^2-t^2)^\gamma(t-r+2A)}dt=\frac{p_2{}^*(A)}{(2A)^\gamma(A-r)^\gamma\sin\pi\gamma}+P_{10}(r),$$

$$\frac{1}{\pi}\int_{-A}^{A}\frac{p_2{}^*(t)}{(A^2-t^2)^\gamma(t-r-2A)}dt=-\frac{p_2{}^*(A)}{(2A)^\gamma(A+r)^\gamma\sin\pi\gamma}+P_{11}(r),$$

$$\frac{1}{\pi}\int_{-A}^{A}\frac{p_2{}^*(t)}{(A^2-t^2)^\gamma(t+r+2A)}dt$$
$$=\frac{p_2{}^*(A)}{(2A)^\gamma(A+r)^\gamma\sin\pi\gamma}+P_{12}(r), \qquad (3.19\mathrm{a}-\mathrm{i})$$

where $M_i(r)$ $(i=1,2)$ and $P_i(r)$ $(i=3-12)$ are bounded functions except at the points $r=a,b,$ $r=\pm c$ and $r=\pm A$.

The characteristic equation for β is obtained by substituting Eq.(3.18a) in Eq.(3.17a), then multiplying the resulting equation for the limiting case $r\to a$ by $(r-a)^\beta$, or for the limiting case $r\to b$ by $(b-r)^\beta$ for an internal crack $(\mathrm{a,b}<A)$:

$$\cot(\pi\beta)=0 \qquad (a,b<A) \qquad (3.20)$$

The well known result for an embedded crack tip in a homogeneous medium is 1/2 for β, Cook and Erdoğan(1972), Gupta (1973), Delale and Erdoğan (1982), Nied and Erdoğan (1983), Geçit (1987), Turgut and Geçit(1988).

The characteristic equation for γ, Eq.(3.21) is obtained by substituting Eq.(3.18b,c) in Eq.(3.17b,c), then multiplying the resulting equation for the limiting case $r\to$ c by $(c-r)^\gamma$ for an internal rigid inclusion $(c<A)$,

$$\cot(\pi\gamma)=0 \qquad (c<A) \qquad (3.21)$$

Similarly, the acceptable value for γ is equal to 1/2, Gupta(1974), Artem and Geçit (2002), Yetmez and Geçit(2005), Kaman and Geçit(2007).

When the concentric ring-shaped crack, located at the symmetry plane of $z = 0$, spread out to the outer surface of the cylinder and it becomes an edge crack. $(b = A)$. The characteristic equation for θ, Eq.(3.22), is obtained by substituting Eq.(3.19a) in Eq.(3.17a). Subsequently the resulting equation is multiplied by $(A - r)^{\theta}$ for the limiting case $r \to A$:

$$\cos(\pi\theta) = 2\theta(\theta - 2) + 1 \qquad (b = A) \qquad (3.22)$$

From the Eq.(2.23), it is clear that the value for θ is zero which is also obtained in the previous works, Williams (1952), Geçit (1984), Geçit and Turgut (1988). This shows that the stresses at the apex of a 90˚ wedge with free sides are bounded.

In case of the penny-shaped inclusions spread out to the outer surface of the cylinder, the portion of the infinite cylinder between $z = \pm L$ planes becomes a finite cylinder of length $2L$ with rigid ends. The characteristic equation for γ at the edge of rigid inclusions (when $c = A$), is obtained by substituting Eq.(3.19b-i) in Eq.(3.17b,c). Subsequently, the resulting equation is multiplied by $(A - r)^{\gamma}$ for the limiting case $r \to A$:

$$2\kappa\cos(\pi\gamma) = \kappa^2 + 1 - 4(\gamma - 1)^2 \qquad (c = A) \qquad (3.23)$$

Eq.(3.23) is in agreement with the results of previous works, Williams(1952), Gupta(1975), Geçit and Turgut (1988), which are obtained for the stress singularity at the apex of a 90^0 wedge with one side fixed and the other side free.

CHAPTER IV

SOLUTION OF INTEGRAL EQUATIONS

Solution of singular integral equations, Eqs.(3.5), subjected to the conditions given in Eqs.(3.9) is given in this chapter. The solution procedure is separated into two main parts (i) finite cylinder and (ii) infinite cylinder problems. Additionally, the solution procedure for each main part is also separated to subsections.

The singular integral equations are expressed in terms of non-dimensional variables $\emptyset$ and ψ on the internal crack and η and ε on the inclusions as a first step in the solution procedures:

$$t = \frac{b-a}{2}\emptyset + \frac{b+a}{2}, \qquad (a < t < b, -1 < \emptyset < 1)$$

$$r = \frac{b-a}{2}\psi + \frac{b+a}{2}, \qquad (a < r < b, -1 < \psi < 1) \qquad (4.1\text{a, b})$$

$$t = c\eta, \qquad (-c < t < c, -1 < \eta < 1)$$

$$r = c\varepsilon. \qquad (-c < r < c, -1 < \varepsilon < 1) \qquad (4.2\text{a, b})$$

Consequently, inserting Eqs.(4.1) and (4.2) into the system of singular integral equations, Eqs.(3.5) and Eqs.(3.9), results in

$$
\begin{aligned}
&-\frac{4\mu}{\pi}\int_{-1}^{1} m\left(\frac{b-a}{2}\emptyset+\frac{b+a}{2}\right)\left[\frac{2}{b-a}\frac{2}{\phi-\psi}\right.\\
&\qquad +2M_3\left(\frac{b-a}{2}\psi+\frac{b+a}{2},\frac{b-a}{2}\emptyset+\frac{b+a}{2}\right)\\
&\qquad +\left(\frac{b-a}{2}\emptyset+\frac{b+a}{2}\right)N_{11}\left(\frac{b-a}{2}\psi+\frac{b+a}{2},\frac{b-a}{2}\emptyset\right.\\
&\qquad \left.\left.+\frac{b+a}{2}\right)\right]\frac{b-a}{2}d\phi\\
&\qquad -\int_{-1}^{1}p_1(c\eta)\left[c\eta T_1\left(\frac{b-a}{2}\psi+\frac{b+a}{2}\ ,|c\eta|\right)\right.\\
&\qquad \left.+\frac{2}{\pi}|c\eta\,|N_{12}\left(\frac{b-a}{2}\psi+\frac{b+a}{2}\ ,c\eta\right)\right]cd\eta\\
&\qquad -\int_{-1}^{1}p_2(c\eta)|c\eta|\left[T_2\left(\frac{b-a}{2}\psi+\frac{b+a}{2}\ ,|c\eta|\right)\right.\\
&\qquad \left.+\frac{2}{\pi}N_{13}\left(\frac{b-a}{2}\psi+\frac{b+a}{2}\ ,c\eta\right)\right]cd\eta\\
&\qquad =2(\kappa+1)p_0,\quad (-1<\psi<1)
\end{aligned}
$$

$$
\begin{aligned}
&-\frac{4\mu}{\kappa}\int_{-1}^{1} m\left(\frac{b-a}{2}\emptyset+\frac{b+a}{2}\right)\left[T_3\left(c\varepsilon\,,\frac{b-a}{2}\emptyset+\frac{b+a}{2}\right)\right.\\
&\qquad \left.+\frac{2}{\pi}N_{21}\left(c\varepsilon,\frac{b-a}{2}\emptyset+\frac{b+a}{2}\right)\right]\left(\frac{b-a}{2}\emptyset+\frac{b+a}{2}\right)\frac{b-a}{2}d\phi\\
&\qquad -\frac{1}{\kappa}\int_{-1}^{1}p_1(c\eta)\left[c\eta T_4(c\varepsilon,|c\eta|)-\frac{2\kappa}{\pi}\frac{1}{c(\eta-\varepsilon)}-\frac{2\kappa}{\pi}M_4(c\varepsilon,c\eta)\right.\\
&\qquad \left.+\frac{2}{\pi}|c\eta\,|N_{22}(c\varepsilon,c\eta)\right]cd\eta\\
&\qquad -\frac{1}{\kappa}\int_{-1}^{1}p_2(c\eta)|c\eta|\left[T_5(c\varepsilon,|c\eta|)+\frac{2}{\pi}N_{23}(c\varepsilon,c\eta)\right]cd\eta\\
&\qquad =\frac{4(\kappa-3)(\kappa+1)}{(7-\kappa)\kappa}\ p_0, \qquad\qquad (-1<\varepsilon<1)
\end{aligned}
$$

$$
\begin{aligned}
-\frac{4\mu}{\kappa}\int_{-1}^{1} m\left(\frac{b-a}{2}\emptyset+\frac{b+a}{2}\right)\Bigg[&T_6\left(c\varepsilon\,,\frac{b-a}{2}\emptyset+\frac{b+a}{2}\right)\\
&+\frac{2}{\pi}N_{31}\left(c\varepsilon,\frac{b-a}{2}\emptyset+\frac{b+a}{2}\right)\Bigg]\left(\frac{b-a}{2}\emptyset+\frac{b+a}{2}\right)\frac{b-a}{2}d\phi\\
&-\frac{1}{\kappa}\int_{-1}^{1} p_1(c\eta)\left[c\eta T_7(c\varepsilon,|c\eta|)+\frac{2}{\pi}|c\eta\,|N_{22}(c\varepsilon,c\eta)\right]cd\eta\\
&-\frac{1}{\kappa}\int_{-1}^{1} p_2(c\eta)\Bigg[|c\eta|T_8(c\varepsilon,|c\eta|)-\frac{2\kappa}{\pi}\frac{1}{c(\eta-\varepsilon)}-\frac{2\kappa}{\pi}M_5(c\varepsilon,c\eta)\\
&+\frac{2}{\pi}|c\eta|N_{33}(c\varepsilon,c\eta)\Bigg]cd\eta\\
&=0\,, \qquad\qquad (-1<\varepsilon<1) \qquad\qquad (4.3\mathrm{a}-\mathrm{c})
\end{aligned}
$$

$$\int_{-1}^{1} m\left(\frac{b-a}{2}\emptyset+\frac{b+a}{2}\right)d\emptyset=0,$$

$$\int_{-1}^{1} p_1(c\eta)\eta d\eta=0,$$

$$\int_{-1}^{1} p_2(c\eta)\eta d\eta=0\,. \qquad (4.4\mathrm{a}-\mathrm{c})$$

Next, the singularities of the unknown functions along the lines of Eqs. (3.16), are imposed

$$\frac{\bar{m}(\emptyset)}{(1-\emptyset^2)^{\beta}}=\frac{4\mu}{p_0}m\left(\frac{b-a}{2}\emptyset+\frac{b+a}{2}\right), \qquad \text{(internal crack)}$$

$$\frac{\bar{p}_1(\eta)}{(1-\eta^2)^{\gamma}}=\frac{p_1(c\eta)}{p_0},$$

$$\frac{\bar{p}_2(\eta)}{(1-\eta^2)^{\gamma}}=\frac{p_2(c\eta)}{p_0}, \qquad (4.5\mathrm{a}-\mathrm{c})$$

where $\bar{m}(\emptyset)$, $\bar{p}_1(\eta)$ and $\bar{p}_2(\eta)$are Hölder-continuous functions in $(-1,1)$, Eqs. (4.3) and (4.4) are rewritten in the form

$$\frac{1}{\pi}\int_{-1}^{1}\frac{\bar{m}(\emptyset)}{(1-\emptyset^2)^{\beta}}\left[\frac{1}{\emptyset-\psi}+\bar{M}_3(\psi,\emptyset)+\bar{N}_{11}(\psi,\emptyset)\right]d\,\emptyset$$
$$+\frac{1}{\pi}\int_{-1}^{1}\frac{\bar{p}_1(\eta)}{(1-\eta^2)^{\gamma}}\left[\eta\bar{T}_1(\psi,|\eta|)+|\eta|\bar{N}_{12}(\psi,\eta)\right]d\eta$$
$$+\frac{1}{\pi}\int_{-1}^{1}\frac{\bar{p}_2(\eta)}{(1-\eta^2)^{\gamma}}|\eta|\left[\bar{T}_2(\psi,|\eta|)+\bar{N}_{13}(\psi,\eta)\right]d\eta$$
$$=-(\kappa+1),\qquad\qquad (-1<\psi<1)$$

$$\frac{1}{\pi}\int_{-1}^{1}\frac{\bar{m}(\emptyset)}{(1-\emptyset^2)^{\beta}}\left[\bar{T}_3(\varepsilon,\emptyset)+\bar{N}_{21}(\varepsilon,\emptyset)\right]d\,\emptyset$$
$$+\frac{1}{\pi}\int_{-1}^{1}\frac{\bar{p}_1(\eta)}{(1-\eta^2)^{\gamma}}\left[\eta\bar{T}_4(\varepsilon,|\eta|)+\frac{1}{\eta-\varepsilon}+\bar{M}_4(\varepsilon,\eta)+|\eta|\bar{N}_{22}(\varepsilon,\eta)\right]d\eta$$
$$+\frac{1}{\pi}\int_{-1}^{1}\frac{\bar{p}_2(\eta)}{(1-\eta^2)^{\gamma}}|\eta|\left[\bar{T}_5(\varepsilon,|\eta|)+\bar{N}_{23}(\varepsilon,\eta)\right]d\eta$$
$$=\frac{2(\kappa-3)(\kappa+1)}{(7-\kappa)\kappa},\qquad (-1<\varepsilon<1)$$

$$\frac{1}{\pi}\int_{-1}^{1}\frac{\bar{m}(\emptyset)}{(1-\emptyset^2)^{\beta}}\left[\bar{T}_6(\varepsilon,\emptyset)+\bar{N}_{31}(\varepsilon,\emptyset)\right]d\emptyset$$
$$+\frac{1}{\pi}\int_{-1}^{1}\frac{\bar{p}_1(\eta)}{(1-\eta^2)^{\gamma}}\left[\eta\bar{T}_7(\varepsilon,|\eta|)+|\eta|\bar{N}_{32}(\varepsilon,\eta)\right]d\eta$$
$$+\frac{1}{\pi}\int_{-1}^{1}\frac{\bar{p}_2(\eta)}{(1-\eta^2)^{\gamma}}\left[|\eta|\bar{T}_8(\varepsilon,|\eta|)+\frac{1}{\eta-\varepsilon}+\bar{M}_5(\varepsilon,\eta)\right.$$
$$\left.+|\eta|\bar{N}_{33}(\varepsilon,\eta)\right]d\eta=0\qquad(-1<\varepsilon<1)\qquad\qquad(4.6\mathrm{a}-\mathrm{c})$$

and

$$\int_{-1}^{1}\frac{\bar{m}(\emptyset)}{(1-\emptyset^2)^{\beta}}d\emptyset=0,\qquad\qquad\text{(internal crack)}$$

$$\int_{-1}^{1} \frac{\bar{p}_1(\eta)}{(1-\eta^2)^{\gamma}} \eta \, d\eta = 0,$$

$$\int_{-1}^{1} \frac{\bar{p}_2(\eta)}{(1-\eta^2)^{\gamma}} \eta \, d\eta = 0, \qquad (4.7\text{a} - \text{c})$$

where

$$\bar{M}_3(\psi, \emptyset) = \frac{b-a}{2} M_3 \left(\frac{b-a}{2}\psi + \frac{b+a}{2}, \frac{b-a}{2}\emptyset + \frac{b+a}{2} \right),$$

$$\bar{M}_i(\psi, \emptyset) = c M_i(c\varepsilon, c\eta), \qquad (\ i = 4,5)$$

$$\bar{N}_{11}(\psi, \emptyset) = \frac{1}{2} \left(\frac{b-a}{2} \right)^2 \left(\emptyset + \frac{b+a}{b-a} \right) N_{11} \left(\frac{b-a}{2}\psi + \frac{b+a}{2}, \frac{b-a}{2}\emptyset + \frac{b+a}{2} \right),$$

$$\bar{N}_{i1}(\varepsilon, \emptyset) = -\frac{1}{\kappa} \left(\frac{b-a}{2} \right)^2 \left(\emptyset + \frac{b+a}{b-a} \right) N_{i1} \left(c\varepsilon, \frac{b-a}{2}\emptyset + \frac{b+a}{2} \right), \qquad (\ i = 2,3)$$

$$\bar{N}_{1i}(\varepsilon, \eta) = c^2 N_{1i} \left(\frac{b-a}{2}\psi + \frac{b+a}{2}, c\eta \right), \qquad (\ i = 2,3)$$

$$\bar{N}_{ij}(\varepsilon, \eta) = -\frac{1}{\kappa} c^2 N_{ij}(c\varepsilon, c\eta), \qquad (\ i,j = 2,3)$$

$$\bar{T}_i(\psi, \eta) = \frac{\pi}{2} c^2 T_i \left(\frac{b-a}{2}\psi + \frac{b+a}{2}, c\eta \right), \qquad (\ i = 1,2)$$

$$\bar{T}_i(\varepsilon, \emptyset) = -\frac{\pi}{2\kappa} \left(\frac{b-a}{2} \right)^2 \left(\emptyset + \frac{b+a}{b-a} \right) T_i \left(c\varepsilon, \frac{b-a}{2}\emptyset + \frac{b+a}{2} \right), \qquad (\ i = 3,6)$$

$$\bar{T}_i(\varepsilon, \eta) = -\frac{\pi}{2\kappa} c^2 T_i(c\varepsilon, c\eta). \qquad (i = 4,5,7,8) \qquad (4.8\text{a} - \text{i})$$

4.1 Infinite Cylinder Problem

In this section, the solution procedure for the infinite cylinder problem is presented.

4.1.1 Infinite Cylinder Having an Internal Crack and two Inclusions

The general solution of the problem is obtained by considering an infinite cylinder of radius A containing a ring-shaped internal crack located at $z = 0$ plane and two concentric penny-shaped rigid inclusions of radius c located at $z = \pm L$. The infinite cylinder is subjected to axial tensile loads of uniform intensity p_0 on both ends at infinity (Fig. 2.1). β and γ are the powers of singularity determined from Eqs. (3.20) and (3.21):

$$\beta = 1/2,$$

$$\gamma = 1/2. \qquad (4.9\text{a, b})$$

Gauss-Lobatto integration formula, Krenk (1978), Artem and Geçit (2002), may be used to calculate the integrals appearing in Eq.(4.5) and Eq.(4.6),. Then, Eqs. (4.6) and (4.7) become

$$\sum_{i=1}^{n} C_i \bar{m}(\emptyset_i)\left[\frac{1}{\emptyset_i - \psi_j} + \bar{M}_3(\psi_j, \emptyset_i) + \bar{N}_{11}(\psi_j, \emptyset_i)\right]$$
$$+ \sum_{i=1}^{n} C_i \bar{p}_1(\eta_i)\left[\eta_i \bar{T}_1(\psi_j, |\eta_i|) + |\eta_i| \bar{N}_{12}(\psi_j, \eta_i)\right]$$
$$+ \sum_{i=1}^{n} C_i \bar{p}_2(\eta_i)\left[|\eta_i| \bar{T}_2(\psi_j, |\eta_i|) + |\eta_i| \bar{N}_{13}(\psi_j, \eta_i)\right]$$
$$= -(\kappa + 1), \qquad (j = 1, \ldots\ldots n-1)$$

$$\sum_{i=1}^{n} C_i \bar{m}(\emptyset_i)\left[\bar{T}_3(\varepsilon_j, \emptyset_i) + \bar{N}_{21}(\varepsilon_j, \emptyset_i)\right]$$

$$+ \sum_{i=1}^{n} C_i \bar{p}_1(\eta_i)\left[\eta_i \bar{T}_4(\varepsilon_j, |\eta_i|) + \frac{1}{\eta_i - \varepsilon_j} + \bar{M}_4(\varepsilon_j, \eta_i) \right.$$

$$\left. + |\eta_i| \bar{N}_{22}(\varepsilon_j, \eta_i)\right]$$

$$+ \sum_{i=1}^{n} C_i \bar{p}_2(\eta_i)\left[|\eta_i| \bar{T}_5(\varepsilon_j, |\eta_i|) + |\eta_i| \bar{N}_{23}(\varepsilon_j, \eta_i)\right]$$

$$= \frac{2(\kappa - 3)(\kappa + 1)}{(7 - \kappa)\kappa}, \qquad (j = 1, \ldots\ldots n - 1)$$

$$\sum_{i=1}^{n} C_i \bar{m}(\emptyset_i)\left[\bar{T}_6(\varepsilon_j, \emptyset_i) + \bar{N}_{31}(\varepsilon_j, \emptyset_i)\right]$$

$$+ \sum_{i=1}^{n} C_i \bar{p}_1(\eta_i)\left[\eta_i \bar{T}_7(\varepsilon_j, |\eta_i|) + |\eta_i| \bar{N}_{32}(\varepsilon_j, \eta_i)\right]$$

$$+ \sum_{i=1}^{n} C_i \bar{p}_2(\eta_i)\left[|\eta_i| \bar{T}_8(\varepsilon_j, |\eta_i|) + \frac{1}{\eta_i - \varepsilon_j} + \bar{M}_5(\varepsilon_j, \eta_i) \right.$$

$$\left. + |\eta_i| \bar{N}_{33}(\varepsilon_j, \eta_i)\right] = 0, \qquad (j = 1, \ldots\ldots n - 1) \qquad (4.10\text{a} - \text{c})$$

$$\sum_{i=1}^{n} C_i \bar{m}(\emptyset_i) = 0,$$

$$\sum_{i=1}^{n} C_i \bar{p}_1(\eta_i)\eta_i = 0,$$

$$\sum_{i=1}^{n} C_i \bar{p}_2(\eta_i)\eta_i = 0, \qquad (4.11\text{a} - \text{c})$$

where the roots $\emptyset_i, \eta_i$ and ψ_j, ε_j are given by

$$\emptyset_i = \eta_i = \cos\left[\frac{(i-1)\pi}{n-1}\right], \qquad (i = 1, \ldots., n)$$

$$\psi_j = \varepsilon_j = \cos\left[\frac{(2j-1)\pi}{2(n-1)}\right], \qquad (j = 1, \ldots., n-1) \qquad (4.12\text{a}, \text{b})$$

C_i $(i = 1, \ldots, n)$, are the weighting constants of the Lobatto polynomials

$$C_1 = C_n = \frac{1}{2(n-1)}, \quad C_i = \frac{1}{(n-1)}. \qquad (i = 2, \ldots., n-1) \qquad (4.13)$$

Equations (4.10) and (4.11) form a system of $3n \times 3n$ linear algebraic equations. The roots and weighting constants of the Lobatto polynomials are symmetric. In addition to that, the unknown functions $\overline{m}(\emptyset)$, $\bar{p}_1(\eta)$ are odd and $\bar{p}_2(\eta)$ is even. Consequently, the $(3n-3) \times 3n$ system of algebraic equations, Eqs. (4.10), may be reduced to the following $(2n-2) \times 2n$ system

$$\begin{aligned}
\sum_{i=1}^{n} C_i \overline{m}(\emptyset_i)\left[m_6(\psi_j, \emptyset_i) + \overline{N}_{11}(\psi_j, \emptyset_i)\right] \\
+ 2\sum_{i=1}^{n/2} C_i \bar{p}_1(\eta_i)\eta_i\left[\overline{T}_1(\psi_j, \eta_i) + \overline{N}_{12}(\psi_j, \eta_i)\right] \\
+ 2\sum_{i=1}^{n/2} C_i \bar{p}_2(\eta_i)\eta_i\left[\overline{T}_2(\psi_j, \eta_i) + \overline{N}_{13}(\psi_j, \eta_i)\right] \\
= -(\kappa + 1), \qquad (j = 1, \ldots.. n-1)
\end{aligned}$$

$$\sum_{i=1}^{n} C_i \bar{m}(\emptyset_i)\left[\bar{T}_3(\varepsilon_j,\emptyset_i) + \bar{N}_{21}(\varepsilon_j,\emptyset_i)\right]$$
$$+ 2\sum_{i=1}^{n/2} C_i \bar{p}_1(\eta_i)\left[\eta_i \bar{T}_4(\varepsilon_j,\eta_i) + m_7(\varepsilon_j,\eta_i) + \eta_i \bar{N}_{22}(\varepsilon_j,\eta_i)\right]$$
$$+ 2\sum_{i=1}^{n/2} C_i \bar{p}_2(\eta_i)\eta_i\left[\bar{T}_5(\varepsilon_j,\eta_i) + \bar{N}_{23}(\varepsilon_j,\eta_i)\right]$$
$$= \frac{2(\kappa-3)(\kappa+1)}{(7-\kappa)\kappa}, \qquad (j = 1, \ldots\ldots n/2)$$

$$\sum_{i=1}^{n} C_i \bar{m}(\emptyset_i)\left[\bar{T}_6(\varepsilon_j,\emptyset_i) + \bar{N}_{31}(\varepsilon_j,\emptyset_i)\right] + 2\sum_{i=1}^{n/2} C_i \bar{p}_1(\eta_i)\eta_i\left[\bar{T}_7(\varepsilon_j,\eta_i) + \bar{N}_{32}(\varepsilon_j,\eta_i)\right]$$
$$+ 2\sum_{i=1}^{n/2} C_i \bar{p}_2(\eta_i)\left[\eta_i \bar{T}_8(\varepsilon_j,\eta_i) + m_8(\varepsilon_j,\eta_i) + \eta_i \bar{N}_{33}(\varepsilon_j,\eta_i)\right]$$
$$= 0, \qquad (j = 1, \ldots\ldots n/2 - 1) \qquad (4.14\text{a} - \text{c})$$

where

$$m_6(\psi_j,\emptyset_i)$$
$$= \begin{cases} \dfrac{2f}{f\psi_j + g} K\left(\dfrac{f\emptyset_i + g}{f\psi_j + g}\right) + \dfrac{2f(f\emptyset_i + g)}{(f\emptyset_i + g)^2 - \left(f\psi_j + g\right)^2} E\left(\dfrac{f\emptyset_i + g}{f\psi_j + g}\right) & \emptyset_i < \psi_j \\ \dfrac{2f(f\emptyset_i + g)}{(f\emptyset_i + g)^2 - \left(f\psi_j + g\right)^2} E\left(\dfrac{f\psi_j + g}{f\emptyset_i + g}\right) & \emptyset_i > \psi_j \end{cases},$$

$$m_7(\varepsilon_j,\eta_i) = \begin{cases} \dfrac{1}{\varepsilon_j} K\left(\dfrac{\eta_i}{\varepsilon_j}\right) + \dfrac{\varepsilon_j}{{\eta_i}^2 - {\varepsilon_j}^2} E\left(\dfrac{\eta_i}{\varepsilon_j}\right), & \eta_i < \varepsilon_j \\ \dfrac{\eta_i}{{\eta_i}^2 - {\varepsilon_j}^2} E\left(\dfrac{\varepsilon_j}{\eta_i}\right), & \eta_i > \varepsilon_j \end{cases},$$

$$m_8(\varepsilon_j,\eta_i) = \begin{cases} \dfrac{\eta_i}{{\eta_i}^2 - {\varepsilon_j}^2} E\left(\dfrac{\eta_i}{\varepsilon_j}\right), & \eta_i < \varepsilon_j \\ \dfrac{1}{\varepsilon_j} K\left(\dfrac{\varepsilon_j}{\eta_i}\right) + \dfrac{{\eta_i}^2}{\varepsilon_j\left({\eta_i}^2 - {\varepsilon_j}^2\right)} E\left(\dfrac{\varepsilon_j}{\eta_i}\right), & \eta_i > \varepsilon_j \end{cases}, \quad (4.15\mathrm{a-c})$$

in which

$$f = \frac{b-a}{2A},$$

$$g = \frac{b+a}{2A}. \qquad (4.16\mathrm{a,b})$$

The system in Eqs.(4.14), contains $2n-2$ equations for $2n$ unknowns, $\bar{m}(\emptyset_i)$ $(i = 1,\ldots,n)$, $\bar{p}_1(\eta_i)$, $\bar{p}_2(\eta_i)$ $(i = 1,\ldots,n/2)$. Consequently, to complete the number of equations to $2n$, the equilibrium equation, Eq.(4.11c), and the single-valuedness condition, Eqs.(4.11a) are added to the system:

$$\sum_{i=1}^{n} C_i \bar{m}(\emptyset_i) = 0,$$

$$\sum_{i=1}^{n/2} C_i \bar{p}_2(\eta_i)\eta_i = 0. \qquad (4.17\mathrm{a,b})$$

For this case, if n is chosen to be an even integer, the coefficients for $j = n/2$ that correspond to $r = 0$ in Eqs. (4.14b) must be particularly considered. In order to make this, the kernels $N_{ij}(r,t)$ $(i,j = 1-3)$ must be calculated separately for $r = 0$. Let

$$L_{ij_{\infty 0}}(t,\alpha) = \lim_{\alpha\to\infty} L_{ij}(0,t,\alpha),$$

$$N_{ij_{s0}}(t) = \int_0^\infty L_{ij_{\infty 0}}(t,\alpha)\,d\alpha,$$

$$N_{ij}(0,t) = N_{ij_{s0}}(t) + \int_0^\infty \left[L_{ij}(0,t,\alpha) - L_{ij_{\infty 0}}(t,\alpha)\right] d\alpha, \qquad (i = 2; j = 1-3)$$

$$(4.18\text{a} - \text{c})$$

where $K_{ij_{\infty 0}}(t,\alpha)$ and $N_{ij_{s0}}(t)$ $(i = 2; j = 1-3)$ are given in Appendix E and F, respectively.

Then, noting that

$$K(0) = E(0) = \frac{\pi}{2}, \tag{4.19}$$

Eqs.(4.14b) for $j = n/2$ may be replaced by

$$\begin{aligned}\sum_{i=1}^{n} C_i \overline{m}(\emptyset_i)[\overline{T}_3(0,\emptyset_i) + \overline{N}_{21}(0,\emptyset_i)] \\ + 2\sum_{i=1}^{n/2} C_i \bar{p}_1(\eta_i)\left[\eta_i \overline{T}_4(0,\eta_i) + \frac{\pi}{2\eta_i} + \eta_i \overline{N}_{22}(0,\eta_i)\right] \\ + 2\sum_{i=1}^{n/2} C_i \bar{p}_2(\eta_i)\eta_i[\overline{T}_5(0,\eta_i) + \overline{N}_{23}(0,\eta_i)] \\ = \frac{2(\kappa-3)(\kappa+1)}{(7-\kappa)\kappa}.\end{aligned} \tag{4.20}$$

Laguerre integration formula is used to numerically calculate the improper integrals for kernels, $N_{ij}(r,t)$ $(i,j = 1-3)$, Abramowitz and Stegun (1965).

4.1.2 Infinite Cylinder Having two Inclusions

In this section, an infinite axisymmetric cylinder of radius A containing two penny-shaped rigid inclusions of radius c located at $z = \pm L$ planes is considered. The infinite cylinder is subjected to axial tensile loads of uniform intensity p_0 at infinity (Fig 4.1). In this case there is no crack on the cylinder. Therefore, the unknown function $m(r)$ defined on the crack must be eliminated. Consequently, the integral equations Eqs. (4.14a), related to the conditions arise from crack, Eqs. (3.1a), will be unnecessary. The remaining integral equations, Eqs. (4.14b,c), will reduce to

$$\sum_{i=1}^{n/2} C_i \bar{p}_1(\eta_i)\left[\eta_i \bar{T}_4(\varepsilon_j,\eta_i) + m_7(\varepsilon_j,\eta_i) + \eta_i \bar{N}_{22}(\varepsilon_j,\eta_i)\right]$$
$$+ \sum_{i=1}^{n/2} C_i \bar{p}_2(\eta_i)\eta_i\left[\bar{T}_5(\varepsilon_j,\eta_i) + \bar{N}_{23}(\varepsilon_j,\eta_i)\right]$$
$$= \frac{(\kappa-3)(\kappa+1)}{(7-\kappa)\kappa}, \qquad (j = 1, \ldots\ldots n/2)$$

$$\sum_{i=1}^{n/2} C_i \bar{p}_1(\eta_i)\eta_i\left[\bar{T}_7(\varepsilon_j,\eta_i) + \bar{N}_{32}(\varepsilon_j,\eta_i)\right]$$
$$+ \sum_{i=1}^{n/2} C_i \bar{p}_2(\eta_i)\left[\eta_i \bar{T}_8(\varepsilon_j,\eta_i) + m_8(\varepsilon_j,\eta_i) + \eta_i \bar{N}_{33}(\varepsilon_j,\eta_i)\right]$$
$$= 0, \qquad (j = 1, \ldots\ldots n/2 - 1) \qquad (4.21\mathrm{a,b})$$

that must be complemented by the

$$\sum_{i=1}^{n/2} C_i \bar{p}_1(\eta_i)\left[\eta_i \bar{T}_4(0,\eta_i) + \frac{\pi}{2\eta_i} + \eta_i \bar{N}_{22}(0,\eta_i)\right]$$
$$+ \sum_{i=1}^{n/2} C_i \bar{p}_2(\eta_i)\eta_i[\bar{T}_5(0,\eta_i) + \bar{N}_{23}(0,\eta_i)] = \frac{(\kappa-3)(\kappa+1)}{(7-\kappa)\kappa}, \qquad (4.22)$$

the kernels at $r = 0$ cannot be calculated easily, for this reason the $n/2$ th equation in the system is written separately.

In this case, there are $(n-1)$ equations while the number of unknowns is n. Consequently, to complete the number of equations to n, the equilibrium equation is added to the system

$$\sum_{i=1}^{n/2} C_i \bar{p}_2(\eta_i)\eta_i = 0. \tag{4.23}$$

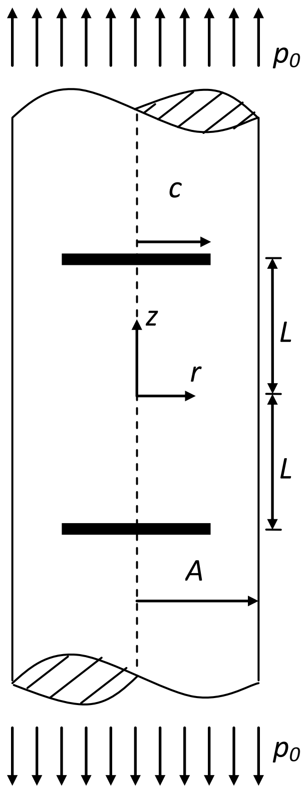

Figure 4.1 Geometry of an infinite cylinder with two penny-shaped inclusions

4.1.3 Infinite Cylinder Having an Internal Crack

An infinite circular cylinder of radius A containing a ring-shaped internal crack of width $(b-a)$ located at $z=0$ plane is considered, in this section. This cylinder is subjected to axial tensile loads of uniform intensity p_0 at infinity (Fig 4.2). In this case, there is no inclusion on the cylinder. Therefore, the unknown functions $p_1(r)$ and $p_2(r)$ defined on the inclusions must be eliminated.

Consequently, the integral equations, Eqs. (4.14b,c), and the associated boundary conditions on the rigid inclusions, Eqs. (3.1b,c), become unnecessary. For this case, the remaining integral equation, Eq. (4.14a), will reduce to

$$\sum_{i=1}^{n} C_i \overline{m}(\emptyset_i)\left[m_6(\psi_j,\emptyset_i)+\overline{N}_{11}(\psi_j,\emptyset_i)\right]=-(\kappa+1). \quad (j=1,\dots\dots n-1) \quad (4.24)$$

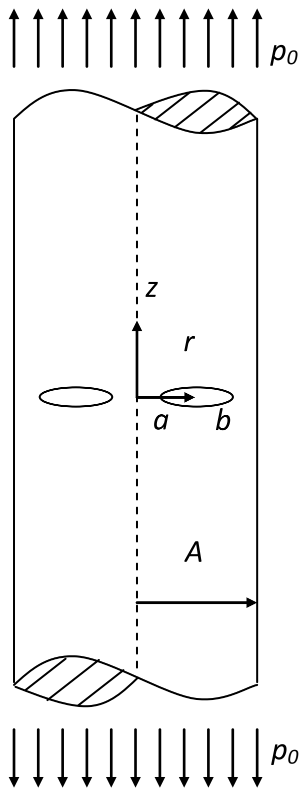

Figure 4.2 Geometry of an infinite cylinder with a ring-shaped crack.

Obviously, there are $(n-1)$ equations while the number of unknowns is n. Therefore, to complete the number of equations to n, the single-valuedness condition, Eqs.(4.25), is added to the system

$$\sum_{i=1}^{n} C_i \overline{m}(\emptyset_i)=0. \quad (4.25)$$

4.1.4 Infinite Cylinder with an Edge Crack

The infinite cylinder, shown in Fig. 4.3, of radius A containing an edge crack of width $(A-a)$ located at $z=0$ plane is considered in this section. Both ends of this cracked infinite cylinder are subjected to axial tensile loads of uniform intensity p_0. The unknown functions $p_1(r)$ and $p_2(r)$ defined on the rigid inclusions must be removed. In this case, Eq. (3.16a) must be replaced by

$$m(t) = \frac{m^*(t)}{(t-a)^{\beta}(A-t)^{\theta}}, \qquad (0 < \mathrm{Re}(\beta, \theta) < 1) \tag{4.26}$$

where β and θ are to be calculated from the characteristic equations, Eq. (3.20) and Eq. (3.22).

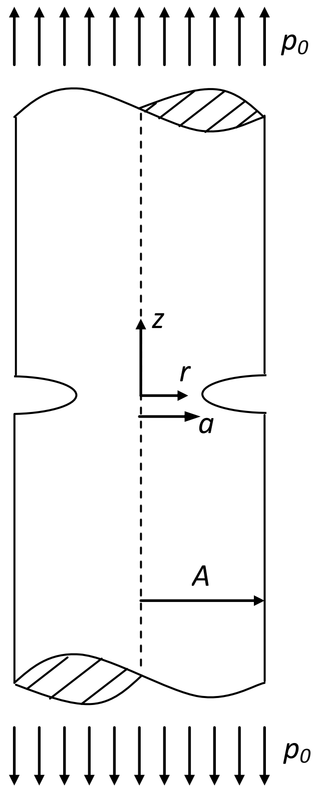

Figure 4.3 Geometry of an infinite cylinder with an edge crack.

Eqs. (4.1) defining non-dimensional variables $\emptyset$, ψ on the edge crack must be replaced by

$$t = (A-a)\emptyset + A, \qquad (a < t < A, -1 < \emptyset < 0)$$

$$r = (A-a)\psi + A, \qquad (a < r < A, -1 < \psi < 0) \qquad (4.27\text{a, b})$$

The integral equations, Eq. (4.14b,c), and the condition on the rigid inclusions, Eq. (3.1b,c), must be removed. For this case, N is chosen as an odd integer and Eqs. (4.14a) reduces to

$$\sum_{i=1}^{(N-1)/2} C_i \bar{m}(\emptyset_i)\left[m_6(\psi_j, \emptyset_i) + \bar{N}_{11}(\psi_j, \emptyset_i)\right] = -(\kappa+1), \qquad (j = 1, \ldots\ldots (N-1)/2) \qquad (4.28)$$

where

$$\frac{\bar{m}(\emptyset)}{(1-\emptyset^2)^{1/2}} = \frac{4\mu}{p_0} m\big((A-a)\emptyset + A\big). \qquad (4.29)$$

4.2 Finite Cylinder Problem

When the rigid inclusions at $z = \pm L$ spread out and their radii c approaches A, the radius of the cylinder, the portion of the infinite cylinder between $z = -L$ and $z = L$ becomes a finite cylinder with rigid ends.

4.2.1 Finite Cylinder without Crack

The finite cylinder, shown in Fig. 4.4, without crack is subjected to uniformly distributed tensile load of intensity p_0 at $z = \pm L$. In this case, Eq. (3.16b,c) must be replaced by

$$p_1(r) = \frac{p_1^*(r)}{(A^2 - r^2)^\gamma}, \qquad (0 < Re(\gamma) < 1)$$

$$p_2(r) = \frac{p_2^*(r)}{(A^2 - r^2)^\gamma}, \qquad (0 < Re(\gamma) < 1) \tag{4.30a, b}$$

where γ has to be obtained from the characteristic equation, Eq. (3.23). Also, Eqs. (3.2a,b) defining non-dimensional variables η and ε on the rigid inclusion must be replaced by

$$t = A\eta, \qquad (-A < t < A, -1 < \eta < 1)$$

$$r = A\varepsilon. \qquad (-A < r < A, -1 < \varepsilon < 1) \tag{4.31a, b}$$

Gauss-Jacobi integration formula is used to calculate the integrals containing $\bar{p}_1(\eta)$ and $\bar{p}_2(\eta)$ in Eqs.(4.6) and (4.7), Erdoğan et al. (1973), Gupta (1974), Geçit (1986), Yetmez and Geçit (2005). Consequently, Eqs. (4.14) are replaced by

$$\begin{aligned} &\frac{1}{\pi}\sum_{i=1}^{n/2} W_i \bar{p}_1(\eta_i)\left[\eta_i \bar{T}_4(\varepsilon_j,\eta_i) + m_7(\varepsilon_j,\eta_i) + \eta_i \bar{N}_{22}(\varepsilon_j,\eta_i)\right] \\ &\qquad + \frac{1}{\pi}\sum_{i=1}^{n/2} W_i \bar{p}_2(\eta_i)\eta_i\left[\bar{T}_5(\varepsilon_j,\eta_i) + \bar{N}_{23}(\varepsilon_j,\eta_i)\right] \\ &\qquad = \frac{(\kappa-3)(\kappa+1)}{(7-\kappa)\kappa}, \qquad (j = 1, \ldots\ldots n/2) \end{aligned}$$

$$\begin{aligned} &\frac{1}{\pi}\sum_{i=1}^{n/2} W_i \bar{p}_1(\eta_i)\eta_i\left[\bar{T}_7(\varepsilon_j,\eta_i) + \bar{N}_{32}(\varepsilon_j,\eta_i)\right] \\ &\qquad + \frac{1}{\pi}\sum_{i=1}^{n/2} W_i \bar{p}_2(\eta_i)\left[\eta_i \bar{T}_8(\varepsilon_j,\eta_i) + m_8(\varepsilon_j,\eta_i) + \eta_i \bar{N}_{33}(\varepsilon_j,\eta_i)\right] \\ &\qquad = 0, \qquad (j = 1, \ldots\ldots n/2 - 1) \end{aligned} \tag{4.32a, b}$$

where

$$\frac{\bar{p}_1(\eta)}{(1-\eta^2)^\gamma} = \frac{p_1(A\eta)}{p_0},$$

$$\frac{\bar{p}_2(\eta)}{(1-\eta^2)^\gamma} = \frac{p_2(A\eta)}{p_0}, \tag{4.33a, b}$$

and $C_i, \emptyset_i, \psi_j$ $(i, j = 1, \ldots, n)$ are Lobatto weights and integration points, given by Eqs. (4.12) and (4.13). On the other hand, W_i, η_i and ε_j $(i, j = 1, \ldots, n/2)$, are the weights and the roots of the Jacobi polynomials:

$$P_n^{(-\gamma,-\gamma)}(\eta_i) = 0, \qquad (i, \ldots, n)$$

$$P_{n-1}^{(1-\gamma,1-\gamma)}(\varepsilon_j) = 0, \qquad (j, \ldots, n-1)$$

$$W_i = -\frac{2(n-\gamma+1)}{(n+1)!}\frac{[\Gamma(n-\gamma+1)]^2}{\Gamma(n-2\gamma+1)}\frac{(n-2\gamma+1)^{-1}2^{-2\gamma}}{P_n^{(-\gamma,-\gamma)}(\eta_i)P_{n+1}^{(-\gamma,-\gamma)}(\eta_i)}. \qquad (i, \ldots, n)$$

$$(4.34a - c)$$

Note that calculation of kernels of Eqs. (4.32b) for $j = \mathrm{n}/2$ that correspond to $r = 0$ must be particularly considered. Then, this equation is expressed separately in the form

$$\frac{1}{\pi}\sum_{i=1}^{n/2} W_i\bar{p}_1(\eta_i)\left[\eta_i\bar{T}_4(0,\eta_i) + \frac{\pi}{2\eta_i} + \eta_i\bar{N}_{22}(0,\eta_i)\right]$$
$$+\frac{1}{\pi}\sum_{i=1}^{n/2} W_i\bar{p}_2(\eta_i)\eta_i[\bar{T}_5(0,\eta_i) + \bar{N}_{23}(0,\eta_i)] = \frac{(\kappa-3)(\kappa+1)}{(7-\kappa)\kappa}. \tag{4.35}$$

For this case, there are $(n-1)$ equations while the number of unknowns is n. Therefore, in order to increase the number of equations to n, the equilibrium equation is added to the system.

$$\frac{1}{\pi}\sum_{i=1}^{n/2} W_i\bar{p}_2(\eta_i)\eta_i = 0. \tag{4.36}$$

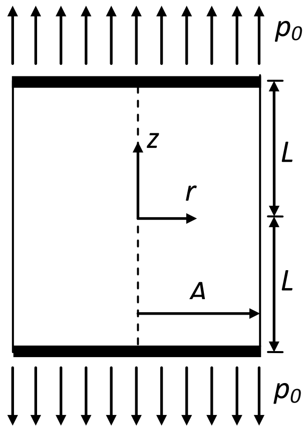

Figure 4.4 Geometry of a finite cylinder

4.2.2 Finite Cylinder Having a Crack

The finite cylinder, shown in Fig. 4.5, containing a transverse ring-shaped crack of width $(b-a)$ located at $z = 0$ plane is subjected to uniformly distributed tensile load intensity p_0 at $z = \pm L$.

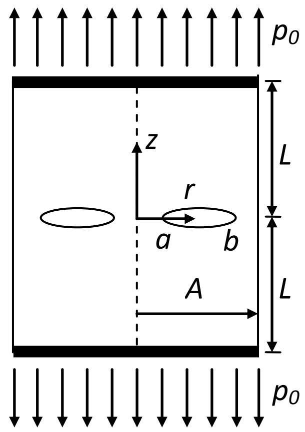

Figure 4.5 Finite cylinder having a ring-shaped crack

In this case, Eqs. (4.14) are replaced by

$$\sum_{i=1}^{n} C_i \bar{m}(\emptyset_i)\left[m_6\left(\psi_j, \emptyset_i\right) + \bar{N}_{11}\left(\psi_j, \emptyset_i\right)\right]$$
$$+\frac{2}{\pi}\sum_{i=1}^{n/2} W_i \bar{p}_1(\eta_i)\eta_i\left[\bar{T}_1\left(\psi_j, \eta_i\right) + \bar{N}_{12}\left(\psi_j, \eta_i\right)\right]$$
$$+\frac{2}{\pi}\sum_{i=1}^{n/2} W_i \bar{p}_2(\eta_i)\eta_i\left[\bar{T}_2\left(\psi_j, \eta_i\right) + \bar{N}_{13}\left(\psi_j, \eta_i\right)\right]$$
$$= -(\kappa + 1), \qquad (j = 1, \ldots\ldots n-1)$$

$$\sum_{i=1}^{n} C_i \bar{m}(\emptyset_i)\left[\bar{T}_3\left(\varepsilon_j, \emptyset_i\right) + \bar{N}_{21}\left(\varepsilon_j, \emptyset_i\right)\right]$$
$$+\frac{2}{\pi}\sum_{i=1}^{n/2} W_i \bar{p}_1(\eta_i)\left[\eta_i \bar{T}_4\left(\varepsilon_j, \eta_i\right) + m_7\left(\varepsilon_j, \eta_i\right) + \eta_i \bar{N}_{22}\left(\varepsilon_j, \eta_i\right)\right]$$
$$+\frac{2}{\pi}\sum_{i=1}^{n/2} W_i \bar{p}_2(\eta_i)\eta_i\left[\bar{T}_5\left(\varepsilon_j, \eta_i\right) + \bar{N}_{23}\left(\varepsilon_j, \eta_i\right)\right]$$
$$= \frac{2(\kappa-3)(\kappa+1)}{(7-\kappa)\kappa}, \qquad (j = 1, \ldots\ldots n/2)$$

$$\sum_{i=1}^{n} C_i \bar{m}(\emptyset_i)\left[\bar{T}_6\left(\varepsilon_j, \emptyset_i\right) + \bar{N}_{31}\left(\varepsilon_j, \emptyset_i\right)\right] + \frac{2}{\pi}\sum_{i=1}^{n/2} W_i \bar{p}_1(\eta_i)\eta_i\left[\bar{T}_7\left(\varepsilon_j, \eta_i\right) + \bar{N}_{32}\left(\varepsilon_j, \eta_i\right)\right]$$
$$+\frac{2}{\pi}\sum_{i=1}^{n/2} W_i \bar{p}_2(\eta_i)\left[\eta_i \bar{T}_8\left(\varepsilon_j, \eta_i\right) + m_8\left(\varepsilon_j, \eta_i\right) + \eta_i \bar{N}_{33}\left(\varepsilon_j, \eta_i\right)\right]$$
$$= 0. \qquad (j = 1, \ldots\ldots n/2 - 1) \qquad (4.37\text{a} - \text{c})$$

Note here that calculation of kernels of Eqs. (4.37b) for $j = n/2$ that corresponds to $r = 0$ must be considered with special attention, which may be written separately in the form

$$\sum_{i=1}^{n} C_i \bar{m}(\phi_i)[\bar{T}_3(0,\phi_i) + \bar{N}_{21}(0,\phi_i)]$$

$$+\frac{2}{\pi}\sum_{i=1}^{n/2} W_i \bar{p}_1(\eta_i)\left[\eta_i \bar{T}_4(0,\eta_i) + \frac{\pi}{2\eta_i} + \eta_i \bar{N}_{22}(0,\eta_i)\right]$$

$$+\frac{2}{\pi}\sum_{i=1}^{n/2} W_i \bar{p}_2(\eta_i)\eta_i[\bar{T}_5(0,\eta_i) + \bar{N}_{23}(0,\eta_i)]$$

$$= \frac{2(\kappa-3)(\kappa+1)}{(7-\kappa)\kappa}. \tag{4.38}$$

For this case, there are $(2n-2)$ equations while the number of unknowns is $2n$. Accordingly, to complete the number of equations to n , the single-valuedness condition and equilibrium equation are added to the system:

$$\sum_{i=1}^{n} C_i \bar{m}(\phi_i) = 0,$$

$$\frac{1}{\pi}\sum_{i=1}^{n/2} W_i \bar{p}_2(\eta_i)\eta_i = 0. \tag{4.39a, b}$$

4.2.3 Finite Cylinder Having an Edge Crack

In this case, the finite cylinder, shown in Fig. 4.5, containing a transverse edge crack of width $(A-a)$ located at $z = 0$ plane subjected to an axial tensile load of uniform intensity p_0 at $z = \pm L$ is considered. Eqs. (4.14) are replaced by

$$\sum_{i=1}^{(N-1)/2} C_i \bar{m}(\emptyset_i)\left[m_6(\psi_j,\emptyset_i)+\bar{N}_{11}(\psi_j,\emptyset_i)\right]$$

$$+\frac{2}{\pi}\sum_{i=1}^{n/2} W_i \bar{p}_1(\eta_i)\eta_i\left[\bar{T}_1(\psi_j,\eta_i)+\bar{N}_{12}(\psi_j,\eta_i)\right]$$

$$+\frac{2}{\pi}\sum_{i=1}^{n/2} W_i \bar{p}_2(\eta_i)\eta_i\left[\bar{T}_2(\psi_j,\eta_i)+\bar{N}_{13}(\psi_j,\eta_i)\right]$$

$$=-(\kappa+1), \qquad (j=1,\ldots\ldots(N-1)/2)$$

$$\sum_{i=1}^{(N-1)/2} C_i \bar{m}(\emptyset_i)\left[\bar{T}_3(\varepsilon_j,\emptyset_i)+\bar{N}_{21}(\varepsilon_j,\emptyset_i)\right]$$

$$+\frac{2}{\pi}\sum_{i=1}^{n/2} W_i \bar{p}_1(\eta_i)\left[\eta_i\bar{T}_4(\varepsilon_j,\eta_i)+m_7(\varepsilon_j,\eta_i)+\eta_i\bar{N}_{22}(\varepsilon_j,\eta_i)\right]$$

$$+\frac{2}{\pi}\sum_{i=1}^{n/2} W_i \bar{p}_2(\eta_i)\eta_i\left[\bar{T}_5(\varepsilon_j,\eta_i)+\bar{N}_{23}(\varepsilon_j,\eta_i)\right]$$

$$=\frac{2(\kappa-3)(\kappa+1)}{(7-\kappa)\kappa}, \qquad (j=1,\ldots\ldots n/2)$$

$$\sum_{i=1}^{(N-1)/2} C_i \bar{m}(\emptyset_i)\left[\bar{T}_6(\varepsilon_j,\emptyset_i)+\bar{N}_{31}(\varepsilon_j,\emptyset_i)\right]$$

$$+\frac{2}{\pi}\sum_{i=1}^{n/2} W_i \bar{p}_1(\eta_i)\eta_i\left[\bar{T}_7(\varepsilon_j,\eta_i)+\bar{N}_{32}(\varepsilon_j,\eta_i)\right]$$

$$+\frac{2}{\pi}\sum_{i=1}^{n/2} W_i \bar{p}_2(\eta_i)\left[\eta_i\bar{T}_8(\varepsilon_j,\eta_i)+m_8(\varepsilon_j,\eta_i)+\eta_i\bar{N}_{33}(\varepsilon_j,\eta_i)\right]$$

$$=0, \qquad (j=1,\ldots\ldots n/2-1) \qquad (4.40\mathrm{a}-\mathrm{c})$$

which are subjected to the condition

$$\frac{1}{\pi}\sum_{i=1}^{n/2} \mathrm{W_i}\eta_i\ \bar{p}_2(\eta_i)=0. \qquad (4.41)$$

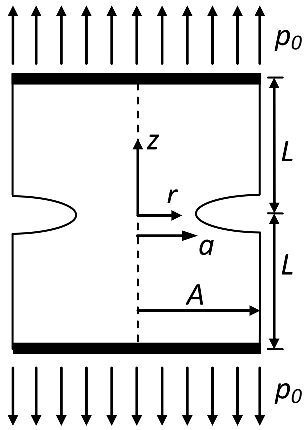

Figure 4.6 Finite cylinder having an edge crack

The equation corresponding to $j = n/2$ $(r = 0)$ in Eqs.(4.14) is again written separately as

$$\sum_{i=1}^{(N-1)/2} C_i \overline{m}(\emptyset_i)[\overline{T}_3(0,\emptyset_i) + \overline{N}_{21}(0,\emptyset_i)]$$

$$+\frac{2}{\pi}\sum_{i=1}^{\frac{n}{2}} W_i \bar{p}_1(\eta_i)\left[\eta_i \overline{T}_4(0,\eta_i) + \frac{\pi}{2\eta_i} + \eta_i \overline{N}_{22}(0,\eta_i)\right]$$

$$+\frac{2}{\pi}\sum_{i=1}^{\frac{n}{2}} W_i \bar{p}_2(\eta_i)\eta_i[\overline{T}_5(0,\eta_i) + \overline{N}_{23}(0,\eta_i)]$$

$$= \frac{2(\kappa-3)(\kappa+1)}{(7-\kappa)\kappa}. \tag{4.42}$$

CHAPTER V

STRESS INTENSITY FACTORS

Stress intensity factors form a very important basis in fracture mechanics. Stresses become infinity in the vicinity of tips or edges of cracks and inclusions. These infinite stresses are expressed in terms of stress intensity factors.

Stress intensity factors for cracks and inclusions are considered separately in the following subsections.

5.1 Stress Intensity Factors at the Edges of the Internal Crack

The stress intensity factors, used to express the stresses around the edges of an internal crack, are given in this section. Mode-I stress intensity factors, k_{1a}, k_{1b}, at the edges of the crack are defined as

$$k_{1a} = \lim_{r \to a} \sqrt{2(a-r)}\, \sigma_z(r,0),$$

$$k_{1b} = \lim_{r \to b} \sqrt{2(r-b)}\, \sigma_z(r,0), \qquad (5.1\text{a, b})$$

and $\sigma_z(r,0)$ may be expressed from Eq.(2.49d) in the form

$$\sigma_z(r,0) = \frac{4\mu}{\pi(\kappa+1)} \int_a^b \frac{m(t)}{t-r} dt + \sigma_{zb}(r,0), \qquad (5.2)$$

where the bounded part, $\sigma_{zb}(r,0)$, is such that:

$$\sigma_{zb}(r,0)=\frac{2\mu}{\pi(\kappa+1)}\int_a^b m(t)[2M_3(r,t)+tN_{11}(r,t)]dt, \tag{5.3}$$

$m(r)$ is expressed as:

$$m(r)=\frac{m^*(r)}{\sqrt{(r-a)(b-r)}}=\begin{cases}\dfrac{m^*(r)(b-r)^{-1/2}}{(r-a)^{1/2}} & , \text{ around a}\\ \dfrac{m^*(r)(r-a)^{-1/2}}{(b-r)^{1/2}} & , \text{ around b}\end{cases} \tag{5.4}$$

and the integral of the function in Eq. (5.2) is calculated by the method given in Muskhelishvili (1953):

$$\frac{1}{\pi}\int_a^b \frac{m(t)}{t-r}dt=\frac{e^{\pi i/2}}{\sin\pi/2}\frac{m^*(a)}{\sqrt{b-a}}\frac{1}{\sqrt{r-a}}-\frac{e^{-\frac{\pi i}{2}}}{\sin\frac{\pi}{2}}\frac{m^*(b)}{\sqrt{b-a}}\frac{1}{\sqrt{b-r}}+M^*(r), \tag{5.5}$$

where, $M^*(r)$ is bounded for $a<r<b$.

When Eq. (5.5) is rearranged, the following expression is obtained:

$$\frac{1}{\pi}\int_a^b \frac{m(t)}{t-r}dt=\frac{m^*(a)}{\sqrt{b-a}}\frac{1}{\sqrt{a-r}}-\frac{m^*(b)}{\sqrt{b-a}}\frac{1}{\sqrt{r-b}}+M^*(r). \tag{5.6}$$

If Eq. (5.6) is substituted in Eq. (5.2), $\sigma_z(r,0)$ becomes:

$$\sigma_z(r,0)=\frac{4\mu}{(\kappa+1)}\left[\frac{m^*(a)}{\sqrt{b-a}}\frac{1}{\sqrt{a-r}}-\frac{m^*(b)}{\sqrt{b-a}}\frac{1}{\sqrt{r-b}}+M^*(r)\right]. \tag{5.7}$$

The stress intensity factors, k_{1a}, k_{1b}, are related to $m^*(a)$ and $m^*(b)$ by substituting Eq. (5.7) in Eqs. (5.1):

$$k_{1a}=\frac{4\mu}{(\kappa+1)}\frac{m^*(a)}{\sqrt{(b-a)/2}},$$

$$k_{1b} = -\frac{4\mu}{(\kappa+1)}\frac{m^*(b)}{\sqrt{(b-a)/2}}. \qquad (5.8\text{a, b})$$

Furthermore, normalized stress intensity factors may be defined and calculated as:

$$\bar{k}_{1a} = \frac{k_{1a}}{p_0\sqrt{(b-a)/2}} = \frac{\bar{m}(-1)}{\kappa+1},$$

$$\bar{k}_{1b} = \frac{k_{1b}}{p_0\sqrt{(b-a)/2}} = -\frac{\bar{m}(1)}{\kappa+1}. \qquad (5.9\text{a, b})$$

5.2 Stress Intensity Factor for an Edge Crack

The stress intensity factor, used to state the stresses at the vicinity of an edge crack, is given in this sub-section. Mode-I stress intensity factor, k_{1a}, for the inner edge of the crack may be written as

$$k_{1a} = \lim_{r\to a}\sqrt{2}\,(a-r)^{\beta}\sigma_z(r,0), \qquad (5.10)$$

and $\sigma_z(r,0)$ may be stated from Eq.(2.49d) in the form

$$\sigma_z(r,0) = \frac{4\mu}{\pi(\kappa+1)}\int_a^A \frac{m(t)}{t-r}dt + \sigma_{zb}(r,0), \qquad (5.11)$$

where $m(r)$ is expressed as:

$$m(r) = \frac{m^*(r)}{(r-a)^{\beta}(A-r)^{\theta}} = \begin{cases} \dfrac{m^*(r)(A-r)^{\theta}}{(r-a)^{\beta}}, & \text{around a} \\ \dfrac{m^*(r)(r-a)^{-\beta}}{(A-r)^{\theta}}, & \text{around A} \end{cases} \qquad (5.12)$$

and the integral of the function in Eq. (5.11) is obtained by the technique given in Muskhelishvili (1953):

$$\frac{1}{\pi}\int_a^A \frac{m(t)}{t-r}dt = \frac{e^{\pi i/2}}{\sin\pi/2}\frac{m^*(a)}{\sqrt{r-a}} + \frac{m^*(A)}{\sqrt{A-a}}\log(r-A) + M^*(r), \tag{5.13}$$

where, $M^*(r)$ is bounded for $a < r < A$.

The stress intensity factor, k_{1a} may be related to the $m^*(a)$ by substituting Eq. (5.11) in Eqs. (5.10):

$$k_{1a} = \frac{4\sqrt{2}\mu}{(\kappa+1)}m^*(a). \tag{5.14}$$

Furthermore, normalized stress intensity factors can be defined as:

$$\bar{k}_{1a} = \frac{k_{1a}}{p_0\sqrt{2(A-a)}} = \frac{\bar{m}(1)}{\kappa+1}. \tag{5.15}$$

5.3 Stress Intensity Factors at the Edges of the Rigid Internal Inclusions

The stress intensity factors, used to express the stresses at the edges of a rigid inclusion, are given in this section. The normal (Mode I) and shear stress (Mode II) components of the stress intensity factors, k_{1c} and k_{2c} at the edges of a rigid inclusion, for the case $c < A$, may be obtained as

$$k_{1c} = \lim_{r\to c}\sqrt{2(r-c)}\sigma_z(r,L),$$

$$k_{2c} = \lim_{r\to c}\sqrt{2(r-c)}\tau_{rz}(r,L). \tag{5.16a, b}$$

From Eqs.(2.49c,d), the expressions for normal and shearing stresses may be written

$$\sigma_z(r,L) = \sigma_{zs}(r,L) + \sigma_{zb}(r,L),$$

$$\tau_{rz}(r,L) = \tau_{rzs}(r,L) + \tau_{rzb}(r,L), \tag{5.17a, b}$$

where subscripts s and b refer to the singular and the bounded parts of stresses, respectively.

Eqs. (G.1)−(G.3), given in Appendix G, may be used to express the singular parts in the form

$$\sigma_{zs}(r,L) = \frac{\kappa-1}{2\pi(\kappa+1)}\int_{-c}^{c} p_1(t)\frac{1}{t-r}dt - \frac{1}{2}p_2(r),$$

$$\tau_{rzs}(r,L) = -\frac{\kappa-1}{2\pi(\kappa+1)}\int_{-c}^{c} p_2(t)\frac{1}{t-r}dt - \frac{1}{2}p_1(r). \qquad (5.18\text{a, b})$$

$p_1(r)$ and $p_2(r)$ are expressed as:

$$p_1(r) = \frac{{p_1}^*(r)}{\sqrt{c^2-r^2}} = \begin{cases} \dfrac{{p_1}^*(r)(c+r)^{-1/2}}{(c-r)^{1/2}} &, \ r=c \\ \dfrac{{p_1}^*(r)(c-r)^{-1/2}}{(c+r)^{1/2}} &, \ r=-c \end{cases}$$

$$p_2(r) = \frac{{p_2}^*(r)}{\sqrt{c^2-r^2}} = \begin{cases} \dfrac{{p_2}^*(r)(c+r)^{-1/2}}{(c-r)^{1/2}} &, \ r=c \\ \dfrac{{p_2}^*(r)(c-r)^{-1/2}}{(c+r)^{1/2}} &, \ r=-c \end{cases} \qquad (5.19\text{a, b})$$

The stress intensity factors, k_{1c} , k_{2c}, may be related to ${p_1}^*(c)$ and ${p_2}^*(c)$ by substituting Eq. (5.18) in Eqs. (5.16.):

$$k_{1c} = \frac{\sqrt{2}}{2}\left[\frac{1-\kappa}{1+\kappa}{p_1}^*(1) - \frac{1}{\sqrt{2}}{p_2}^*(1)\right]p_0\sqrt{c},$$

$$k_{2c} = -\frac{\sqrt{2}}{2}\left[\frac{1}{\sqrt{2}}{p_1}^*(1) + \frac{1-\kappa}{1+\kappa}{p_2}^*(1)\right]p_0\sqrt{c}. \qquad (5.20\text{a, b})$$

Stress intensity factors k_{1c} and k_{2c} may be normalized as follows:

$$\bar{k}_{ic} = \frac{k_{ic}}{p_0\sqrt{c}} \qquad (i = 1,2) \tag{5.21}$$

5.4 Stress Intensity Factors at the Corners of the Finite Cylinder

Stress intensity factors, used to express the stresses at the corners of a finite cylinder, are given in this section. For the finite cylinder $(c \to A)$, the normal (Mode I) and shear stress (Mode II) components of stress intensity factors, k_{1A} and k_{2A} are defined as:

$$k_{1A} = \lim_{r \to A} \sqrt{2}(A - r)^{\gamma} \sigma_z(r, L),$$

$$k_{2A} = \lim_{r \to A} \sqrt{2}(A - r)^{\gamma} \tau_{rz}(r, L). \tag{5.22a, b}$$

One may write

$$\sigma_z(r, L) = \sigma_{zs}(r, L) + \sigma_{zb}(r, L),$$

$$\tau_{rz}(r, L) = \tau_{rzs}(r, L) + \tau_{rzb}(r, L), \tag{5.23a, b}$$

where again subscripts s and b refer to the singular and the bounded parts of stresses, respectively.

The singular parts in are the form

$$\sigma_{zs}(r, L) = \frac{\kappa - 1}{2\pi(\kappa + 1)} \int_{-A}^{A} p_1(t) \frac{1}{t - r} dt + \frac{1}{2\pi(\kappa + 1)} \int_{-A}^{A} p_1(t) t N_{52s}(r, t, L) dt - \frac{1}{2} p_2(r),$$

$$\tau_{rzs}(r,L) = -\frac{\kappa-1}{2\pi(\kappa+1)}\int_{-A}^{A} p_2(t)\frac{1}{t-r}dt$$

$$+\frac{1}{2\pi(\kappa+1)}\int_{-A}^{A} p_2(t)|t|N_{63s}(r,t,L)dt - \frac{1}{2}p_1(r). \qquad (5.24\text{a, b})$$

Eq. (5.24) can be converted into the form given in Eqs. (3.20):

$$\sigma_{zs}(r,L) = \frac{1}{2(\kappa+1)}\left\{(\kappa-1)\left[\frac{p_1{}^*(-A)\cot\pi\gamma}{(2A)^\gamma(A+r)^\gamma} - \frac{p_1{}^*(A)\cot\pi\gamma}{(2A)^\gamma(A-r)^\gamma}\right]\right.$$

$$+\left[(3\kappa+5)-2\gamma(\kappa+7)+4\gamma(\gamma+1)\right]\frac{-p_1{}^*(A)}{(2A)^\gamma\sin\pi\gamma}\frac{1}{(A-r)^\gamma}$$

$$\left.+\left[(3\kappa+5)-2\gamma(\kappa+7)+4\gamma(\gamma+1)\right]\frac{p_1{}^*(-A)}{(2A)^\gamma\sin\pi\gamma}\frac{1}{(A+r)^\gamma}\right\}$$

$$-\frac{1}{2}\frac{p_2{}^*(A)}{(A+r)^\gamma(A-r)^\gamma},$$

$$\tau_{rzs}(r,L) = \frac{1}{2(\kappa+1)}\left\{(1-\kappa)\left[\frac{p_2{}^*(-A)\cot\pi\gamma}{(2A)^\gamma(A+r)^\gamma} - \frac{p_2{}^*(A)\cot\pi\gamma}{(2A)^\gamma(A-r)^\gamma}\right]\right.$$

$$+\left[(\kappa-1)-2\gamma(\kappa-5)-4\gamma(\gamma+1)\right]\frac{p_2{}^*(A)}{(2A)^\gamma\sin\pi\gamma}\frac{1}{(A-r)^\gamma}$$

$$\left.+\left[(\kappa-1)-2\gamma(\kappa-5)-4\gamma(\gamma+1)\right]\frac{p_2{}^*(-A)}{(2A)^\gamma\sin\pi\gamma}\frac{1}{(A+r)^\gamma}\right\}$$

$$-\frac{1}{2}\frac{p_1{}^*(A)}{(A+r)^\gamma(A-r)^\gamma}. \qquad (5.25\text{a, b})$$

Stress intensity factors, k_{1A} and k_{2A} can be calculated by substituting Eq. (5.25) in Eq. (5.22):

$$k_{1A} = \frac{\sqrt{2}}{2}\left\{\frac{1}{\kappa+1}\frac{p_1{}^*(A)}{(2A)^\gamma\sin\pi\gamma}\left[(1-\kappa)(\cos\pi\gamma+1)+2(\kappa+1)(\gamma-1)\right.\right.$$

$$\left.\left.-4(\gamma-1)^2\right] - \frac{p_2{}^*(A)}{(2A)^\gamma}\right\},$$

$$k_{2A} = \frac{\sqrt{2}}{2}\left\{\frac{1}{\kappa+1}\frac{p_2{}^*(A)}{(2A)^\gamma \sin\pi\gamma}[(\kappa-1)(\cos\pi\gamma+1)+2(\kappa+1)(\gamma-1) + 4(\gamma-1)^2] - \frac{p_1{}^*(A)}{(2A)^\gamma}\right\}. \quad (5.26\text{a, b})$$

Stress intensity factors k_{1A} and k_{2A} may be normalized as follows:

$$\bar{k}_{iA} = \frac{k_{iA}}{p_0 A^\gamma} \qquad (i = 1,2). \quad (5.27)$$

Normalized stress intensity factors at the corner of the finite cylinder, $\bar{k}_{1A}$ and $\bar{k}_{2A}$, become then

$$\bar{k}_{1A} = \frac{\sqrt{2}}{2}\left\{\frac{1}{\kappa+1}\frac{\bar{p}_1(1)}{2^\gamma \sin\pi\gamma}[(1-\kappa)(\cos\pi\gamma+1)+2(\kappa+1)(\gamma-1)-4(\gamma-1)^2] - \frac{\bar{p}_2(1)}{2^\gamma}\right\},$$

$$\bar{k}_{2A} = \frac{\sqrt{2}}{2}\left\{\frac{1}{\kappa+1}\frac{\bar{p}_2(1)}{2^\gamma \sin\pi\gamma}[(\kappa-1)(\cos\pi\gamma+1)+2(\kappa+1)(\gamma-1)+4(\gamma-1)^2] - \frac{\bar{p}_1(1)}{2^\gamma}\right\}, \quad (5.28\text{a, b})$$

CHAPTER VI

RESULTS AND CONCLUSIONS

6.1 Numerical Results

The unknown functions $m(r), (a \leq r \leq b)$, $p_1(r)$ and $p_2(r)$, $(0 \leq r \leq c)$ are converted into $\bar{m}(\emptyset_i)$, $(-1 \leq \emptyset \leq 1)$ for internal crack, $(-1 \leq \emptyset \leq 0)$ for edge crack, $\bar{p}_1(\eta)$, $\bar{p}_2(\eta)$, $(-1 \leq \eta \leq 1)$. Consequently, functions $\bar{m}(\emptyset)$, $\bar{p}_1(\eta)$ and $\bar{p}_2(\eta)$ are calculated numerically at discrete collocation points to determine the stress intensity factors at the edges of the internal and edge cracks as well as the stress intensity factors at the edges of the inclusions for infinite cylinder and at the corners of the finite cylinder.

Comparative numerical results for the cylinder problems are given in the following sections, in the form of normalized stress intensity factors vs. varying geometrical properties, $(b-a)/A, (A-a)/A, c/A, L/A,$ and material property, Poisson's ratio, ν, of the cylinders, where a and b are the inner and the outer radii for the crack, c is the radius of the inclusion, L is the distance from the crack to the inclusions. In numerical analyses, the constants A, radius of the cylinder, μ, modulus of rigidity and p_0, intensity of the uniformly distributed load applied to the cylinder, are used for normalization purposes.

6.1.1 Infinite Cylinder Problem

In this section, the infinite cylinder problem, defined in Chapter 4, is considered for the cases of infinite cylinder having two inclusions and an internal crack or only two inclusions or only an internal crack or an edge crack. Results for the infinite cylinder problem are given in Figs. (6.1) to (6.20).

6.1.1.1 Infinite Cylinder Having a Crack and two Inclusions

Infinite cylinder having a crack and two inclusions is considered in this sub-section. Figures (6.1) to (6.10) present the variation of stress intensity factors vs. varying geometric and material properties.

Figures (6.1) and (6.2) show the variation of the Mode I normalized stress intensity factors, $\bar{k}_{1a}$ and $\bar{k}_{1b}$, respectively, with $(b-a)/A$ when $c = 0.5A$ and $\nu = 0.3$. Results are given for two values of L/A ratio of the infinite cylinder. From the figures, it can be observed that, $\bar{k}_{1a}$ and $\bar{k}_{1b}$ are almost insensitive to L/A and they increase as $(b-a)/A$ increases. Note that $b+a = A$ means that the center line of the ring shaped crack is at $r = A/2$.

Figure (6.3) presents the results for $\bar{k}_{1a}$ vs. c/A ratio for various values of ν when $(b-a)/A = L = 0.5A$. From the figure, it can be observed that, ν is nearly ineffective for small values of c/A. Changes in the value of ν become more effective for relatively large values of inclusion radius.

Figure (6.4), gives the results for $\bar{k}_{1b}$ vs. c/A ratio for various values of ν when $(b-a)/A = L = 0.5A$. From the figure, it can be observed that, c/A and ν have limited effect for small values of c/A as in the case of $\bar{k}_{1a}$. Furthermore, beyond a large value of c/A ratio, magnitude of $\bar{k}_{1b}$ starts varying considerably with ν and c/A.

Figures (6.5) and (6.6) show the variation of $\bar{k}_{1c}$ vs. $(b-a)/A$ for varying values of L/A and ν, respectively, when $c = 0.5$A. From Fig. (6.5), non-uniform behavior may be observed for small values of L/A, in contrary to that a uniform behavior may be observed for large values of L/A. This shows that the effect of internal crack width becomes more pronounced when inclusions get closer to the internal crack. From

Fig. (6.6), similar curves may be observed for various values of ν. Furthermore, it may be observed that increase in ν gives larger values for $\bar{k}_{1c}$. This figure also indicates that $\bar{k}_{1c}$ decreases when crack width approaches A.
Figure (6.7) shows the variation of $\bar{k}_{1c}$ vs. c/A for various values of ν when $(b-a)/A = L = 0.5A$. From the figure, it can be observed that, all curves show similar trend with a change only in the magnitude. Furthermore, it is clear that for relatively larger values of c/A, increasing values of ν increases magnitude of $\bar{k}_{1c}$. In contrary to that a reverse behavior may be observed for smaller values of c/A. This indicates that $\bar{k}_{1c}$ reaches a peak point and beyond that point it decreases for increasing values of inclusion radius.

Figures (6.8) and (6.9) show the variation of $\bar{k}_{2c}$ vs. $(b-a)/A$ for various values of L/A and ν, respectively, when $c = 0.5$A. From Fig. (6.8) it can be observed that, magnitude of $\bar{k}_{2c}$ heavily depends on $(b-a)/A$ for small values of L/A. When L/A gets larger, curves tend to be uniform. This shows that, when the distance between the crack and inclusions increase, magnitude of $\bar{k}_{2c}$ becomes just slightly dependent to crack width. From Fig. (6.9), it can be observed that, all curves follow similar trend until crack width reaches a certain value ($\sim 0.88A$). Beyond that point, the effect of ν becomes more pronounced on the variation of $\bar{k}_{2c}$.

Figure (6.10) shows the magnitude of $\bar{k}_{2c}$ vs. c/A for various values of ν when $(b-a)/A = L = 0.5A$. It can be observed that, all curves follow similar trends. Additionally, it is clear that larger values of ν result in larger magnitudes for $\bar{k}_{2c}$. This shows that, magnitude of $\bar{k}_{2c}$ heavily depends on Poisson's ratio. Also it can be told that, radius of inclusion has considerable effect on the magnitude of $\bar{k}_{2c}$.

6.1.1.2 Infinite Cylinder Having two Inclusions

An infinite cylinder having two inclusions is considered in this section. Figs. (6.11) to (6.16) show the variation of stress intensity factors vs. various geometric and material properties.

Figure (6.11) shows the variation of normalized Mode I stress intensity factor at the edge of the inclusions, $\bar{k}_{1c}$, vs. L/A ratio for various values of c/A when $\nu = 0.3$. From the figure, it can be observed that L/A ratio has only a very slight effect on $\bar{k}_{1c}$ for large values of a L/A ratio. Furthermore, for various values of c/A, all curves show similar trend except for $c/A = 0.01$ when L/A ratio is small. This shows that beyond a distance, $L \cong A$, the distance between the inclusions is not effective on the variation of $\bar{k}_{1c}$.

Figures (6.12) and (6.13) show the variation of $\bar{k}_{1c}$ vs. ν for various values of L/A and c/A, respectively. Figure (6.12) shows that the variation of $\bar{k}_{1c}$ follows a parabolic path with increasing ν for large values of L/A, in contrary to that $\bar{k}_{1c}$ increases with increasing values of ν for small value of L/A. From Fig. (6.13), it may be observed that for increasing values of ν, the variation of $\bar{k}_{1c}$ shows a parabolic tendency. When c/A ratio gets larger $\bar{k}_{1c}$ gets smaller.

Figure (6.14) shows the variation of normalized Mode II stress intensity factor at the edge of the inclusions, $\bar{k}_{2c}$, vs. L/A ratio for various values of c/A when $\nu = 0.3$. From the figure, it can be observed that L/A ratio has a very slight effect on $\bar{k}_{2c}$ for large values of L/A. For varying values of c/A, all curves show similar trend with only a difference in magnitude of $\bar{k}_{2c}$. This behavior indicates that the distance between the inclusions is not very effective on $\bar{k}_{2c}$ when L/A is greater than ~ 1.

Figures (6.15) and (6.16) show the variation of $\bar{k}_{2c}$ vs. ν for various values of L/A and c/A, respectively, when $c = 0.5A$. Figure (6.15) shows that the variation of $\bar{k}_{2c}$ follows an almost linear path with increasing ν. Furthermore, it is observed that L/A ratio has very small effect on the variation of $\bar{k}_{2c}$. From Fig. (6.16), it may be observed that for increasing values of ν, the variation of $\bar{k}_{2c}$ shows a similar trend for all curves. When the edge of the inclusion approaches surface of the cylinder, $\bar{k}_{2c}$ gets smaller.

Figure (6.17) gives comparison of numerical results for $\bar{k}_{2A}$ as a function of c/A ratio with similar results given by Kaman and Geçit (2006). From the figure, it may be observed that results obtained from present study are in very good agreement with Kaman and Geçit (2006).

6.1.1.3 Infinite Cylinder Having an Internal Crack

In this section, an infinite cylinder having an internal crack is considered. Figures (6.18) and (6.19) show the variation of stress intensity factors at the edges of the crack vs. ν for various values of internal crack width ratio $(b-a)/A$. From Figs. (6.18) and (6.19), it may be observed that, the Mode I stress intensity factors $\bar{k}_{1a}$ and $\bar{k}_{1b}$ show uniform trends with a very slight effect of ν. These factors have smaller magnitudes for smaller values of crack width ratio. When internal crack width gets larger, the magnitudes of $\bar{k}_{1a}$ and $\bar{k}_{1b}$ increase. Furthermore, Poisson's ratio is not effective on the variation of $\bar{k}_{1a}$ and $\bar{k}_{1b}$.

The results obtained from the present study are compared in Table (6.1) with those of the Nied and Erdoğan (1983). From Table (6.1), it is clear that, numerical results for Mode I stress intensity factors $\bar{k}_{1a}$ and $\bar{k}_{1b}$ are very close to those given in Nied and Erdoğan (1983).

6.1.1.4 Infinite Cylinder Having an Edge Crack

An infinite cylinder having an edge crack is considered in this section. Figures (6.20) and (6.21) show the variation of normalized Mode I stress intensity factor $\bar{k}_{1a}$ at the root of the edge crack vs. crack width ratio, $(A-a)/A$, and ν, respectively.

Figure (6.20) gives comparison of numerical results for $\bar{k}_{1a}$ as a function of $(A-a)/A$ ratio with similar results given by Nied and Erdoğan (1983). From the figure, it may be observed that results obtained from present study are in very good agreement with Nied and Erdoğan (1983).

Furthermore, from Fig. (6.21), it is observed that ν has very slight effect on the variation of $\bar{k}_{1a}$ and the magnitude of $\bar{k}_{1a}$ increases with increasing crack width ratio $(A-a)/A$ without a change in the trend of the curves.

Numerical results for Mode I stress intensity factor $\bar{k}_{1a}$ at the root of the edge crack in an infinite cylinder are compared in Table (6.2) with those given in the paper by Nied and Erdoğan (1983). Table (6.2) shows that, numerical results for Mode I stress intensity factor $\bar{k}_{1a}$ are almost identical with those given in Nied and Erdoğan (1983).

6.1.2 Finite Cylinder Problem

A finite cylinder, defined in Chapter 4, is considered in this section. The results are obtained for finite cylinder having no crack, having an internal crack and having an edge crack. Results for the finite cylinder are given in Figs. (6.22) to (6.45).

6.1.2.1 Finite Cylinder without Crack

A finite cylinder having no crack is considered in this section. Figures (6.22) and (6.23) present the variation of normalized Mode I and Mode II stress intensity factors $\bar{k}_{1A}$, $\bar{k}_{2A}$ at the corner of the cylinder vs. L/A for various values of ν.

Figures (6.22) and (6.23) show similar curves for $\bar{k}_{1A}$ and $\bar{k}_{2A}$. From both of these figures it can be observed that, L/A ratio is ineffective when it is larger than unity. In contrary to that, ν is very effective on the magnitudes of these factors. Figure (6.22) shows that increase in ν decreases the magnitude of Mode I stress intensity factor, $\bar{k}_{1A}$, however, in Fig. (6.23), increase in ν increases the magnitude of Mode II stress intensity factor, $\bar{k}_{2A}$. These indicate that Poisson's ratio is very effective on the variation of $\bar{k}_{1A}$ and $\bar{k}_{2A}$.

Figure (6.24) gives comparison of numerical results for $\bar{k}_{2A}$ as a function of ν with similar results given by Kaman and Geçit (2006) as well as Gupta (1974). From the figure, it may be observed that results obtained from present study are in very good agreement with Kaman and Geçit (2006). It seems that the results of Gupta (1974) differ from those of the present study and Kaman and Geçit (2006) a little bit.

6.1.2.2 Finite Cylinder Having an Internal Crack

Finite cylinder having an internal ring-shaped crack is considered in this section. Figs. (6.25) to (6.34) present the variation of normalized Mode I stress intensity factors, $\bar{k}_{1a}$, $\bar{k}_{1b,}$ $\bar{k}_{1A}$ and Mode II stress intensity factor $\bar{k}_{2A}$ vs. L/A for various values of ν and geometric properties.

Figures (6.25) and (6.26) show the curves of $\bar{k}_{1a}$, $\bar{k}_{1b,}$ vs. $(b-a)/A$ for various values of L/A when $\nu = 0.3$. From these figures, it can be observed that, all curves follow similar trends. When the outer edge of the crack gets close to the surface of the cylinder, $\bar{k}_{1a}$ and $\bar{k}_{1b}$ increase extensively.

Figures (6.27) and (6.28) show the variation of $\bar{k}_{1a}$, $\bar{k}_{1b,}$ vs. L/A for various values of ν when $b-a = 0.5A$. From these figures, it can be observed that, effect of ν is more pronounced for smaller values of L/A. When L/A gets larger, the effect of ν starts to vanish. This shows that the magnitudes of $\bar{k}_{1a}$ and $\bar{k}_{1b}$ are independent of Poisson's ratio when the length of the finite cylinder is large.

Figure (6.29) shows the variation of $\bar{k}_{1A}$ vs. $(b-a)/A$ for various values of L/A when $\nu = 0.3$. It can be observed from this figure that, for $L/A > 1$, $(b-a)/A$ ratio has a limited effect. However, for smaller values of L/A, the slope of the curves heavily depend on L/A ratio. This indicates that crack width is very effective on the variation of $\bar{k}_{1A}$ for shorter cylinders.

Figure (6.30) shows the variation of $\bar{k}_{1A}$ vs. $(b-a)/A$ for various values of ν when $L = A$. This figure shows that the effect of ν is more pronounced for smaller values of internal crack width with respect to larger crack widths. When crack width gets larger, the curves get closer.

Figure (6.31) shows the variation of $\bar{k}_{1A}$ vs. L/A for various values of ν when $b-a = 0.5A$. As shown in this figure, $\bar{k}_{1A}$ is larger for smaller ν. Starting with a small length, increase in L/A increases $\bar{k}_{1A}$ and then further increase in L/A decreases it.

Figures (6.32) and (6.33) present the variation of $\bar{k}_{2A}$ vs. $(b-a)/A$ for various values of L/A and ν, respectively. As shown in Figure (6.32) for $L/A > 1$, $(b-a)/A$ ratio has a very slight effect on $\bar{k}_{2A}$. However, for smaller values of L/A, $\bar{k}_{2A}$ changes considerably with $(b-a)/A$. From Fig. (6.33), it is observed that $(b-a)/A$ ratio has a very small effect on the variation of $\bar{k}_{2A}$. Furthermore, the magnitude of $\bar{k}_{2A}$ increases with increasing values of ν with a slight change on the trend of the curves. This indicates that Poisson's ratio is very effective on the variation of $\bar{k}_{2A}$.

Figure (6.34) shows the variation of $\bar{k}_{2A}$ vs. L/A for various values of ν when $b-a=0.5A$. As shown in the figure, all of the curves follow the same trend. When rigid ends inclusions get away from the internal crack, all of the curves tend to be straight. This indicates that the distance between central crack and the rigid ends of the finite cylinder becomes nearly ineffective when L/A ratio is larger than unity.

6.1.2.3 Finite Cylinder Having an Edge Crack

In this section, a finite cylinder with an edge crack is considered. Figures (6.35) to (6.45) show the variation of normalized stress intensity factors $\bar{k}_{1a}$, $\bar{k}_{1A}$ and $\bar{k}_{2A}$ vs. geometric properties $(A-a)/A$ and L/A.

Figure (6.35) shows that when ν gets smaller, magnitude of the $\bar{k}_{1a}$ gets larger for relatively small values of L/A. When, L/A increases, all curves tends to coincide. This indicates that, the effect of ν becomes negligible when the length of the cylinder increases.

It can be observed from Figs. (6.36) and (6.37) that $\bar{k}_{1a}$ does not depend on L/A or ν, much. Furthermore, it can be told that, all curves follow similar trends with increasing positive slope. This indicates that, magnitude of $\bar{k}_{1a}$ increases extensively when edge crack width gets larger. Fig. (6.38) supports the observations from Figs. (6.36) and (6.37).

Figure (6.39) shows the variation of $\bar{k}_{1a}$ vs. L/A for various values of edge crack width ratio, $(A-a)/A$ when $\nu = 0.3$. Figure shows that when edge crack width gets larger, magnitude of $\bar{k}_{1a}$ also gets larger. Furthermore, it is also observed that, this behavior is slightly dependent on the length of the finite cylinder.

Figure (6.40) presents the variation of $\bar{k}_{1A}$ vs. L/A for various values of ν when $b-a=0.5A$. It is observed from this figure that, for small values of L/A, when the rigid ends are closer to the edge crack, the smaller values of ν result in smaller magnitudes for $\bar{k}_{1A}$, in contrary to that, for larger values of L/A, when the ends are farther from the edge crack, smaller values of ν result in larger magnitudes of $\bar{k}_{1A}$. This shows that, variation of $\bar{k}_{1A}$ is heavily dependent on the length of the finite cylinder and Poisson's ratio.

Figures (6.41) and (6.42) show the variation of $\bar{k}_{1A}$ and $\bar{k}_{2A}$, respectively, vs. $(A-a)/A$ for two values of L/A when $\nu = 0.3$. It is observed from these figures that, the curves follow totally different trends. This shows that the magnitude of $\bar{k}_{1A}$ is heavily dependent on L/A ratio, also it is observed that the edge crack width ratio $(A-a)/A$ is considerably effective on the magnitude of $\bar{k}_{1A}$ when $L/A = 1$.

Figures (6.43) and (6.44) show the variation $\bar{k}_{1A}$ and $\bar{k}_{2A}$, respectively, vs. $(A-a)/A$ for various values of ν when $L = A$. It may be observed from these figures that, all curves follow the same trend. Additionally, increasing values of ν decrease the magnitude of $\bar{k}_{1A}$ and increase the magnitude of $\bar{k}_{2A}$. Furthermore, $\bar{k}_{1A}$ and $\bar{k}_{2A}$ decrease slightly, in general, with increasing crack width.

Figure (6.45) shows the variation of $\bar{k}_{2A}$ vs. L/A for various values of ν when $b-a=0.5A$. Figure shows that, large values of ν, result in large magnitudes of $\bar{k}_{2A}$. Additionally, it may be observed from the figure that, all curves nearly follow the same trend. Furthermore, it is clear that, beyond a certain value of L/A, ~ 1.5, curves become nearly straight and horizantal. This indicates that, for larger values of L/A ratio, magnitude of $\bar{k}_{2A}$ becomes nearly constant for each value of Poisson's ratio.

6.2 Conclusions

A finite cylinder with a free lateral surface is considered in this research study. The cylinder with rigid ends contains an edge crack and subjected to a tensile axial load of uniform intensity p_0 at both ends. The material of the cylinder is assumed to be linearly elastic and isotropic.

The solution for the finite cylinder problem is obtained by a procedure starting with obtaining a solution to an infinite cylinder containing a ring shaped crack and two rigid penny-shaped inclusions, subjected to tensile axial loads of uniform intensity p_0 at infinity. This infinite cylinder problem is then converted to the target problem, finite cylinder with an edge crack, considered in this research study. For this purpose, the internal ring shaped crack in the infinite cylinder is converted to an edge crack by letting the outer edge of the crack approach the lateral surface of the cylinder. Afterwards, the two rigid penny-shaped inclusions in the infinite cylinder are enlarged until reaching the lateral surface of cylinder. As a result, these rigid inclusions form the rigid ends of the cylinder and a finite cylinder having an edge crack is obtained.

The following conclusions may be deduced from the results of this research study;

1. Effect of Poisson's ratio is minor on the magnitude of the normalized Mode I stress intensity factor at the root of the edge crack, $\bar{k}_{1a}$, when the length of the finite cylinder is considerable.
2. Magnitude of the normalized Mode I stress intensity factor at the root of the edge crack, $\bar{k}_{1a}$, increases considerably when edge crack width gets larger.

3. The length of the finite cylinder, for values larger than $L = A$, has only a slight effect on the variation of normalized Mode I stress intensity factor at the root of the edge crack, $\bar{k}_{1a}$.
4. Variation of normalized Mode I stress intensity factor at the corner of the finite cylinder, $\bar{k}_{1A}$, is heavily dependent on the length of the finite cylinder as well as on the Poisson's ratio.
5. For relatively long cylinders, magnitude of the normalized Mode II stress intensity factor at the corner of the finite cylinder $\bar{k}_{2A}$ becomes nearly constant.
6. When Poisson's ratio increases, a decrease in the magnitude of normalized Mode I stress intensity factor at the corner of the finite cylinder, $\bar{k}_{1A}$, and an increase in the magnitude of normalized Mode II stress intensity factor at the corner of the finite cylinder, $\bar{k}_{2A}$ are observed.

6.3 Suggestions for Further Studies

This research study may be extended to further points by changing the material and geometrical properties as well as loading conditions of the considered problem. The following loading and geometric conditions as well as material properties may be considered in further studies;

1. The finite cylinder with edge crack may be solved subjected to torsional and shear loading as well as bending moment.
2. The finite cylinder with multiple edge or internal cracks may be solved under the action of any one of above mentioned loading to study the interaction between cracks.
3. The finite cylinder problem with inclined cracks may be solved under any loading condition.

Table 6.1 Comparative results of the present study with that of Nied & Erdoğan (1983) for internal crack when $b + a = A$ and $\nu = 0.3$.

Crack width = $(\boldsymbol{b} - \boldsymbol{a})/\boldsymbol{A}$		Present study		Nied & Erdoğan (1983)	
$\boldsymbol{a/A}$	$\boldsymbol{b/A}$	$\bar{\boldsymbol{k}}_{\boldsymbol{1a}}$	$\bar{\boldsymbol{k}}_{\boldsymbol{1b}}$	$\bar{\boldsymbol{k}}_{\boldsymbol{1a}}$	$\bar{\boldsymbol{k}}_{\boldsymbol{1b}}$
0.505	0.595	1.029	0.988	1.028	0.985

Table 6.2 Comparative results of the present study with that of Nied & Erdoğan (1983) for edge crack when $\nu = 0.3$.

Crack width	Present study	Nied & Erdoğan (1983)
$(\boldsymbol{A} - \boldsymbol{a})/\boldsymbol{A}$	$\bar{\boldsymbol{k}}_{\boldsymbol{1a}}$	$\bar{\boldsymbol{k}}_{\boldsymbol{1a}}$
0.01	1.125	1.121

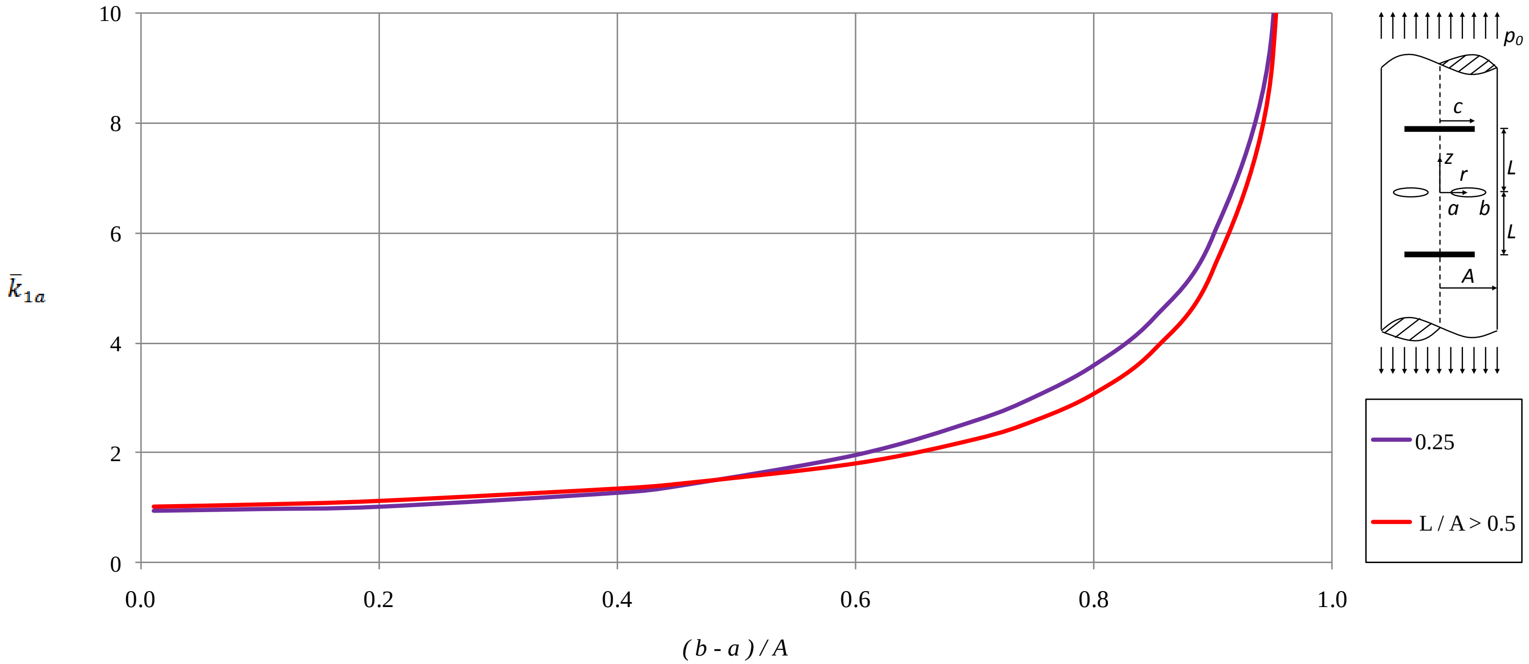

Figure 6.1 Normalized Mode I stress intensity factor $\bar{k}_{1a}$ when $c = 0.5A$, $b + a = A$ and $\nu = 0.3$.

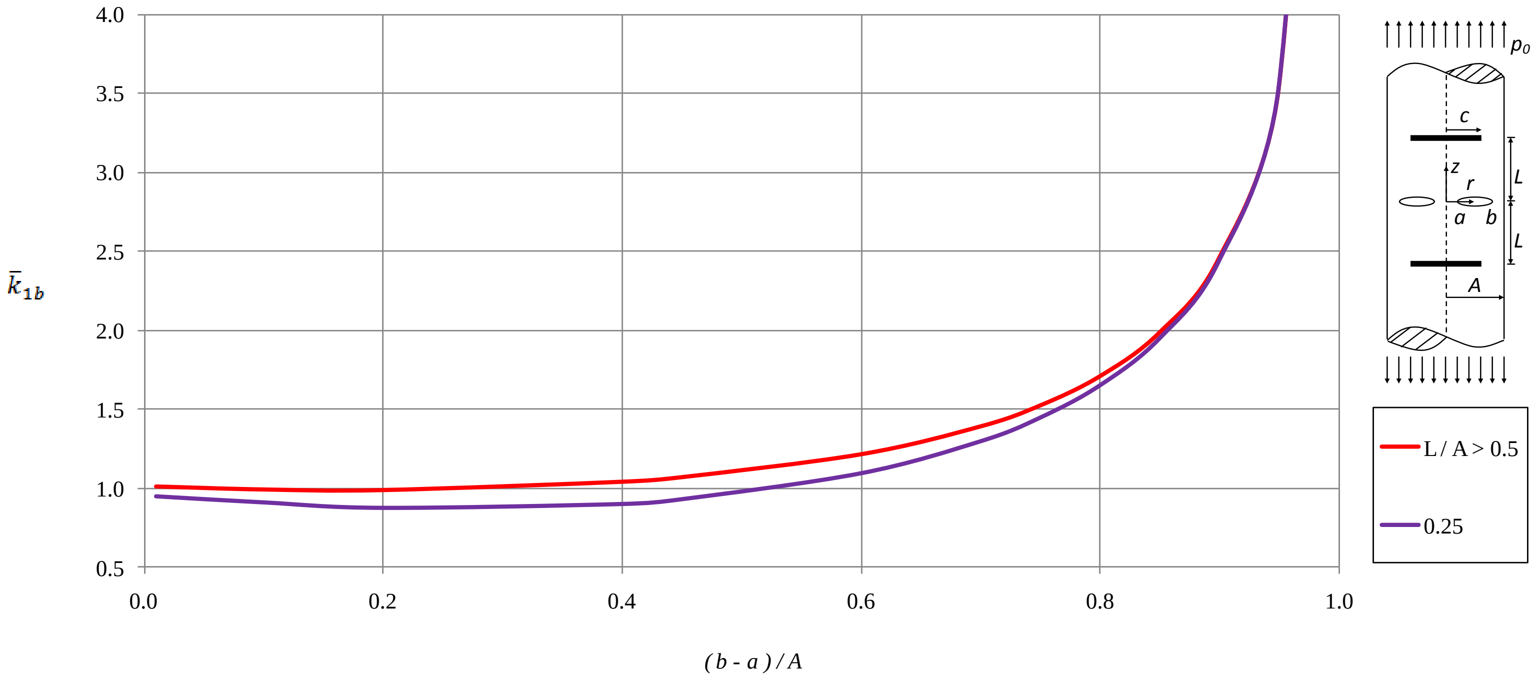

Figure 6.2 Normalized Mode I stress intensity factor $\bar{k}_{1b}$ when $c = 0.5A$, $b + a = A$ and $\nu = 0.3$.

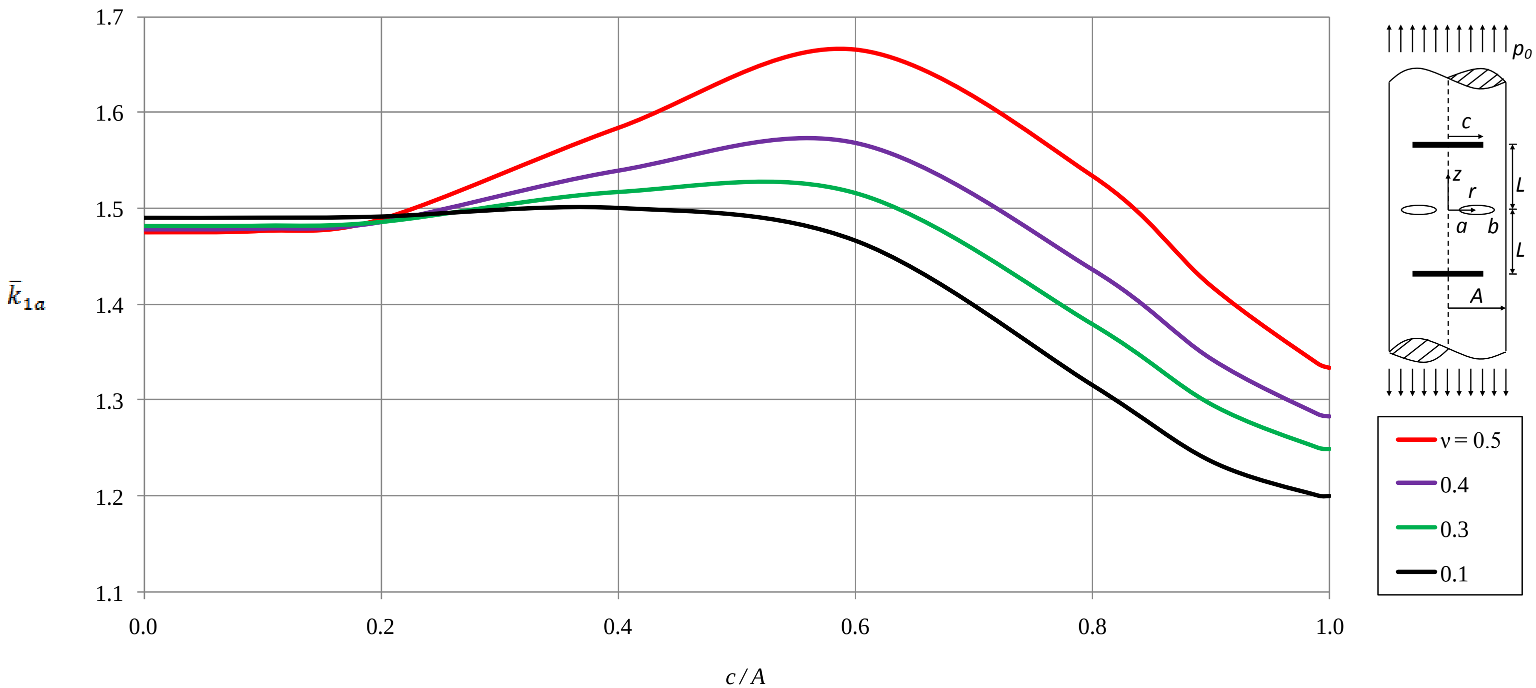

Figure 6.3 Normalized Mode I stress intensity factor $\bar{k}_{1a}$ when $b - a = L = 0.5A$ and $b + a = A$.

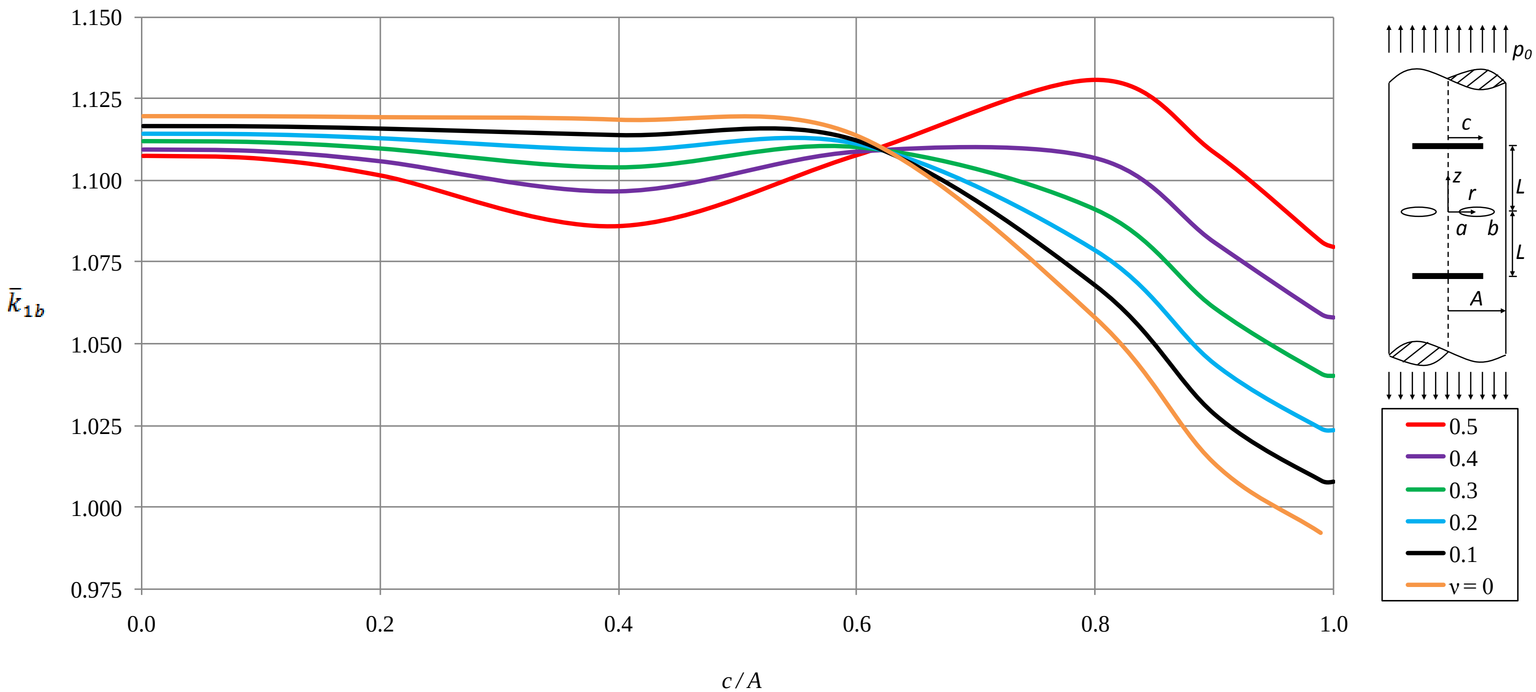

Figure 6.4 Normalized Mode I stress intensity factor $\bar{k}_{1b}$ when $b - a = L = 0.5A$ and $b + a = A$.

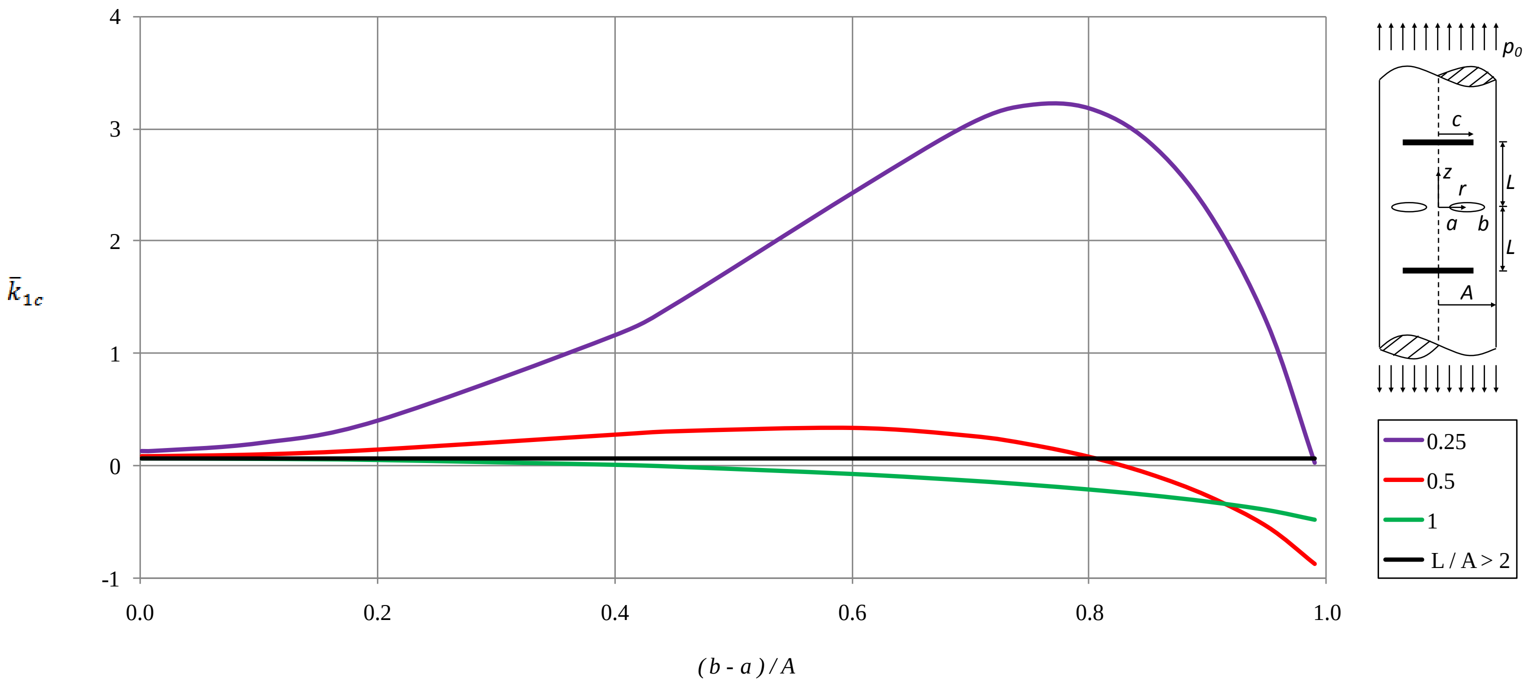

Figure 6.5 Normalized Mode I stress intensity factor $\bar{k}_{1c}$ when $c = 0.5A$, $b + a = A$ and $\nu = 0.3$.

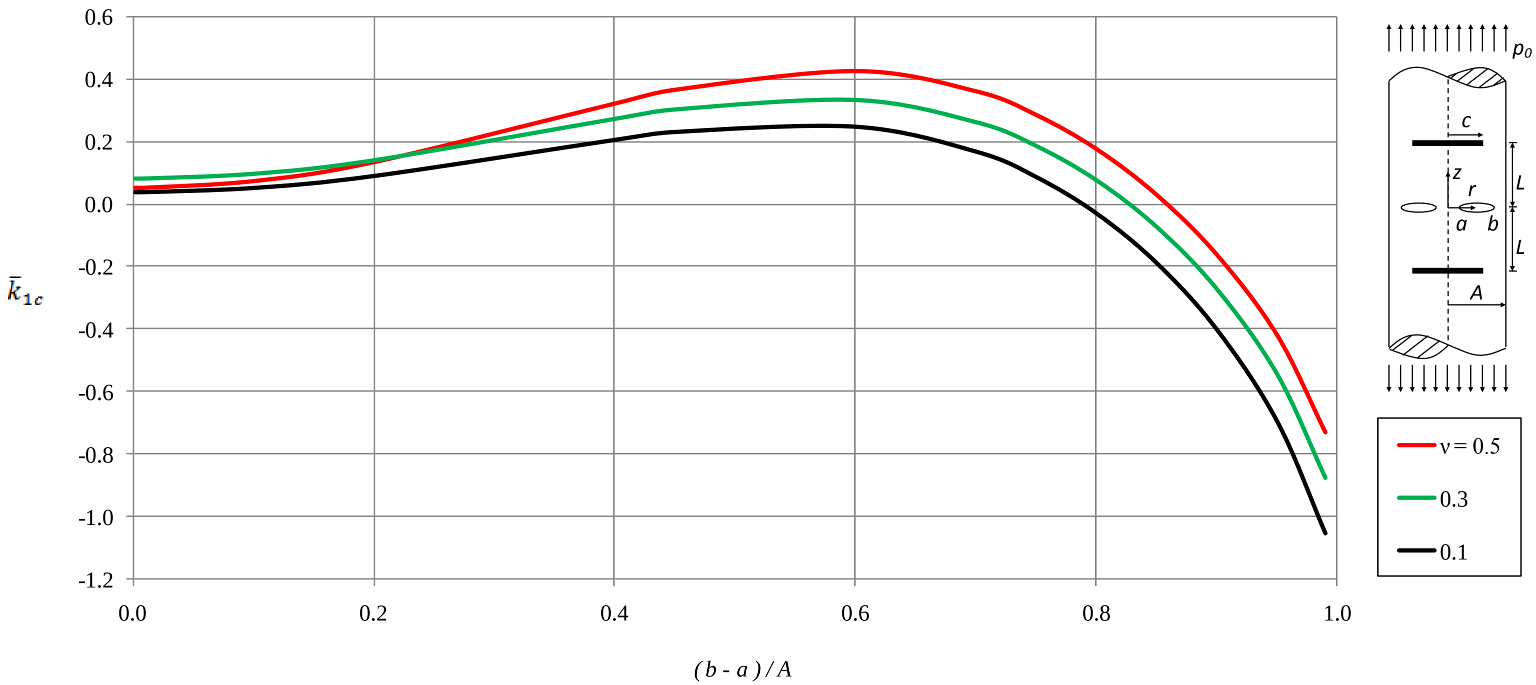

Figure 6.6 Normalized Mode I stress intensity factor $\bar{k}_{1c}$ when $c = L = 0.5A$ and $a + b = A$.

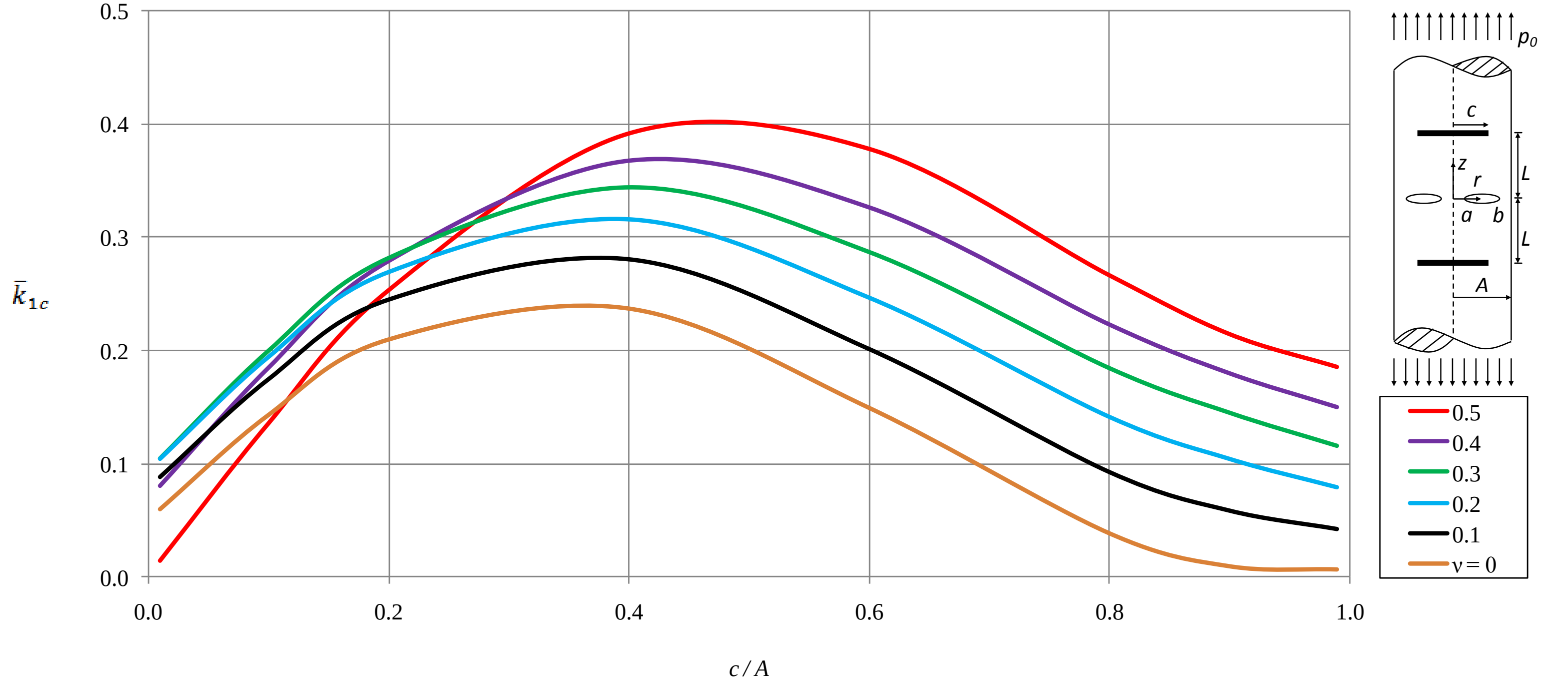

Figure 6.7 Normalized Mode I stress intensity factor $\bar{k}_{1c}$ when $b - a = L = 0.5A$ and $b + a = A$.

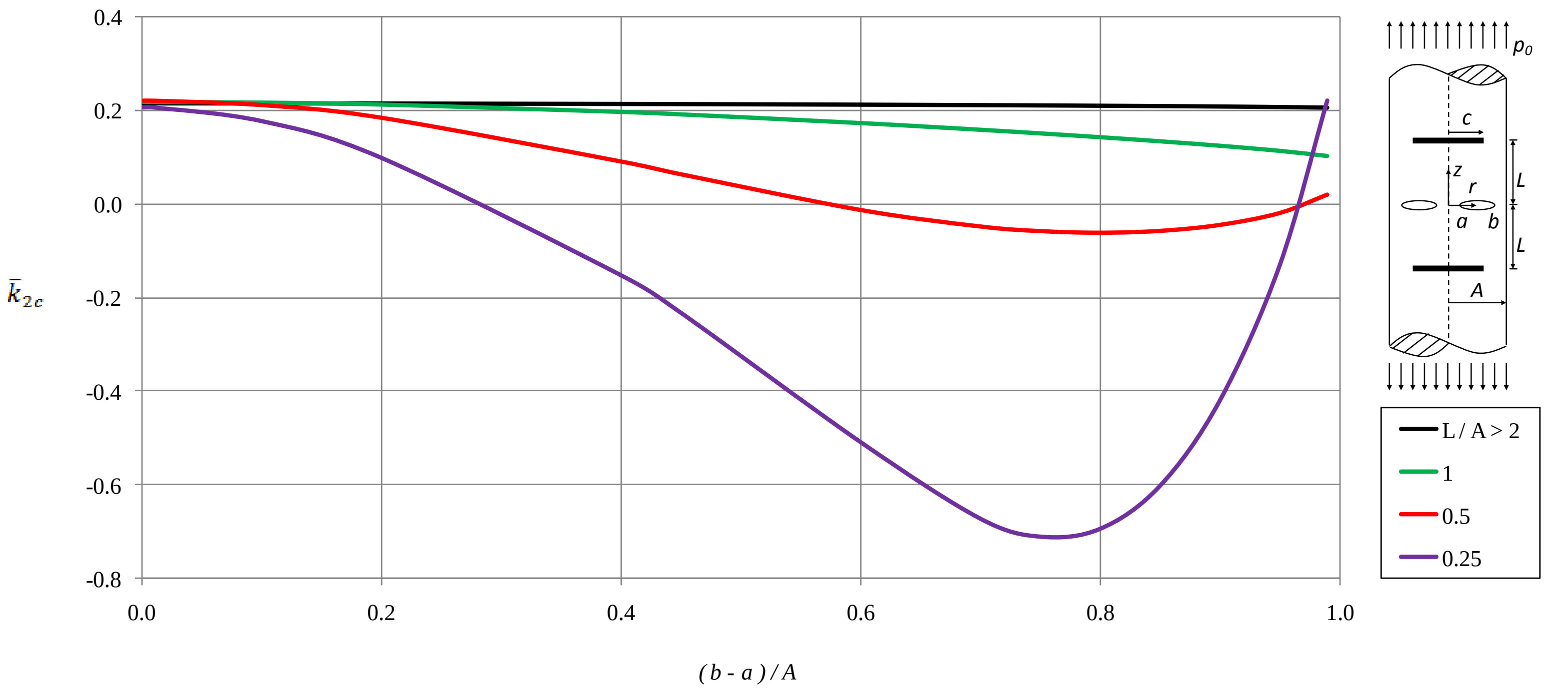

Figure 6.8 Normalized Mode II stress intensity factor $\bar{k}_{2c}$ when $c = 0.5A$, $b + a = A$ and $\nu = 0.3$.

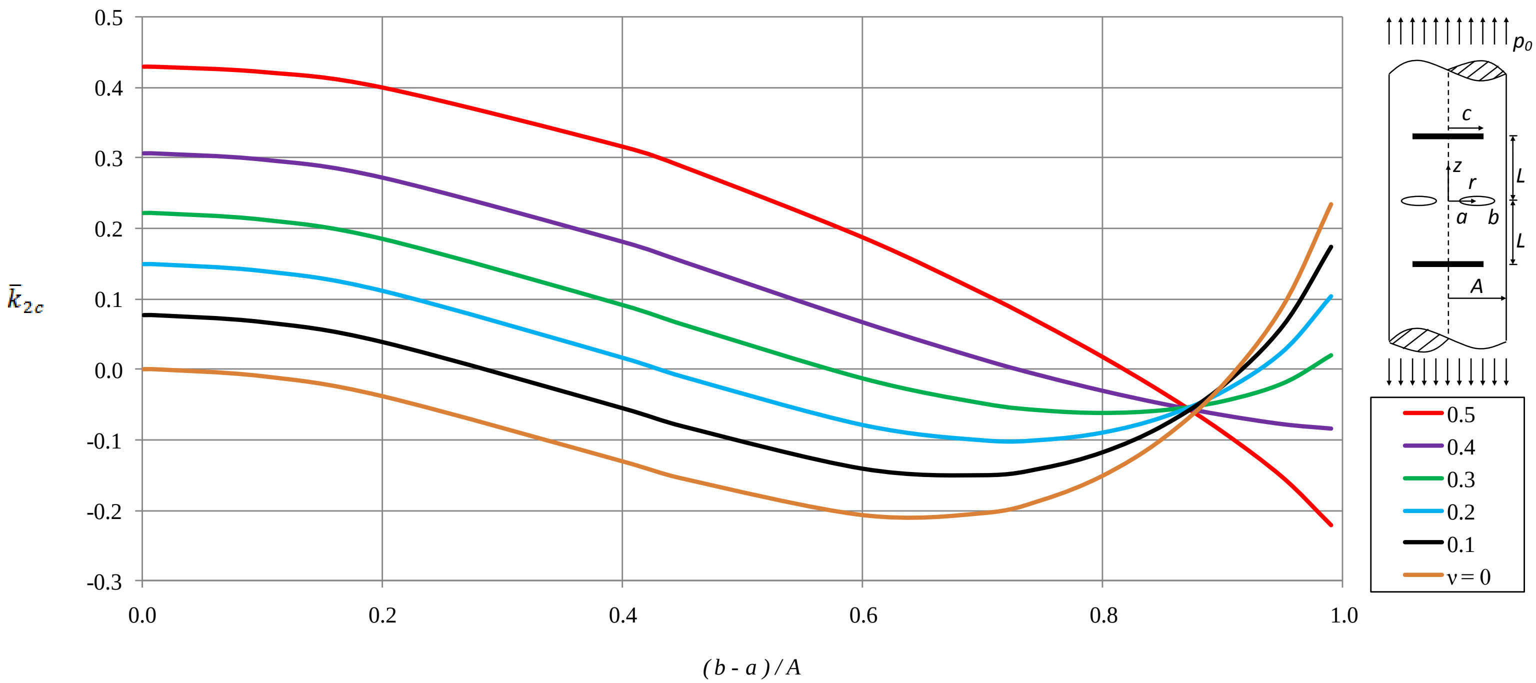

Figure 6.9 Normalized Mode II stress intensity factor $\bar{k}_{2c}$ when $c = L = 0.5A$ and $b + a = A$.

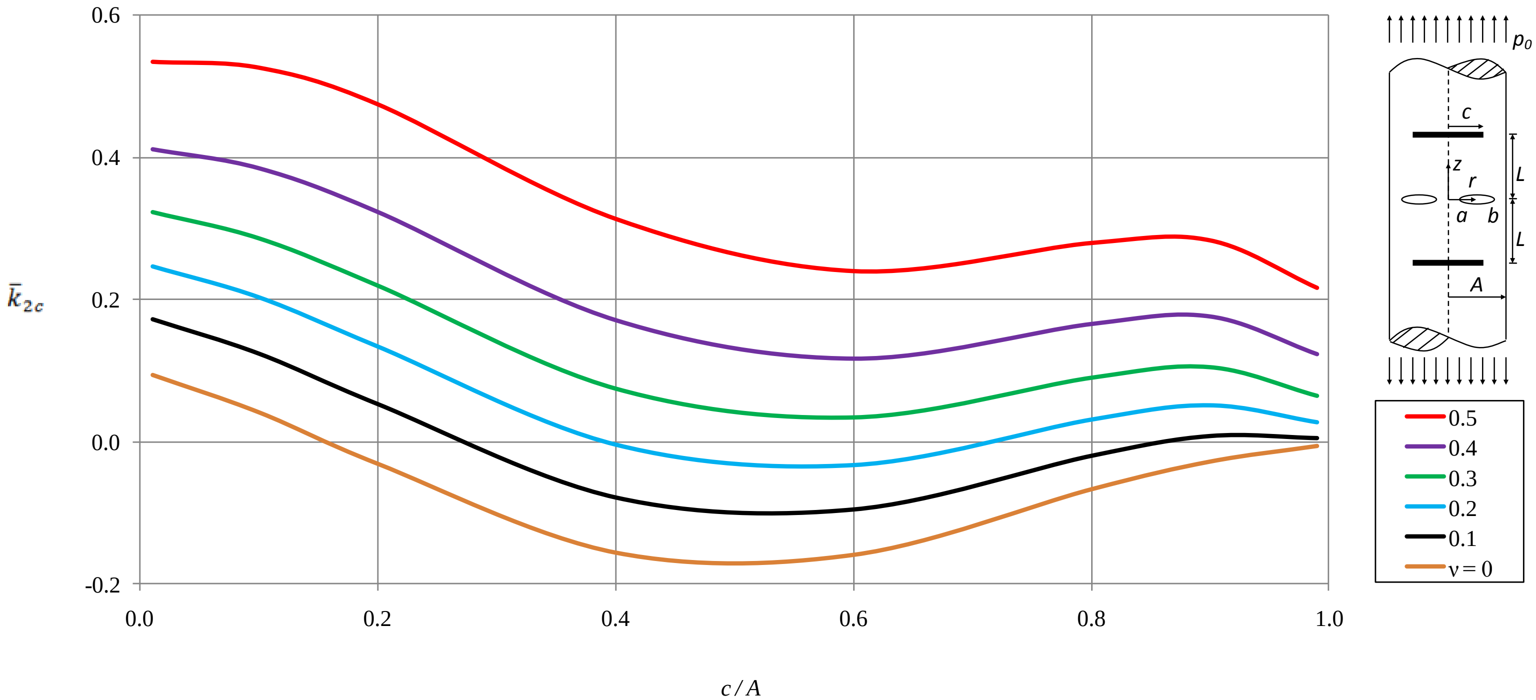

Figure 6.10 Normalized Mode II stress intensity factor $\bar{k}_{2c}$ when $b - a = L = 0.5A$ and $b + a = A$.

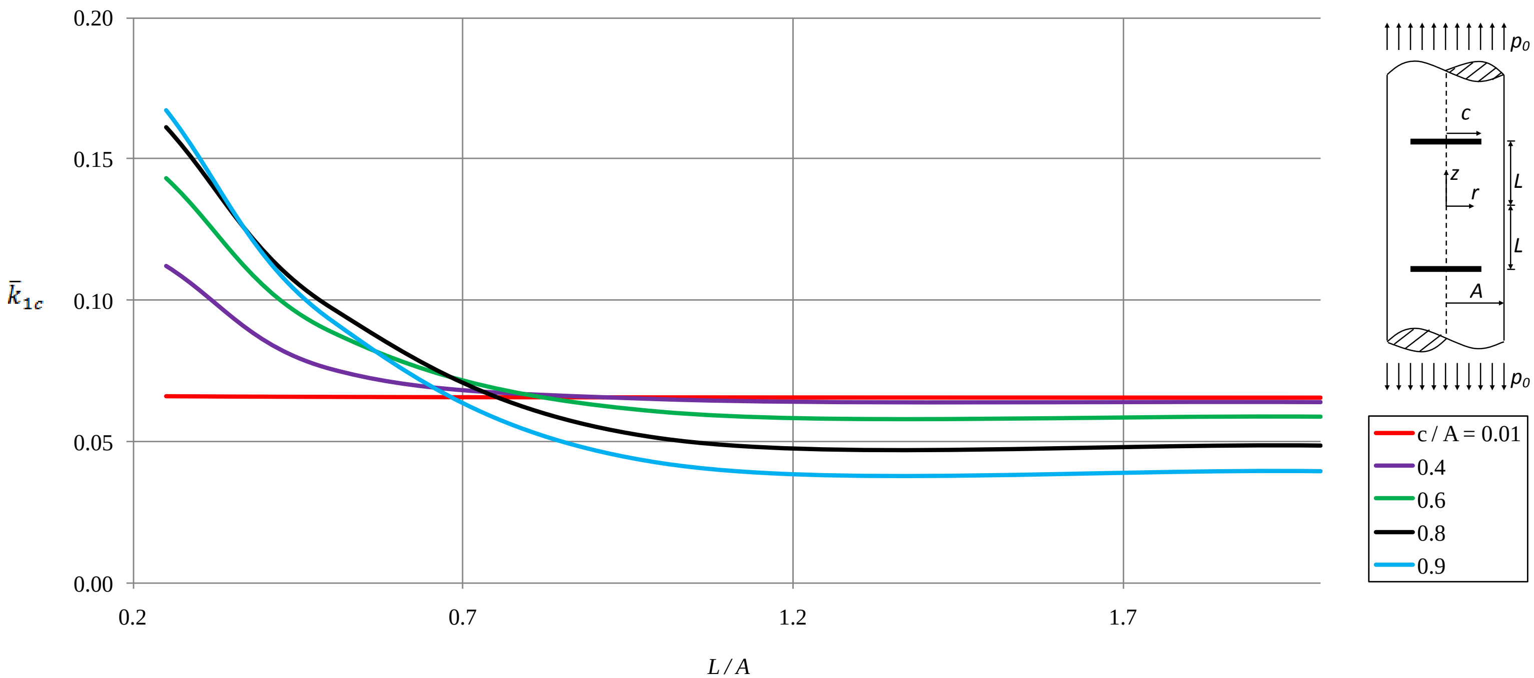

Figure 6.11 Normalized Mode I stress intensity factor $\bar{k}_{1c}$ at the inclusion edge when $\nu = 0.3$.

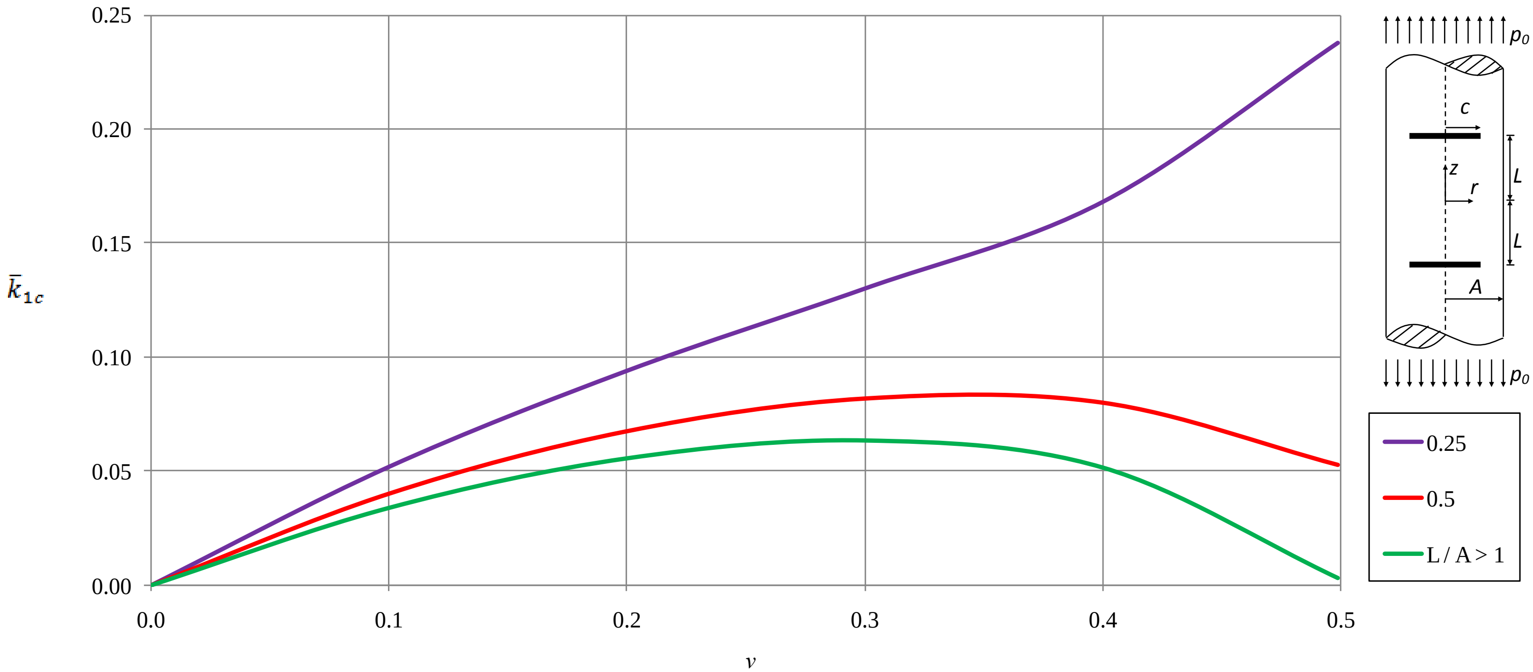

Figure 6.12 Normalized Mode I stress intensity factor $\bar{k}_{1c}$ at the inclusion edge when $c = 0.5A$.

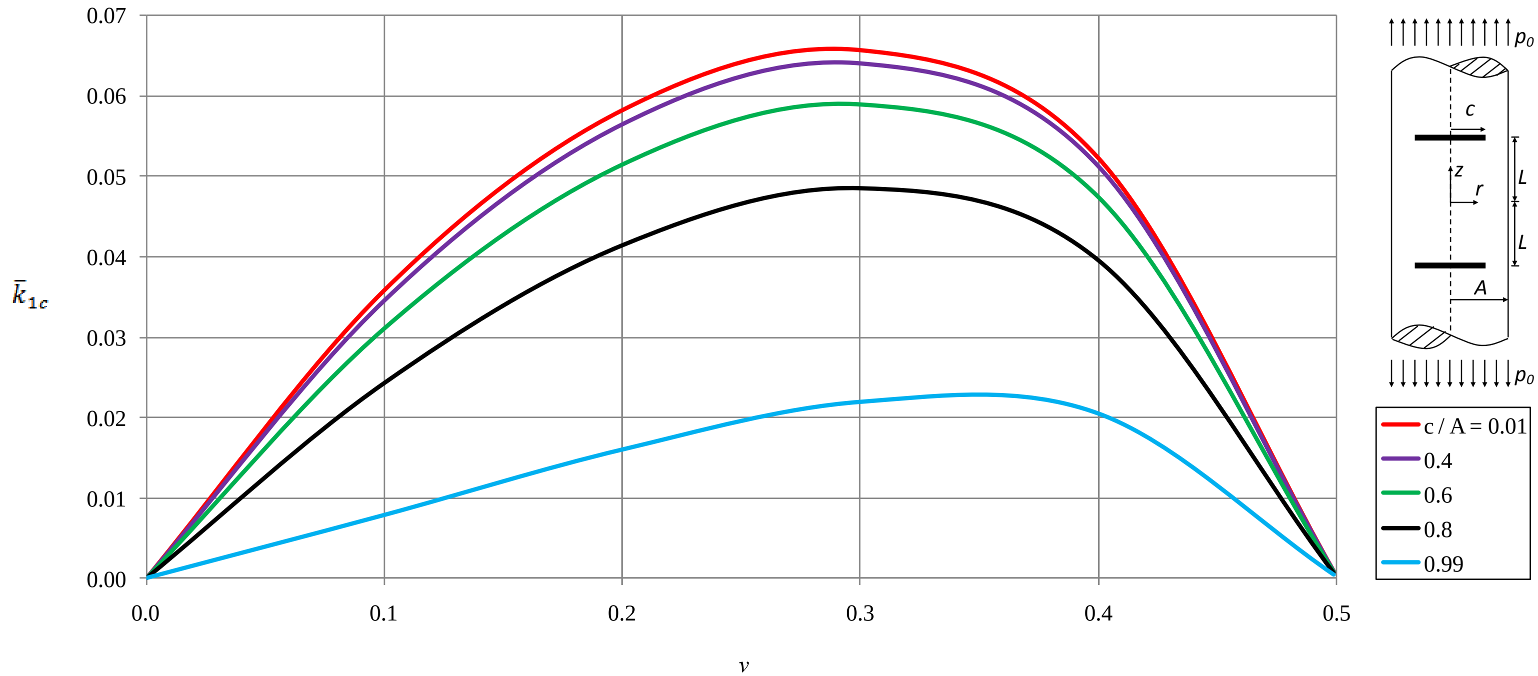

Figure 6.13 Normalized Mode I stress intensity factor $\bar{k}_{1c}$ at the inclusion edge when $L = 2A$.

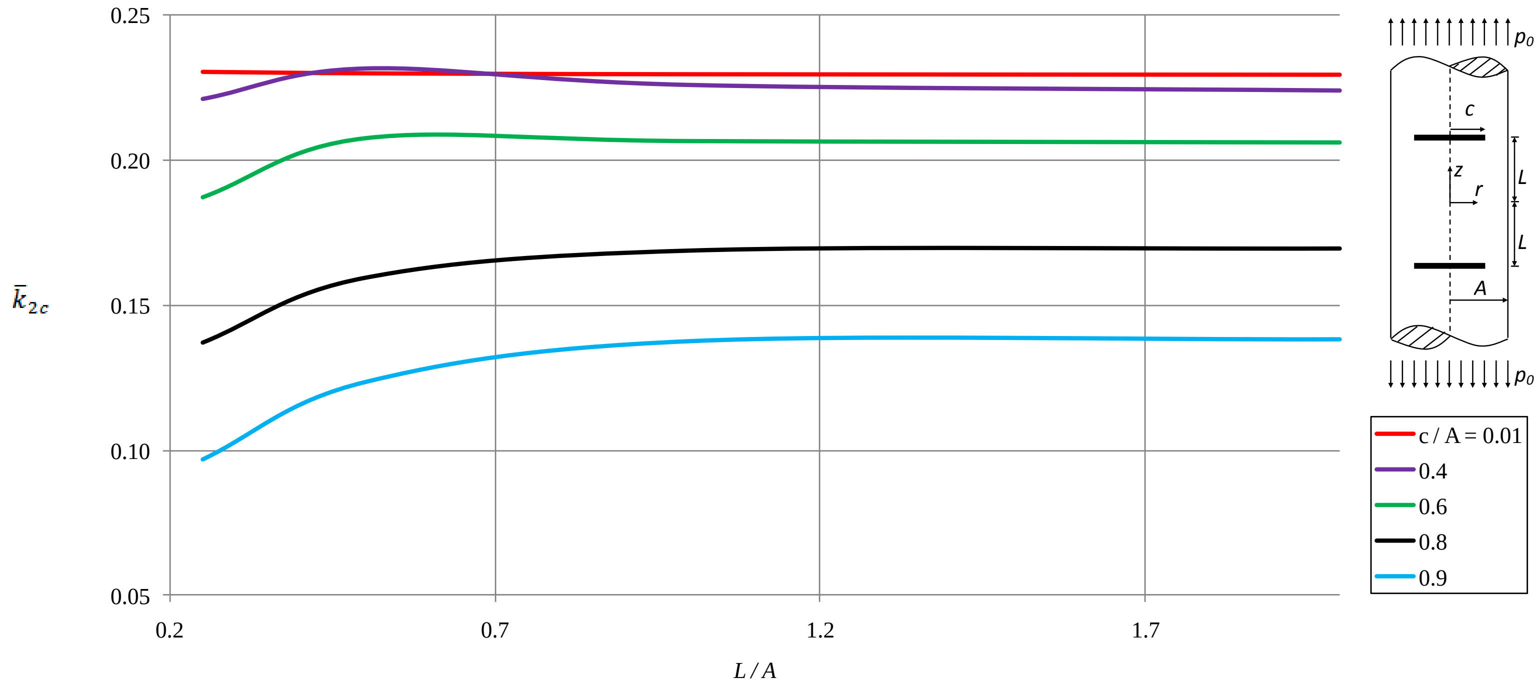

Figure 6.14 Normalized Mode II stress intensity factor $\bar{k}_{2c}$ at the inclusion edge when $\nu = 0.3$.

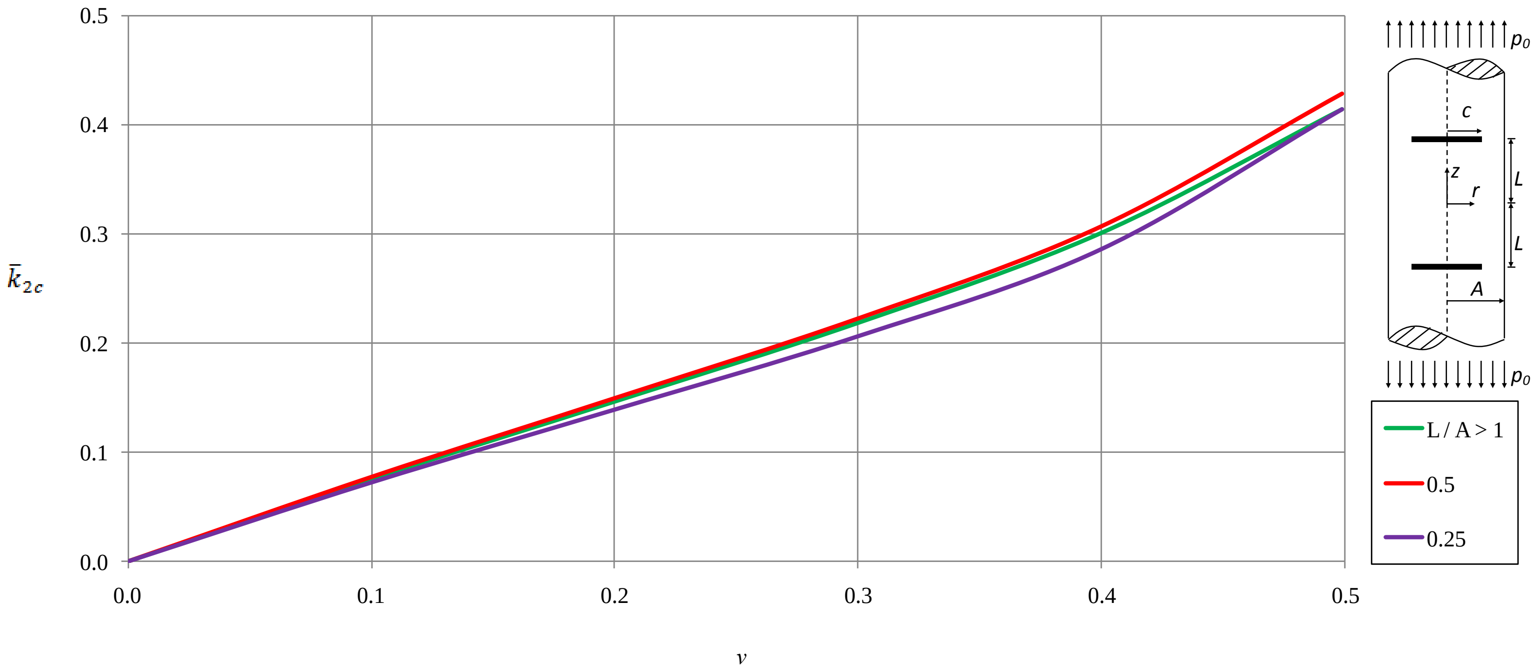

Figure 6.15 Normalized Mode II stress intensity factor $\bar{k}_{2c}$ at the inclusion edge when $c = 0.5A$.

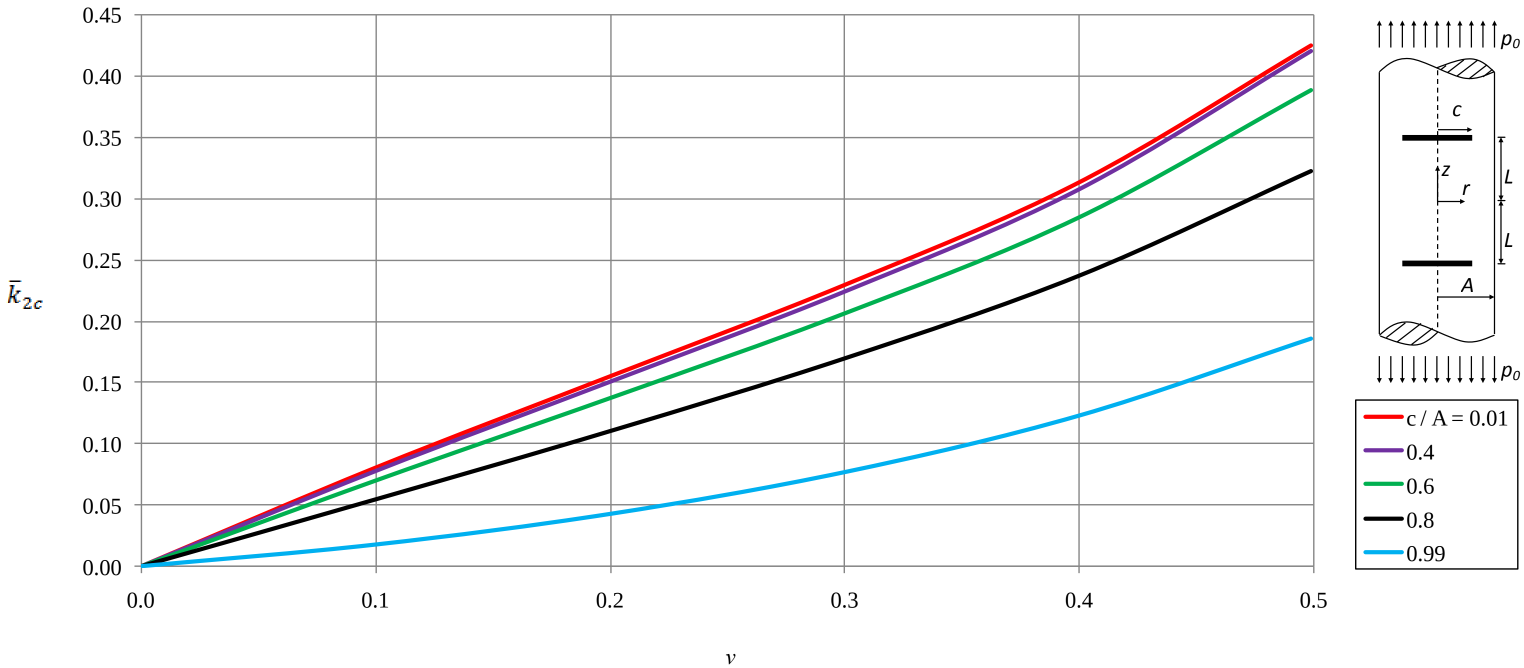

Figure 6.16 Normalized Mode II stress intensity factor $\bar{k}_{2c}$ at the inclusion edge when $L = 2A$.

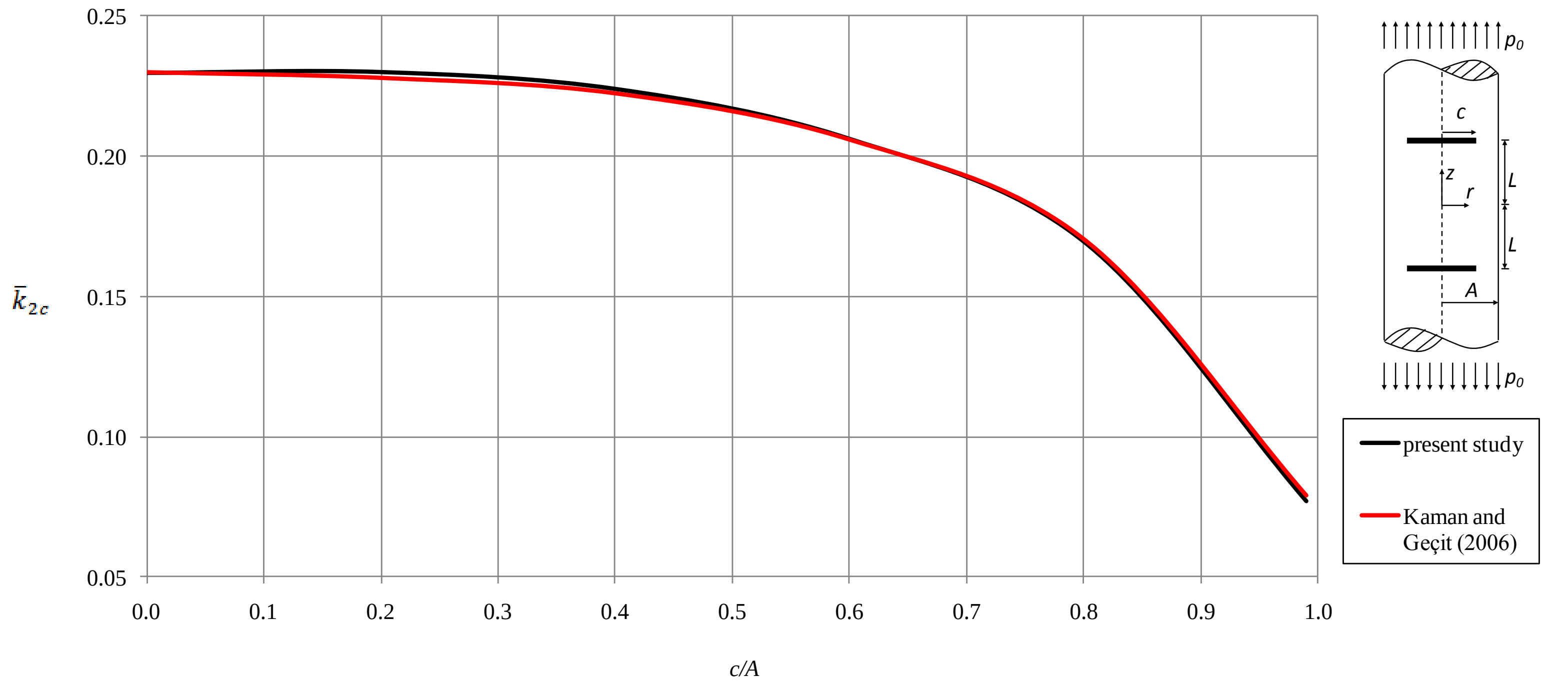

Figure 6.17 Normalized Mode II stress intensity factor $\bar{k}_{2c}$ when $\nu = 0.3$ and $L = 2A$.

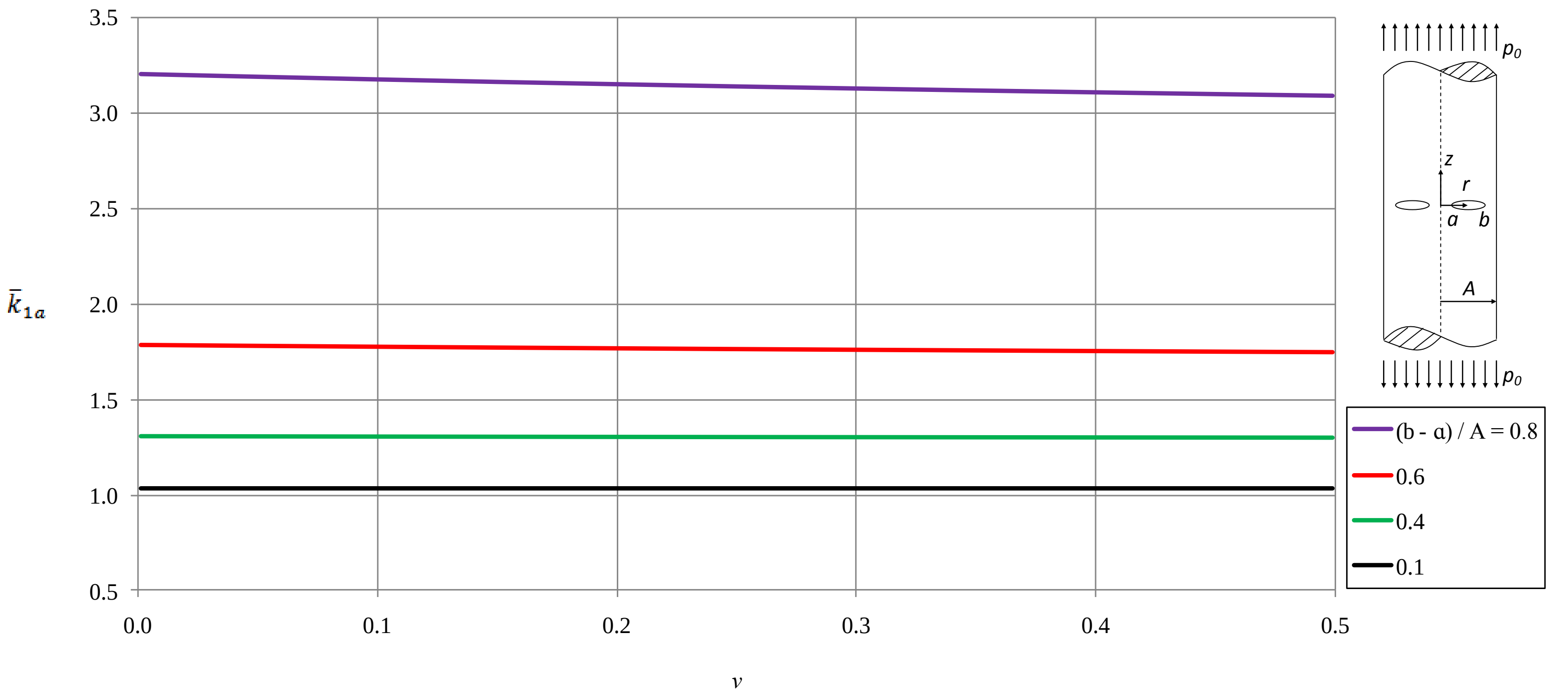

Figure 6.18 Normalized Mode I stress intensity factor $\bar{k}_{1a}$ at the crack edge when $b + a = A$.

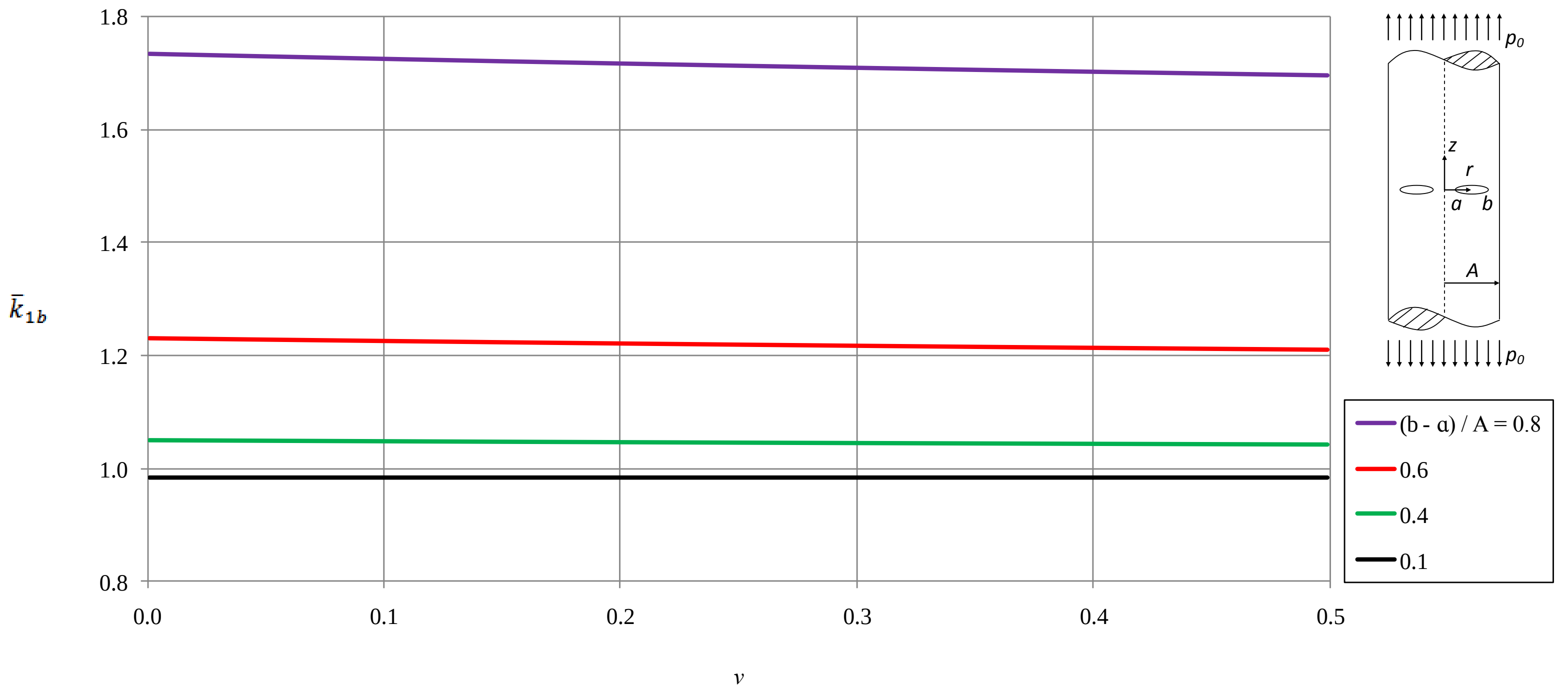

Figure 6.19 Normalized Mode I stress intensity factor $\bar{k}_{1b}$ at the crack edge when $b + a = A$.

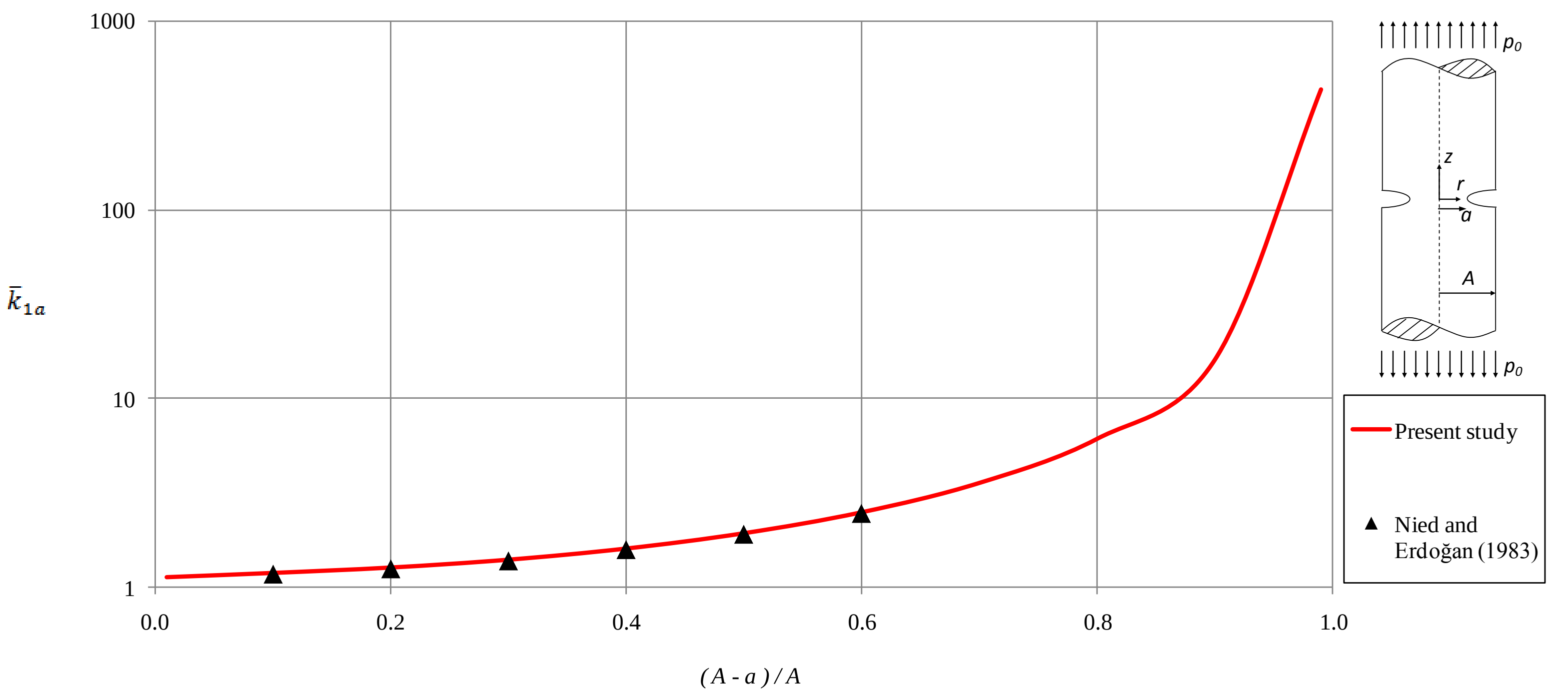

Figure 6.20 Normalized Mode I stress intensity factor $\bar{k}_{1a}$ for the edge crack.

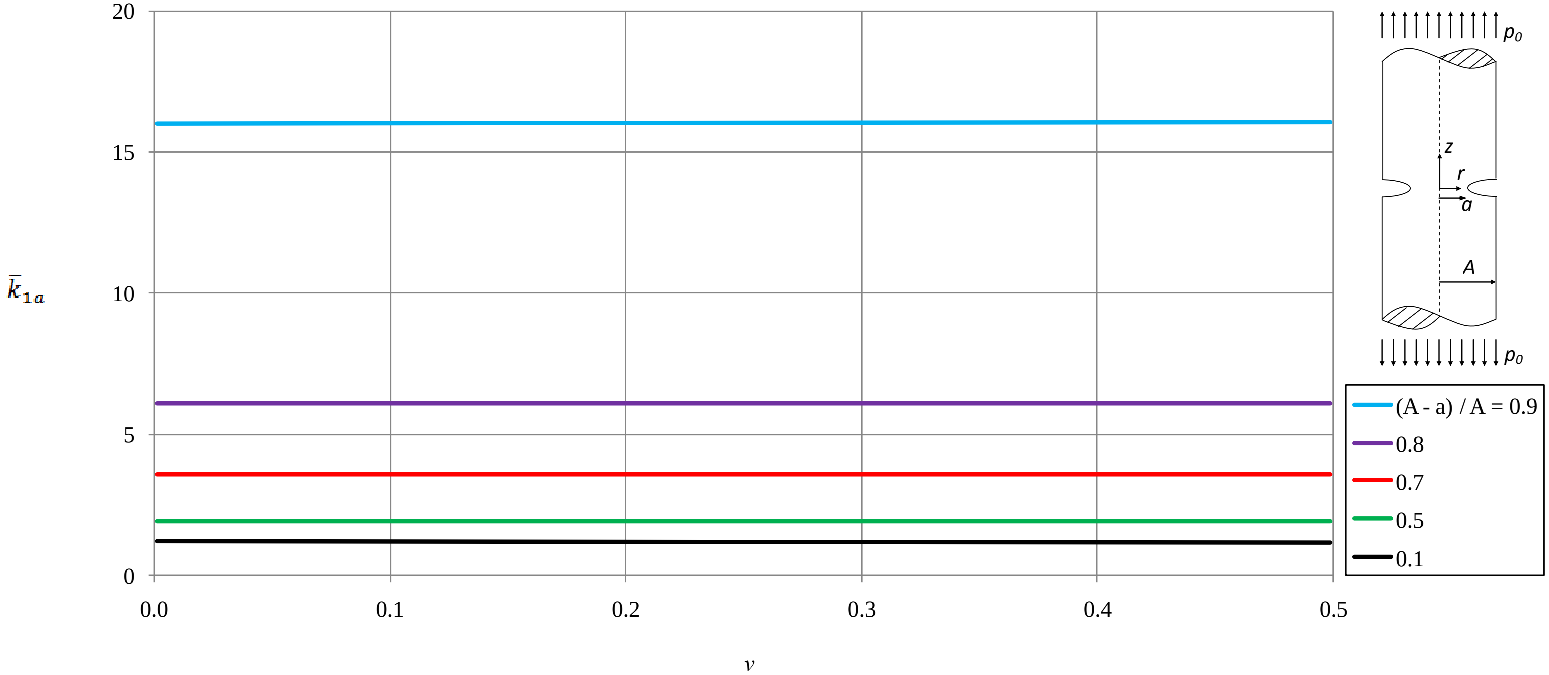

Figure 6.21 Normalized Mode I stress intensity factor $\bar{k}_{1a}$ for the edge crack.

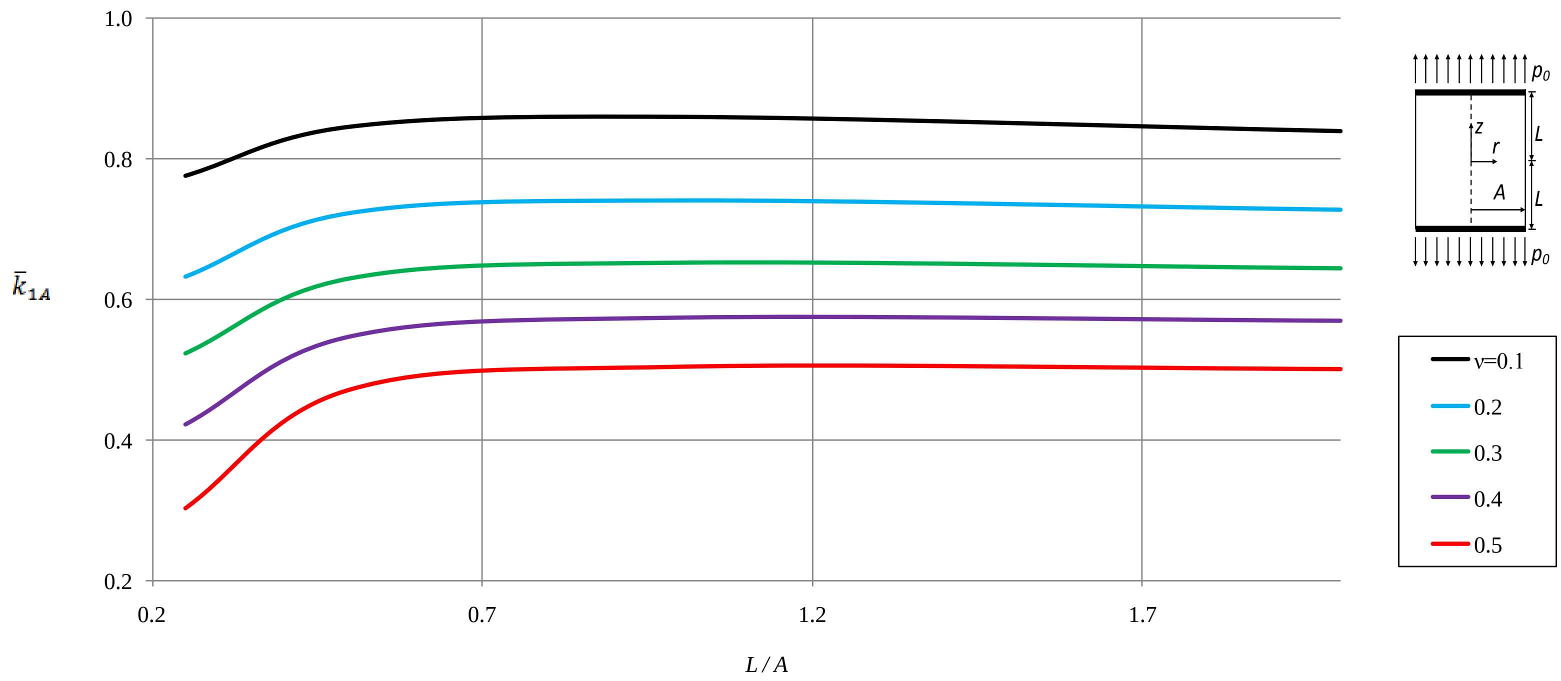

Figure 6.22 Normalized Mode I stress intensity factor $\bar{k}_{1A}$ when at the corner of the finite cylinder .

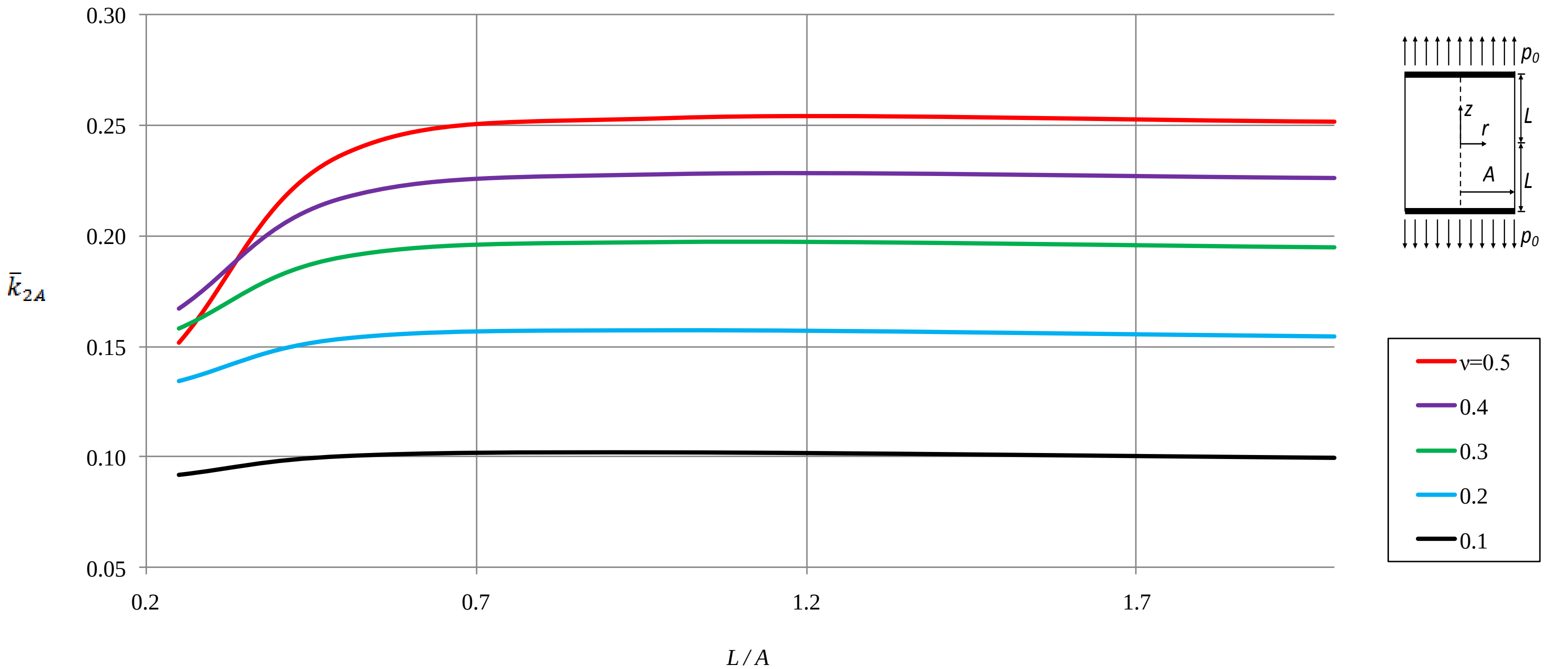

Figure 6.23 Normalized Mode II stress intensity factor $\bar{k}_{2A}$ when at the corner of the finite cylinder .

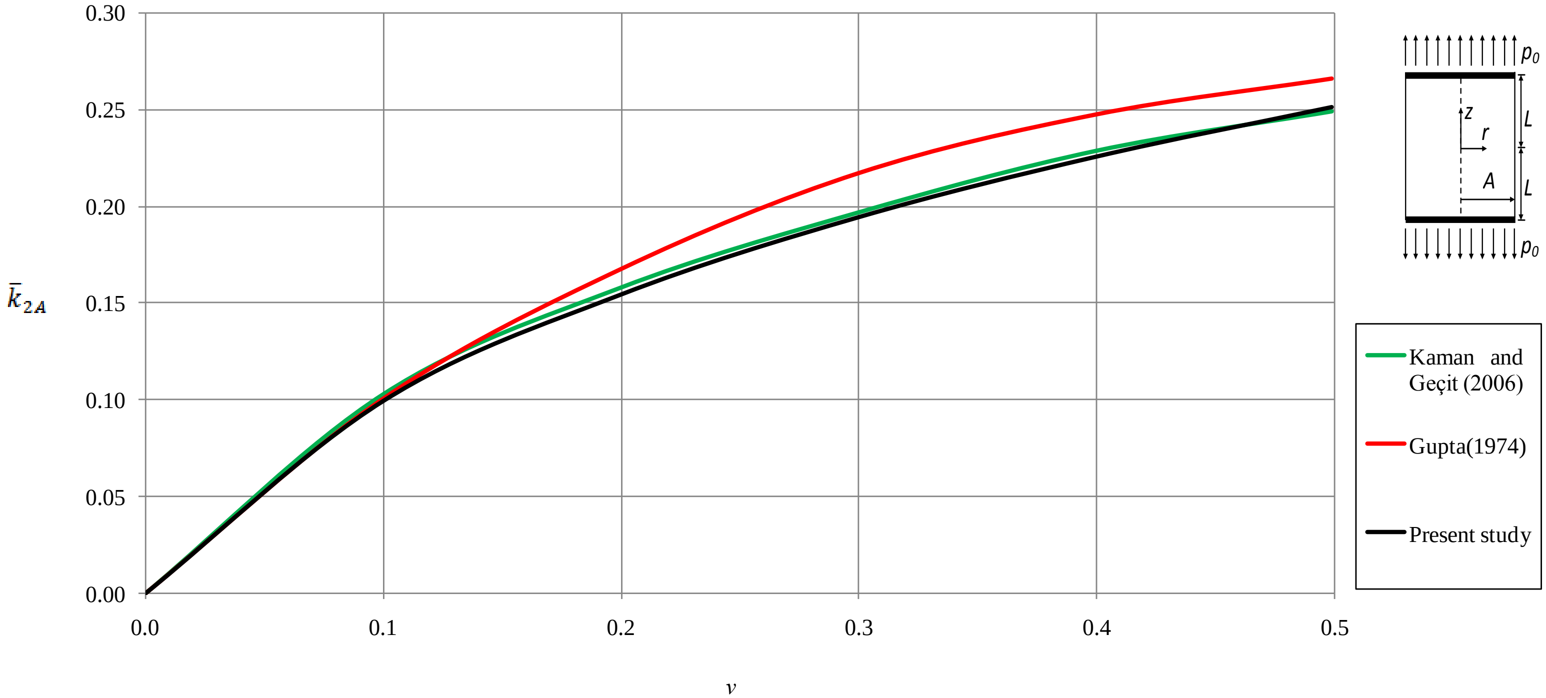

Figure 6.24 Normalized Mode II stress intensity factor $\bar{k}_{2A}$ at the corner of the finite cylinder when $L = 2A$.

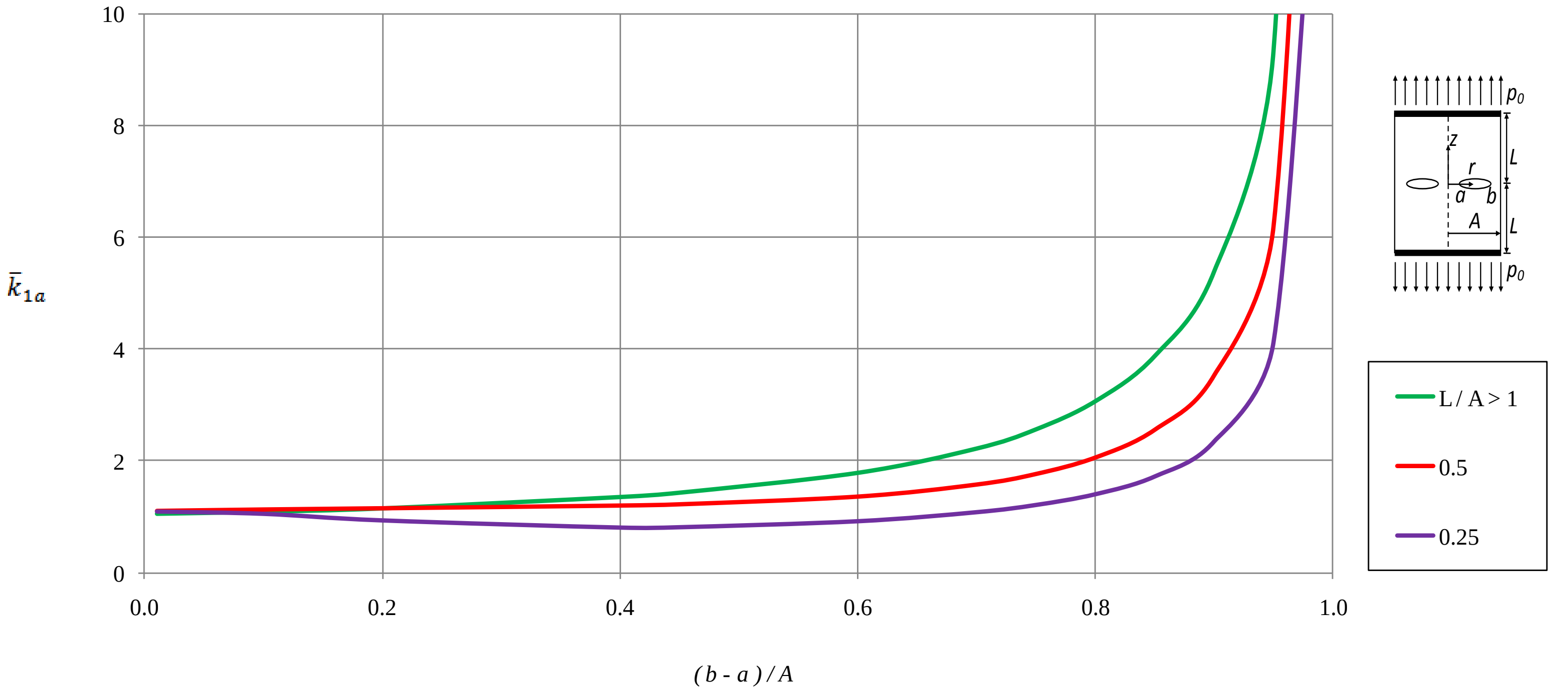

Figure 6.25 Normalized Mode I stress intensity factor $\bar{k}_{1a}$ at the inner edge of the crack when $\nu = 0.3$ and $b + a = A$.

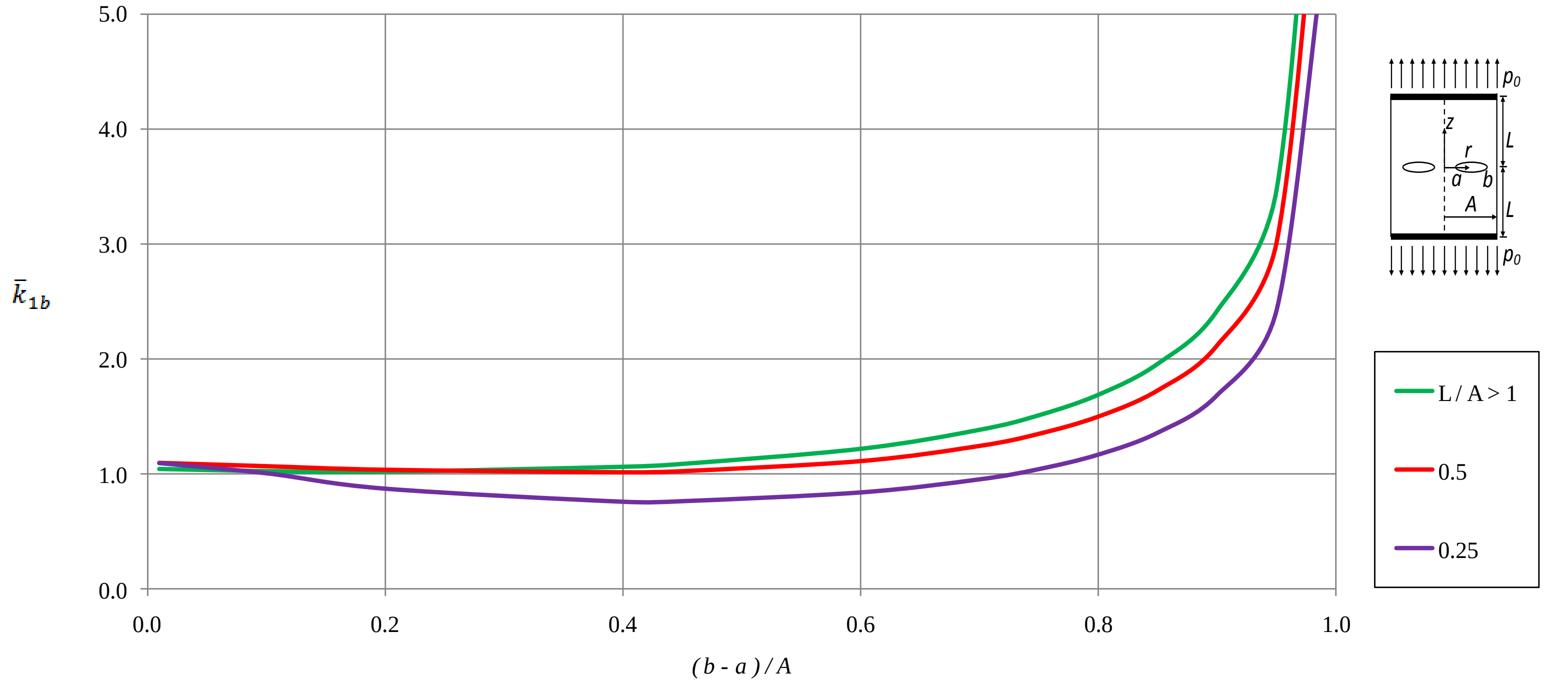

Figure 6.26 Normalized Mode I stress intensity factor $\bar{k}_{1b}$ at the outer edge of the crack when $\nu = 0.3$ and $b + a = A$.

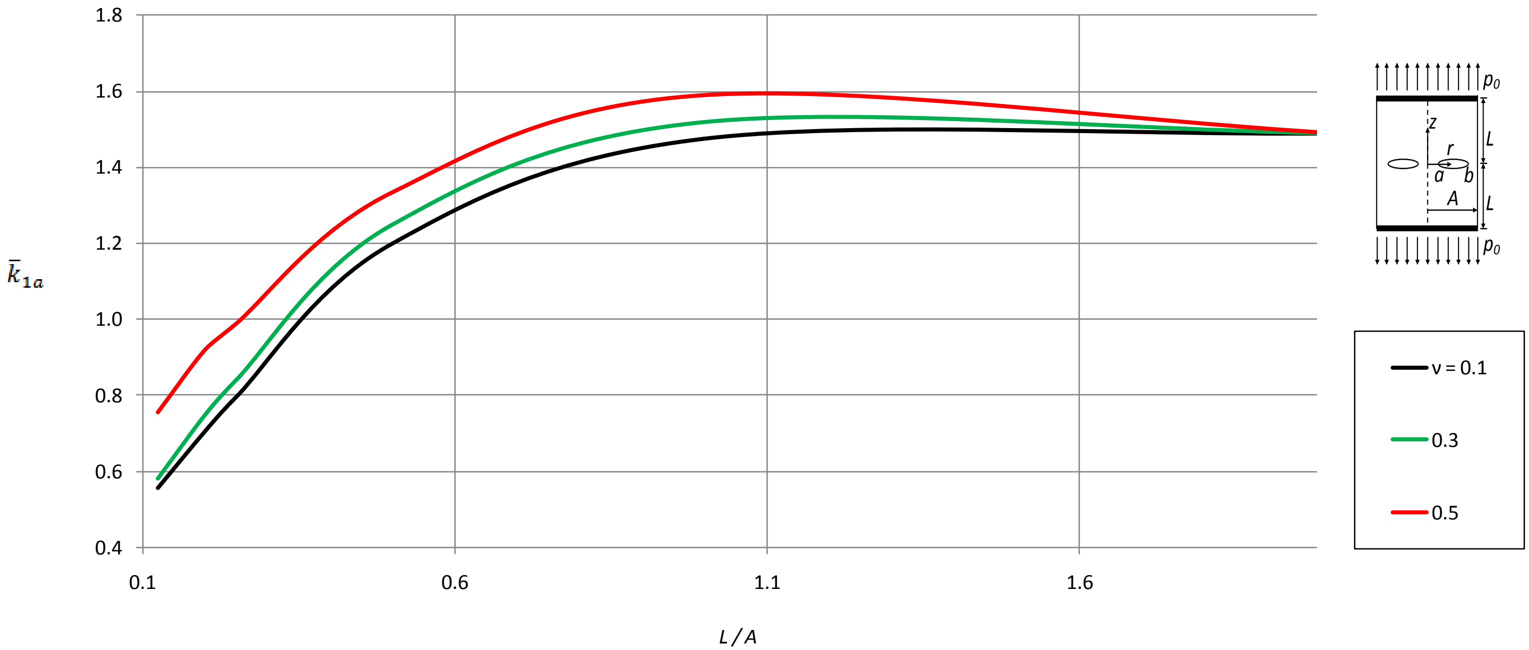

Figure 6.27 Normalized Mode I stress intensity factor $\bar{k}_{1a}$ at the crack edge when $b - a = 0.5A$ and $b + a = A$.

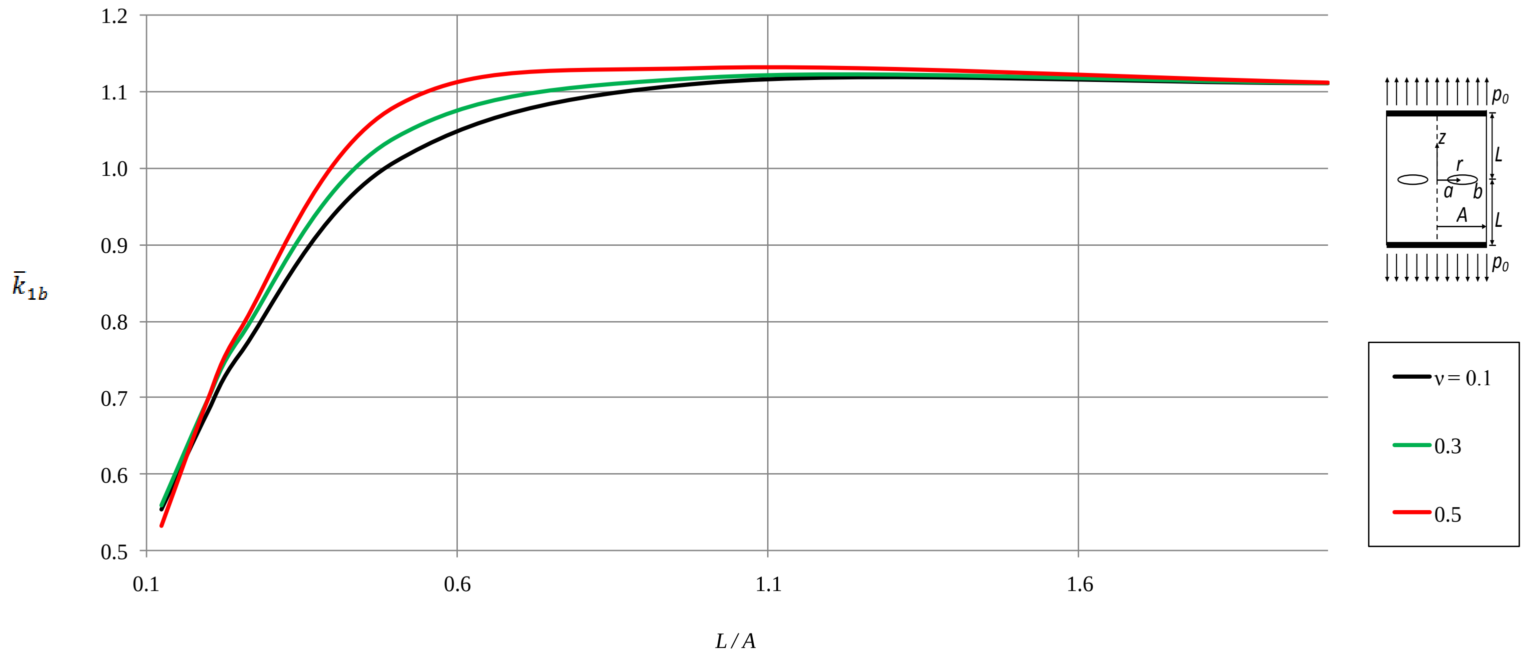

Figure 6.28 Normalized Mode I stress intensity factor $\bar{k}_{1b}$ at the outer edge of the crack when when $b - a = 0.5A$ and $b + a = A$.

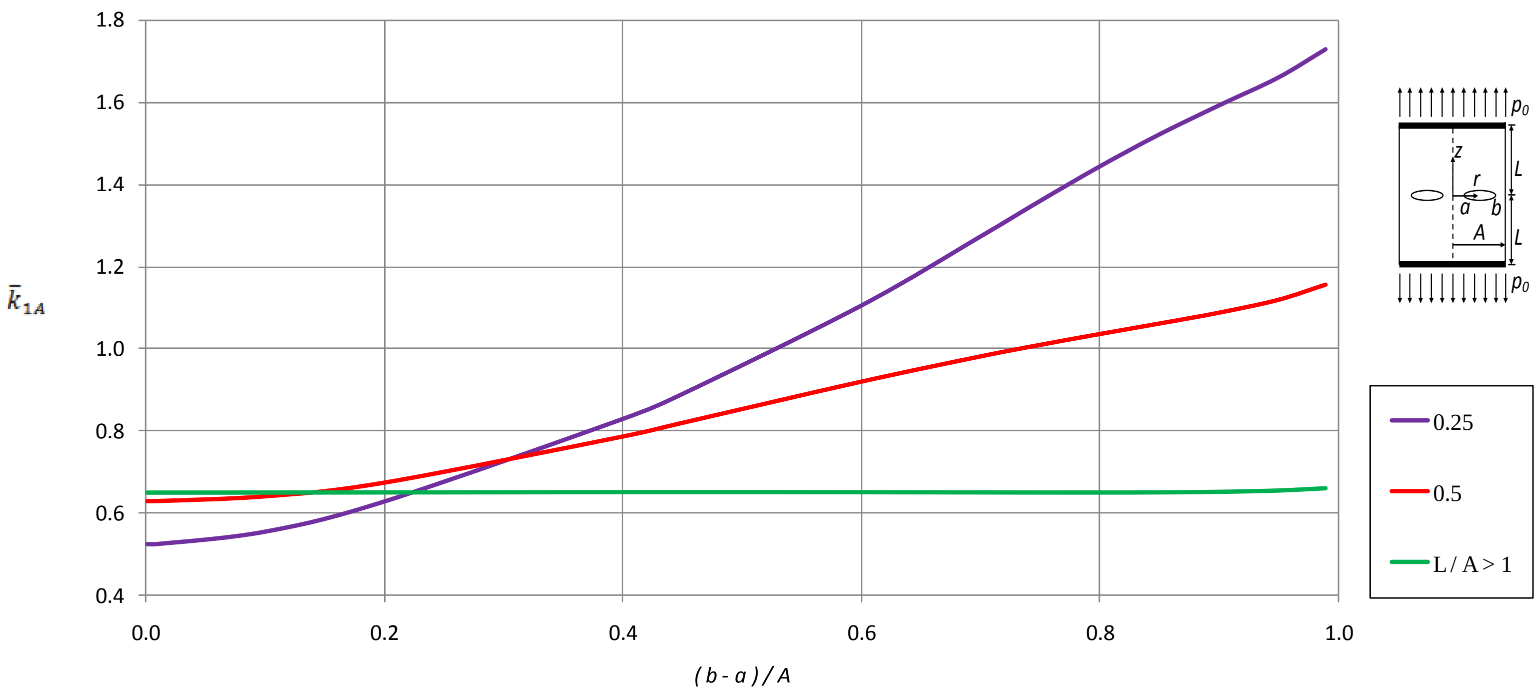

Figure 6.29 Normalized Mode I stress intensity factor $\bar{k}_{1A}$ at the corner of the finite cylinder when $\nu = 0.3$ and $b + a = A$.

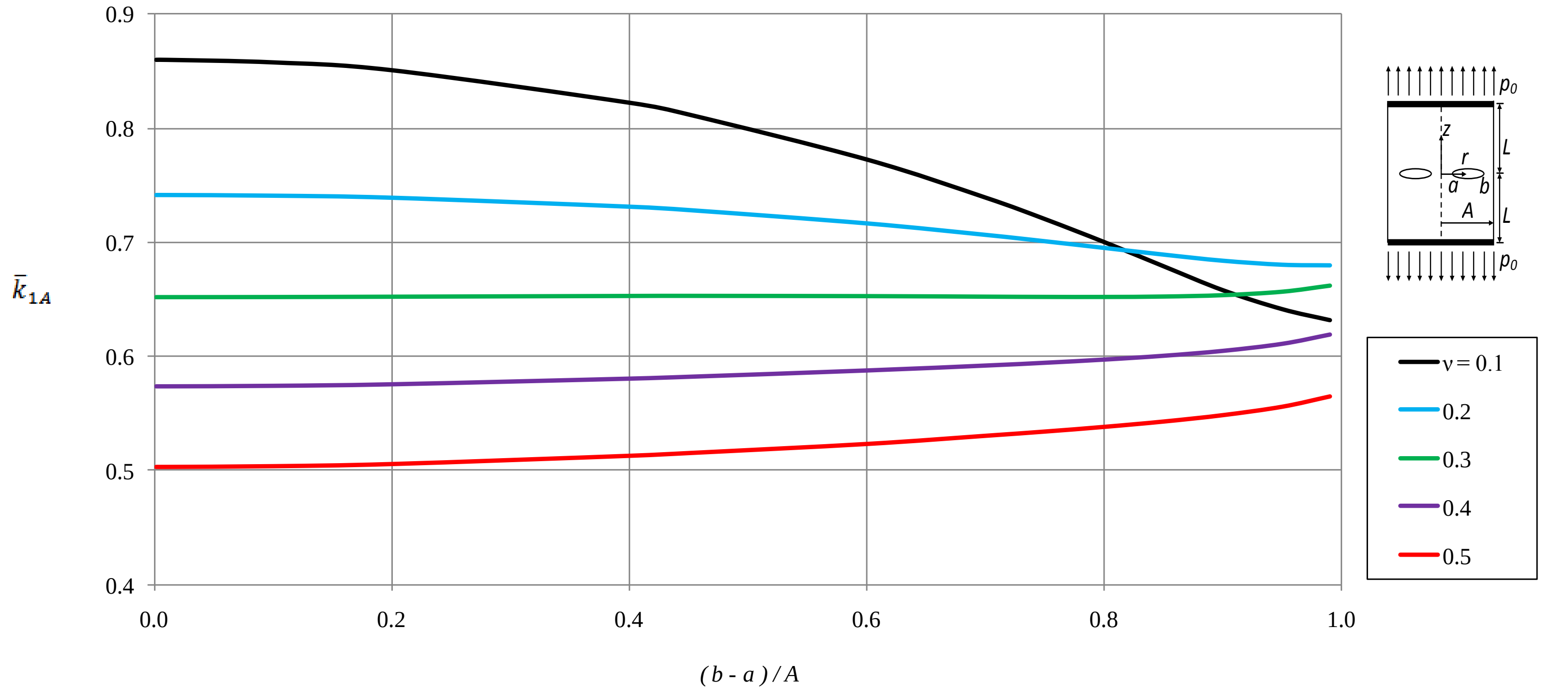

Figure 6.30 Normalized Mode I stress intensity factor $\bar{k}_{1A}$ at the corner of the finite cylinder when $L = A$ and $b + a = A$.

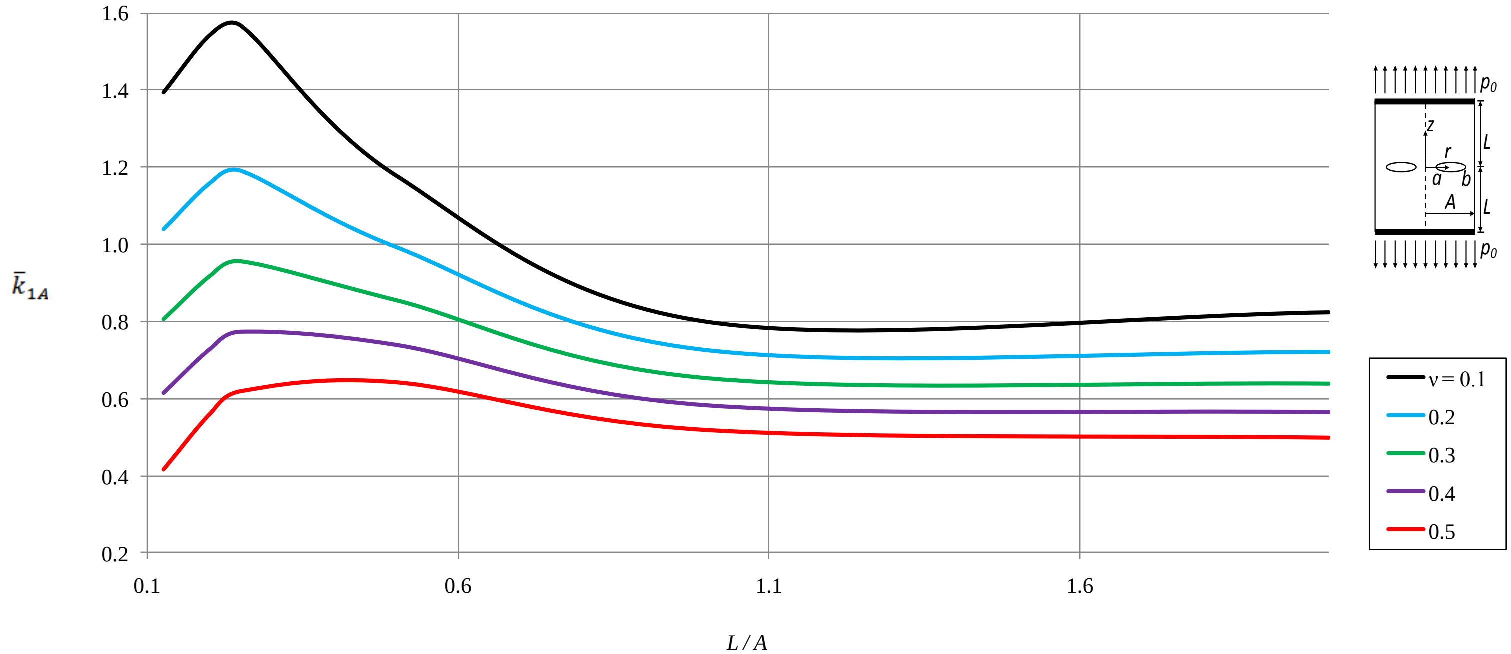

Figure 6.31 Normalized Mode I stress intensity factor $\bar{k}_{1A}$ at the corner of the finite cylinder when $b - a = 0.5A$ and $b + a = A$.

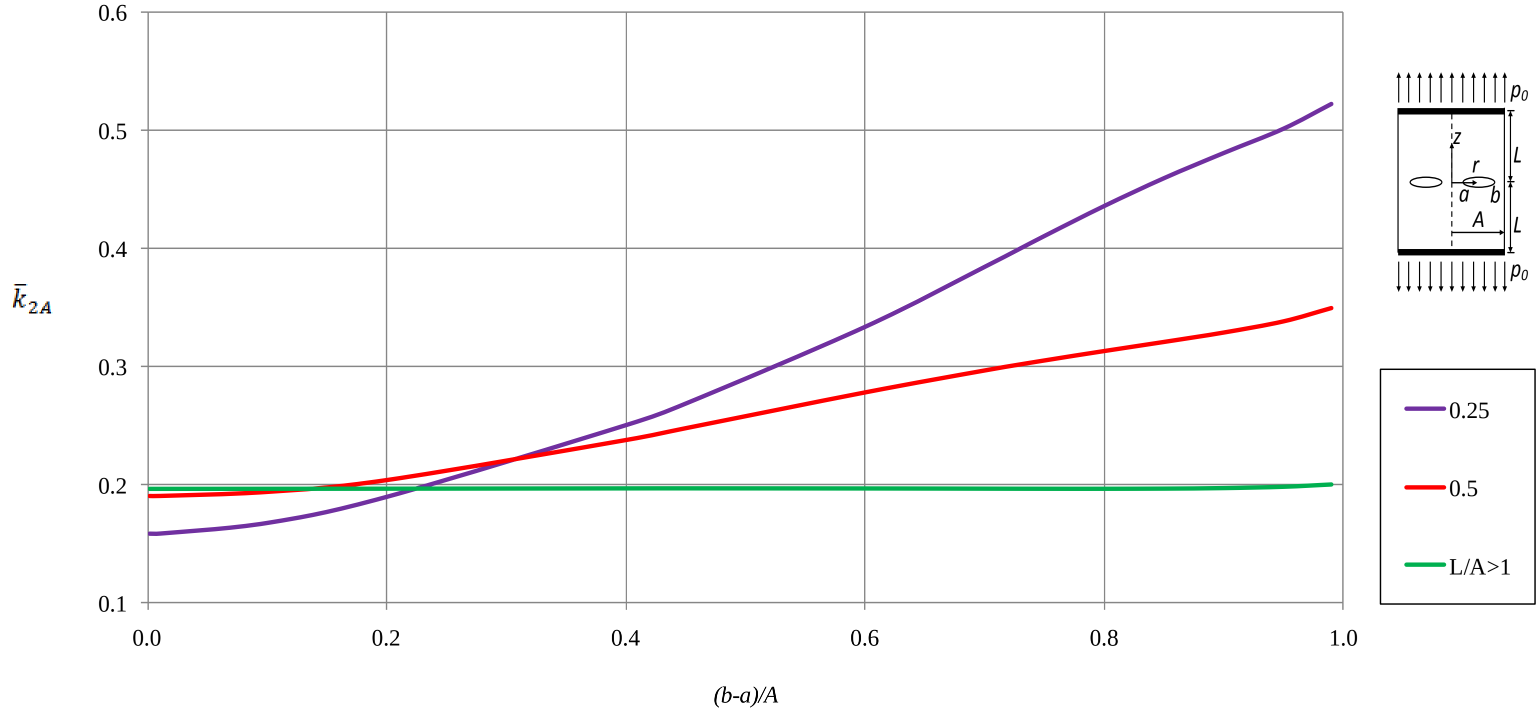

Figure 6.32 Normalized Mode II stress intensity factor $\bar{k}_{2A}$ at the corner of the finite cylinder when $\nu = 0.3$ and $b + a = A$.

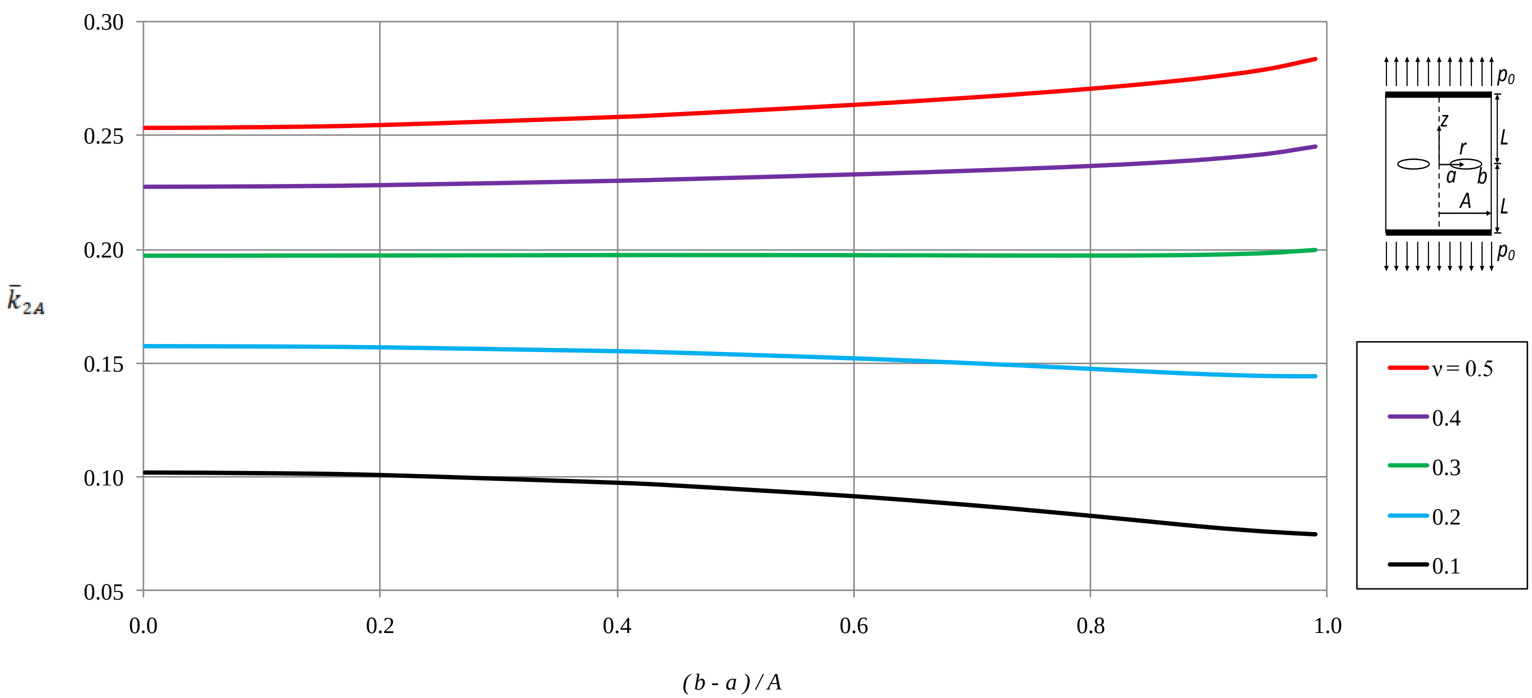

Figure 6.33 Normalized Mode II stress intensity factor $\bar{k}_{2A}$ at the corner of the finite cylinder when $L = A$ and $b + a = A$.

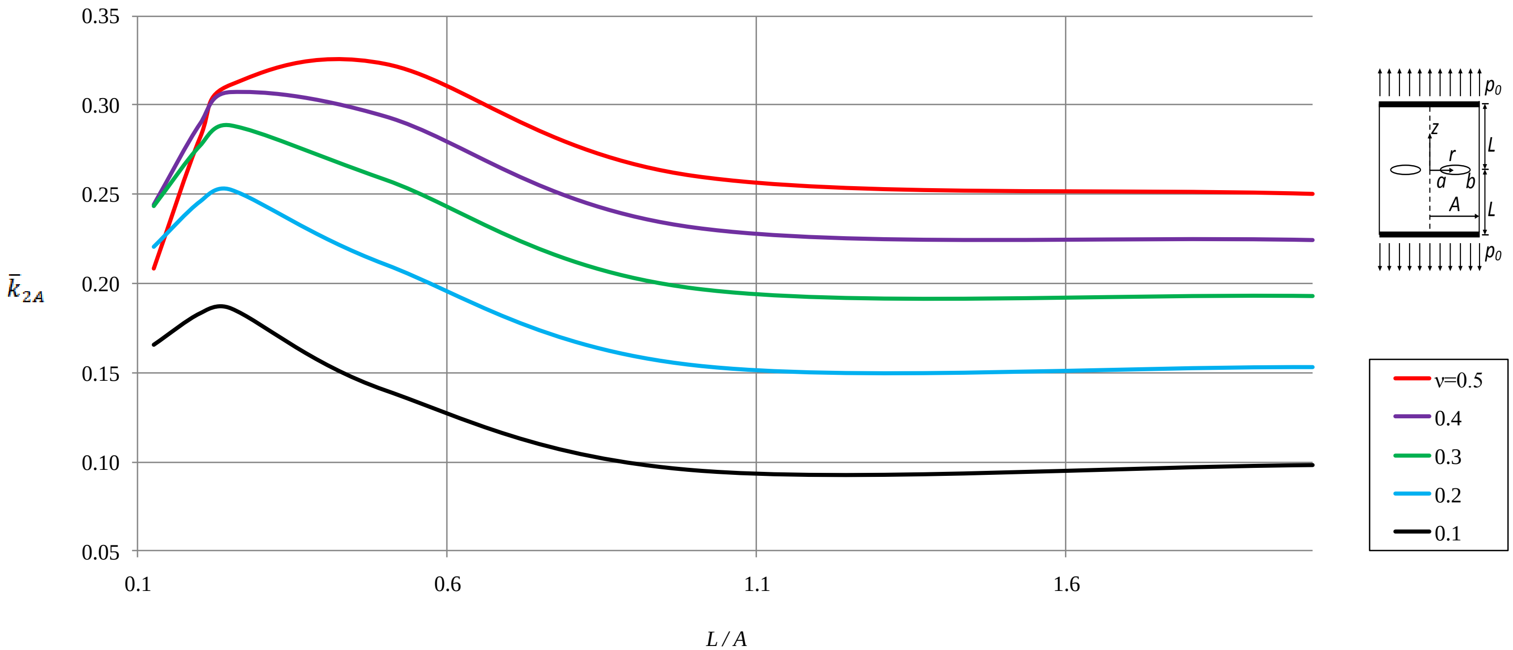

Figure 6.34 Normalized Mode II stress intensity factor $\bar{k}_{2A}$ at the corner of the finite cylinder when $b - a = 0.5A$ and $b + a = A$.

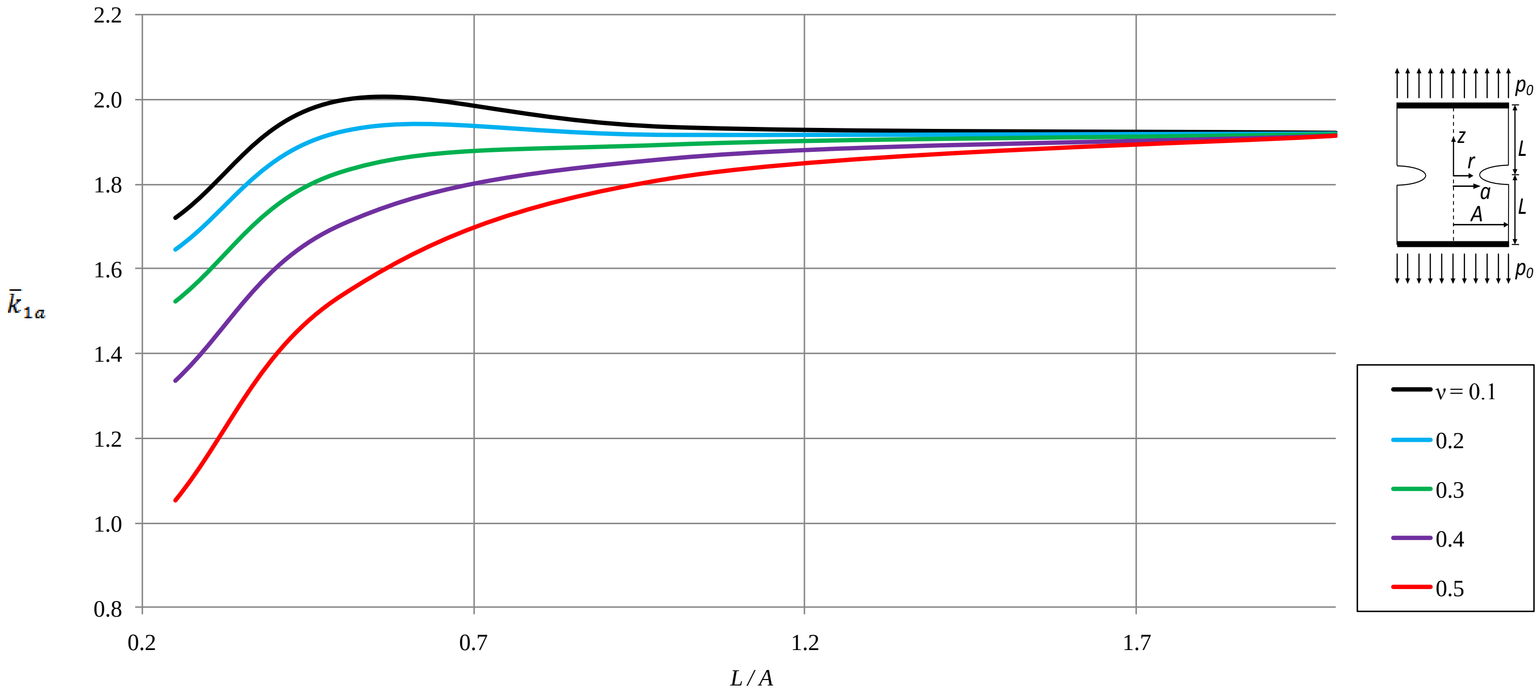

Figure 6.35 Normalized Mode I stress intensity factor $\bar{k}_{1a}$ for the edge crack when $b - a = 0.5A$.

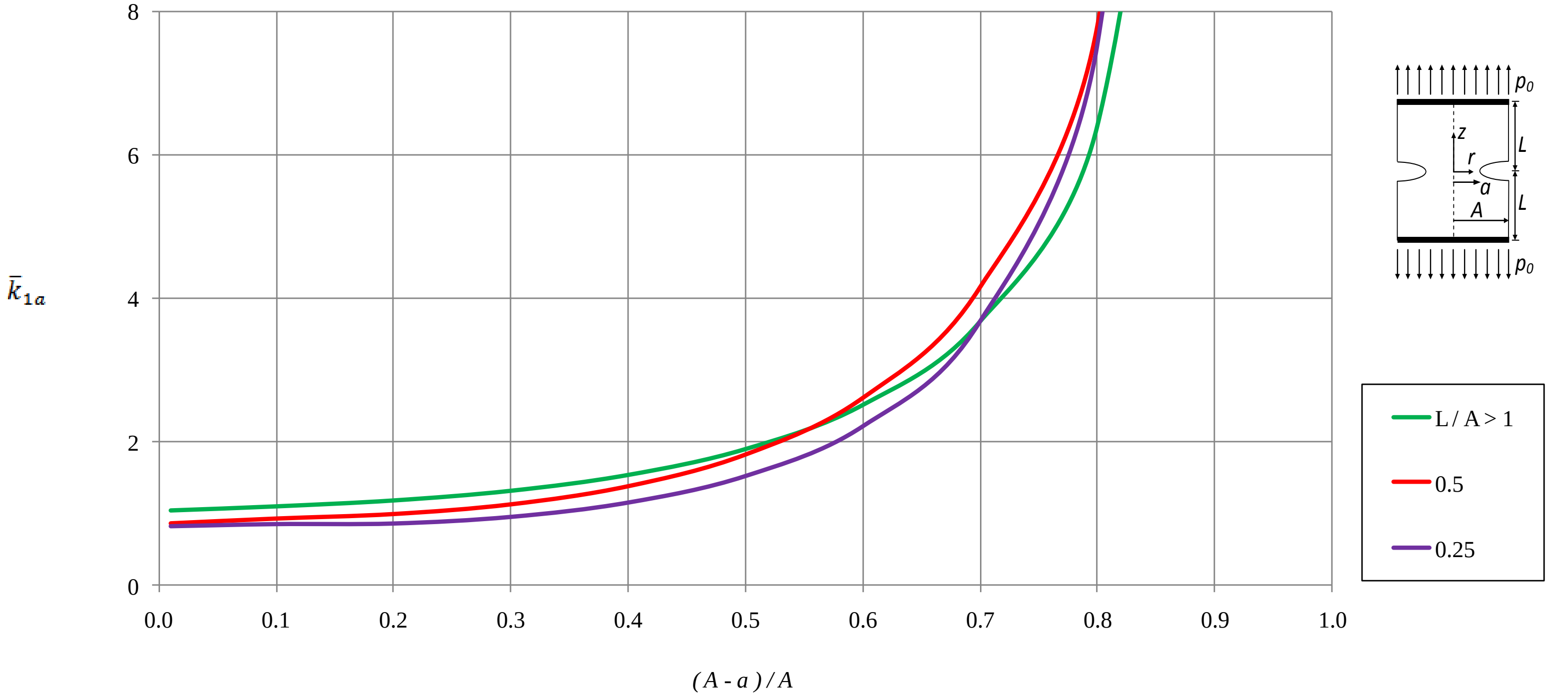

Figure 6.36 Normalized Mode I stress intensity factor $\bar{k}_{1a}$ for the edge crack when $\nu = 0.3$.

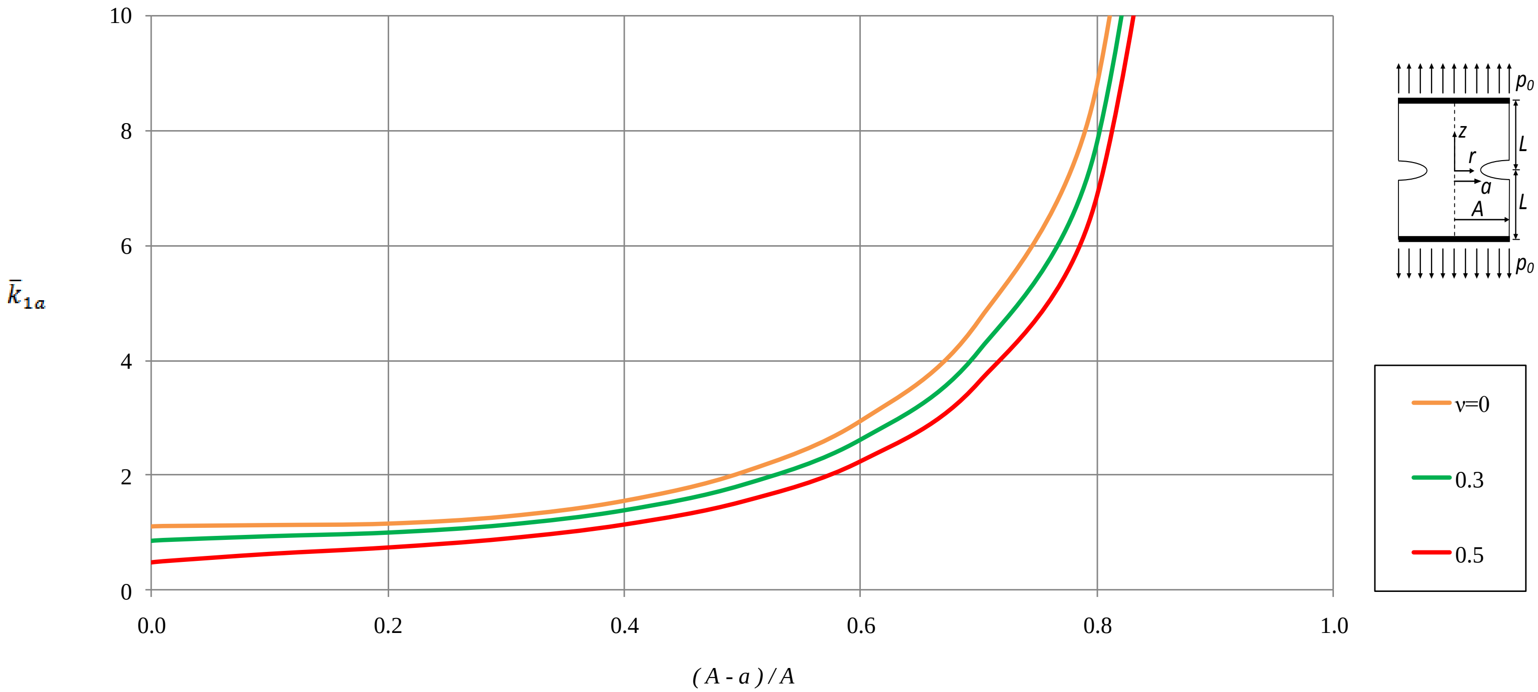

Figure 6.37 Normalized Mode I stress intensity factor $\bar{k}_{1a}$ for the edge crack when $L = 0.5A$.

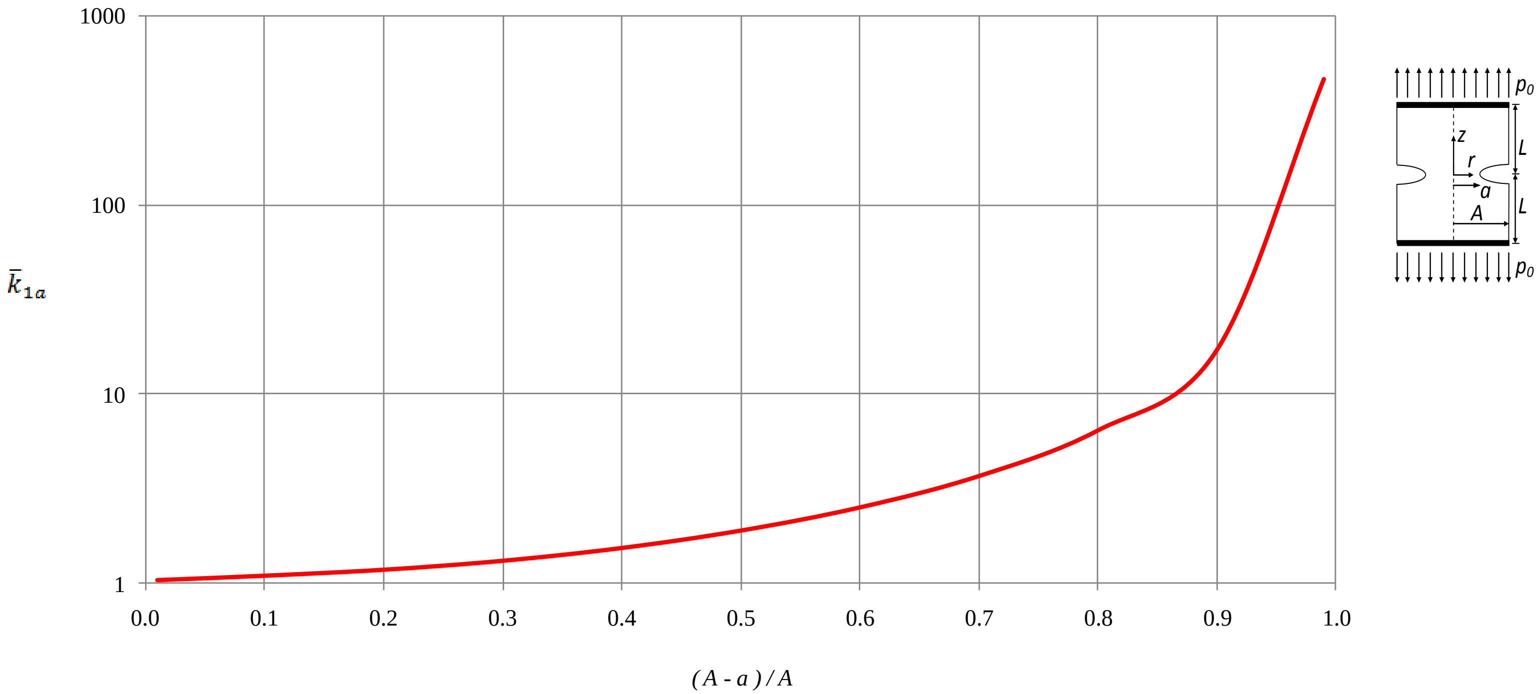

Figure 6.38 Normalized Mode I stress intensity factor $\bar{k}_{1a}$ for the edge crack when $L = A$.

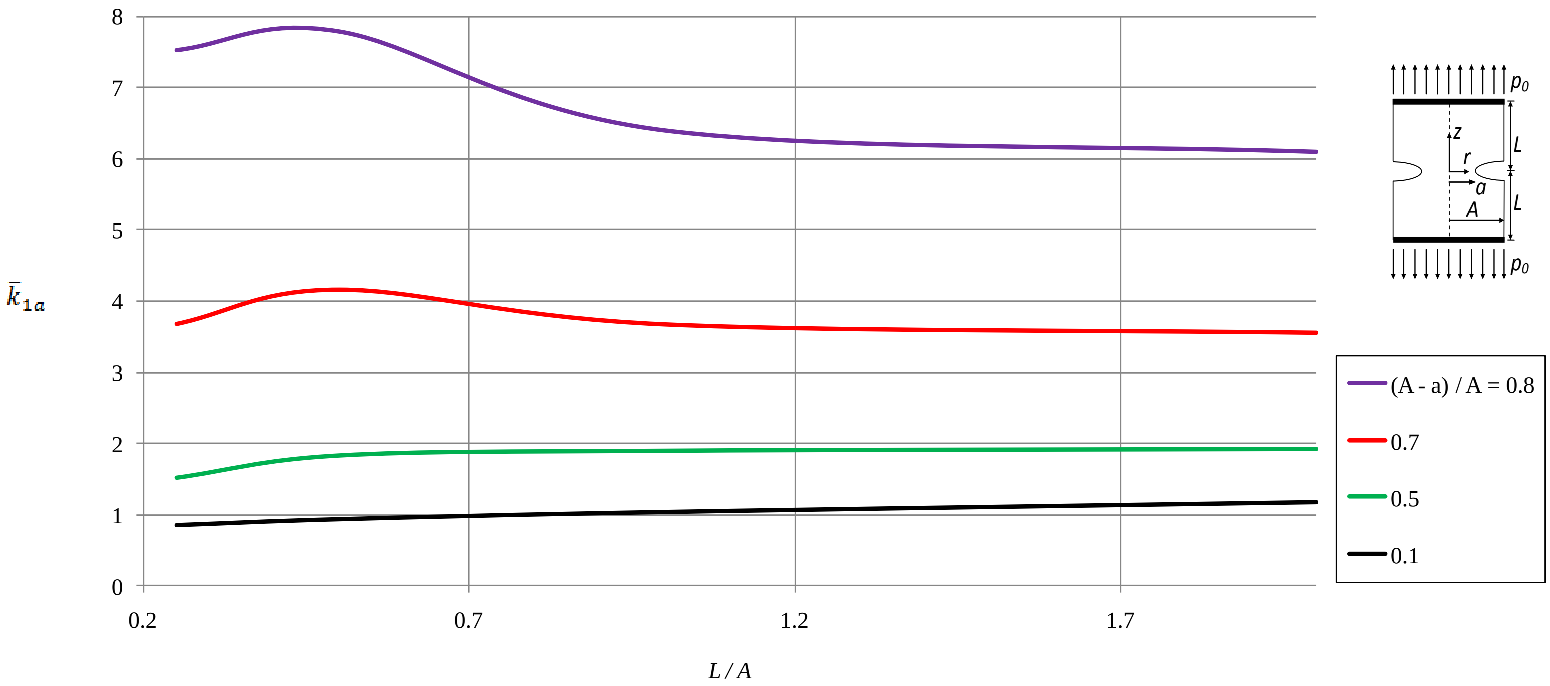

Figure 6.39 Normalized Mode I stress intensity factor $\bar{k}_{1a}$ for the edge crack when $\nu = 0.3$.

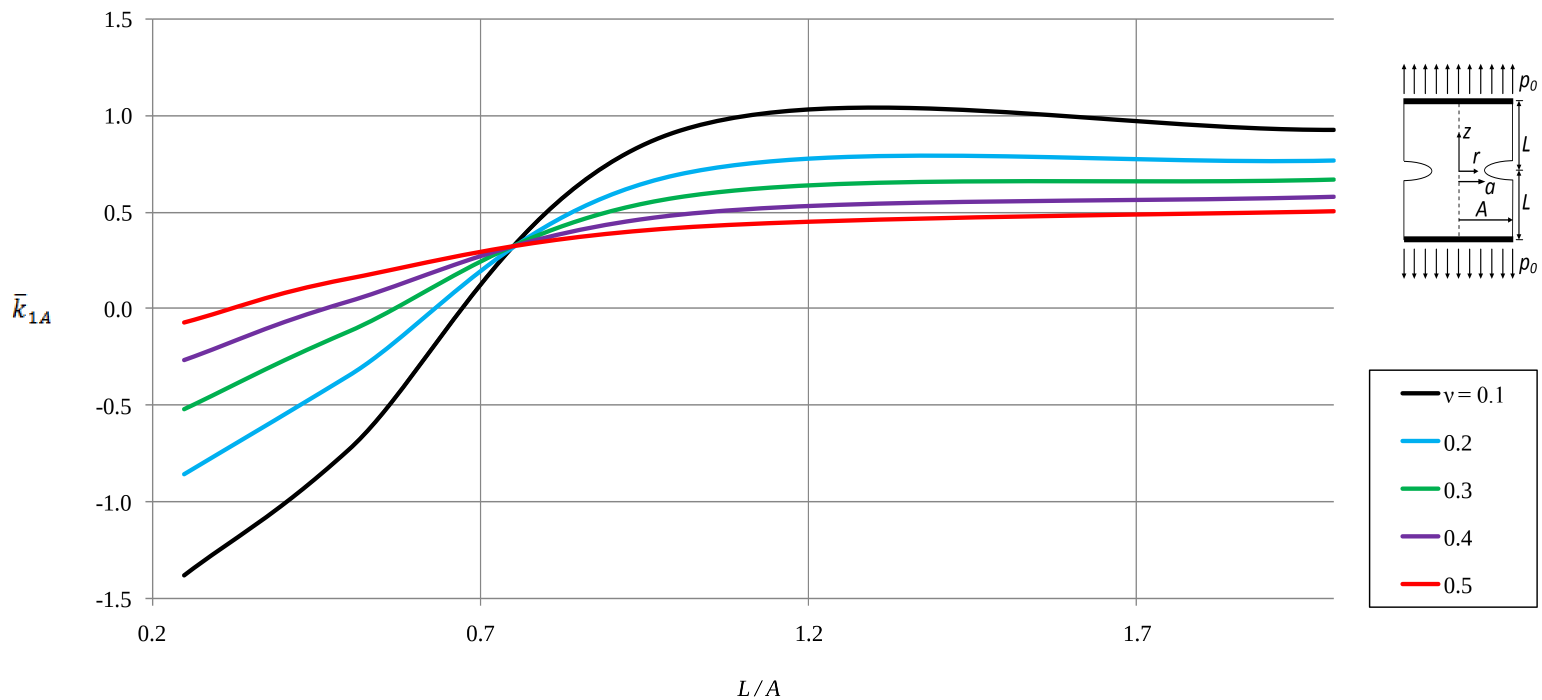

Figure 6.40 Normalized Mode I stress intensity factor $\bar{k}_{1A}$ at the corner of the finite cylinder when $b - a = 0.5A$.

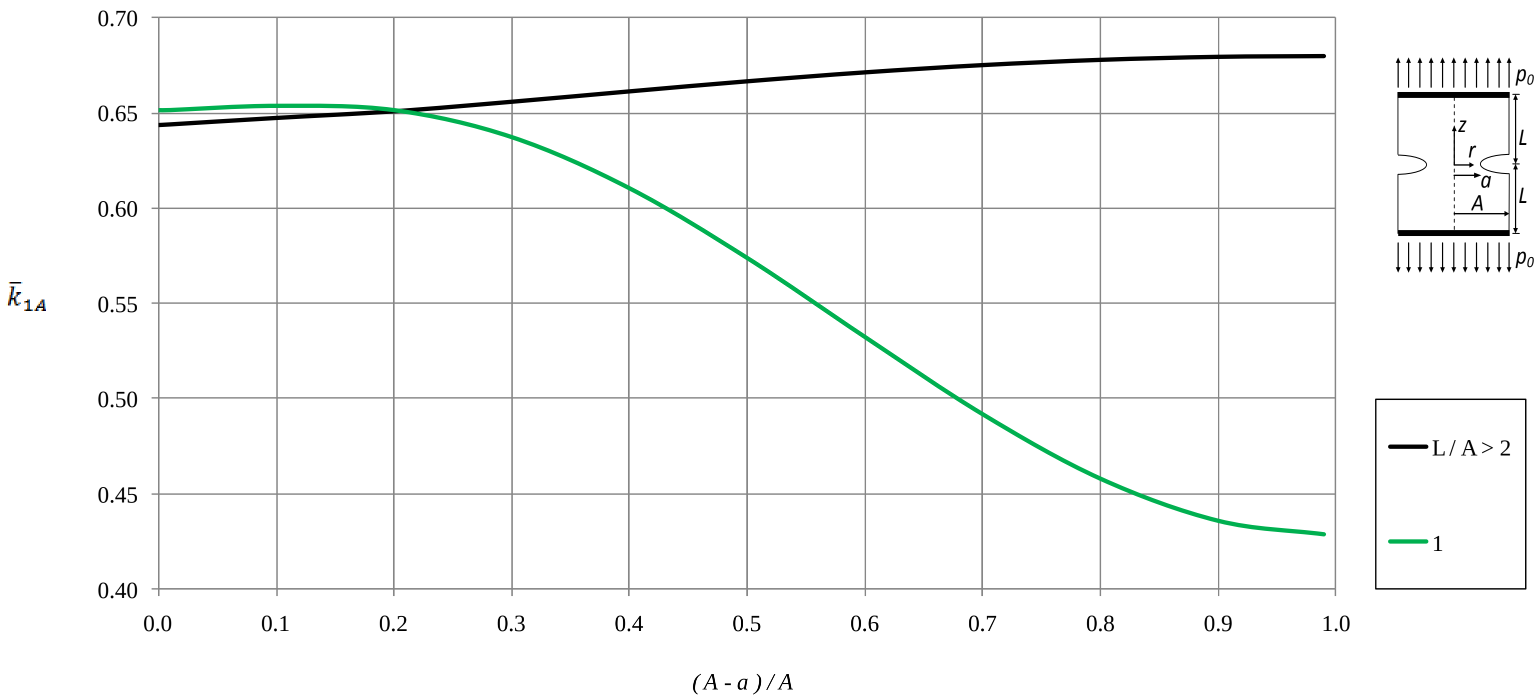

Figure 6.41 Normalized Mode I stress intensity factor $\bar{k}_{1A}$ at the corner of the finite cylinder when $\nu = 0.3$.

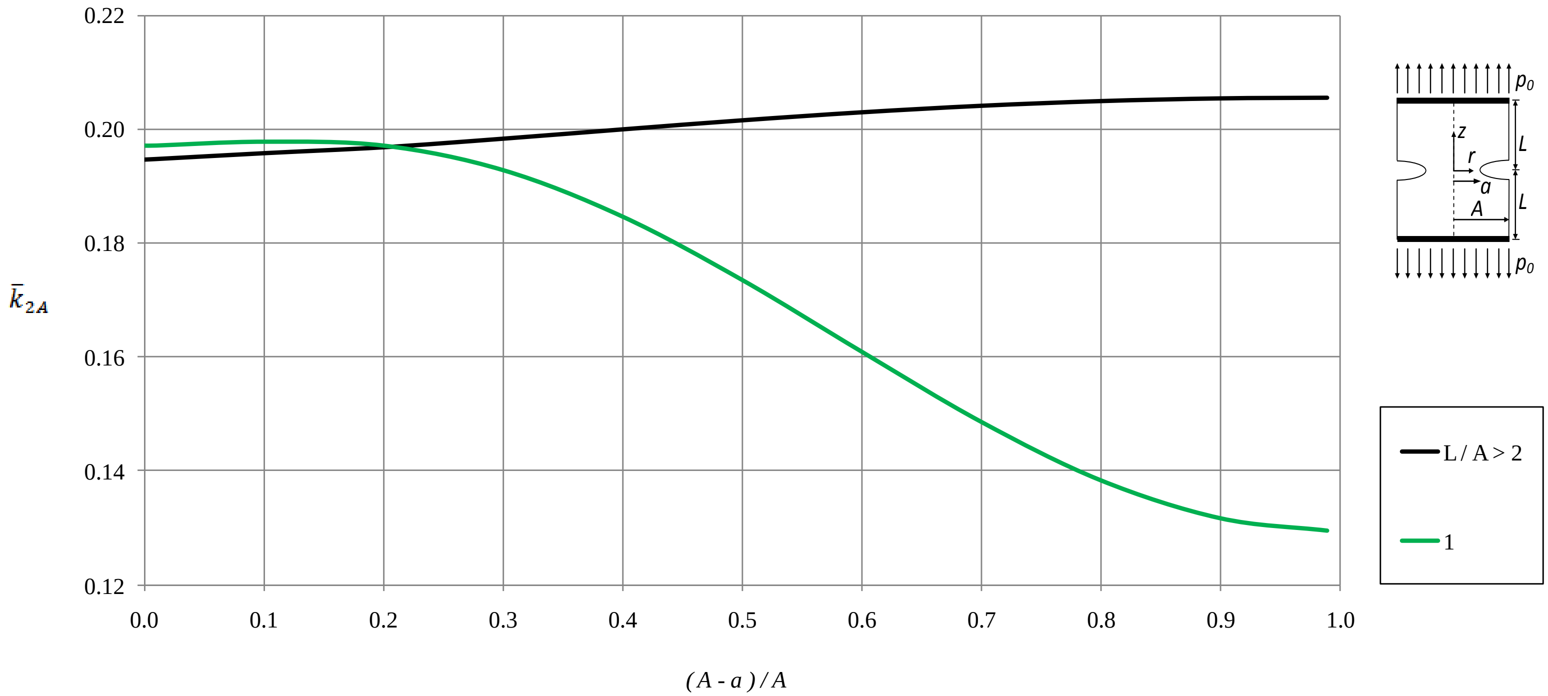

Figure 6.42 Normalized Mode II stress intensity factor $\bar{k}_{2A}$ at the corner of the finite cylinder when $\nu = 0.3$.

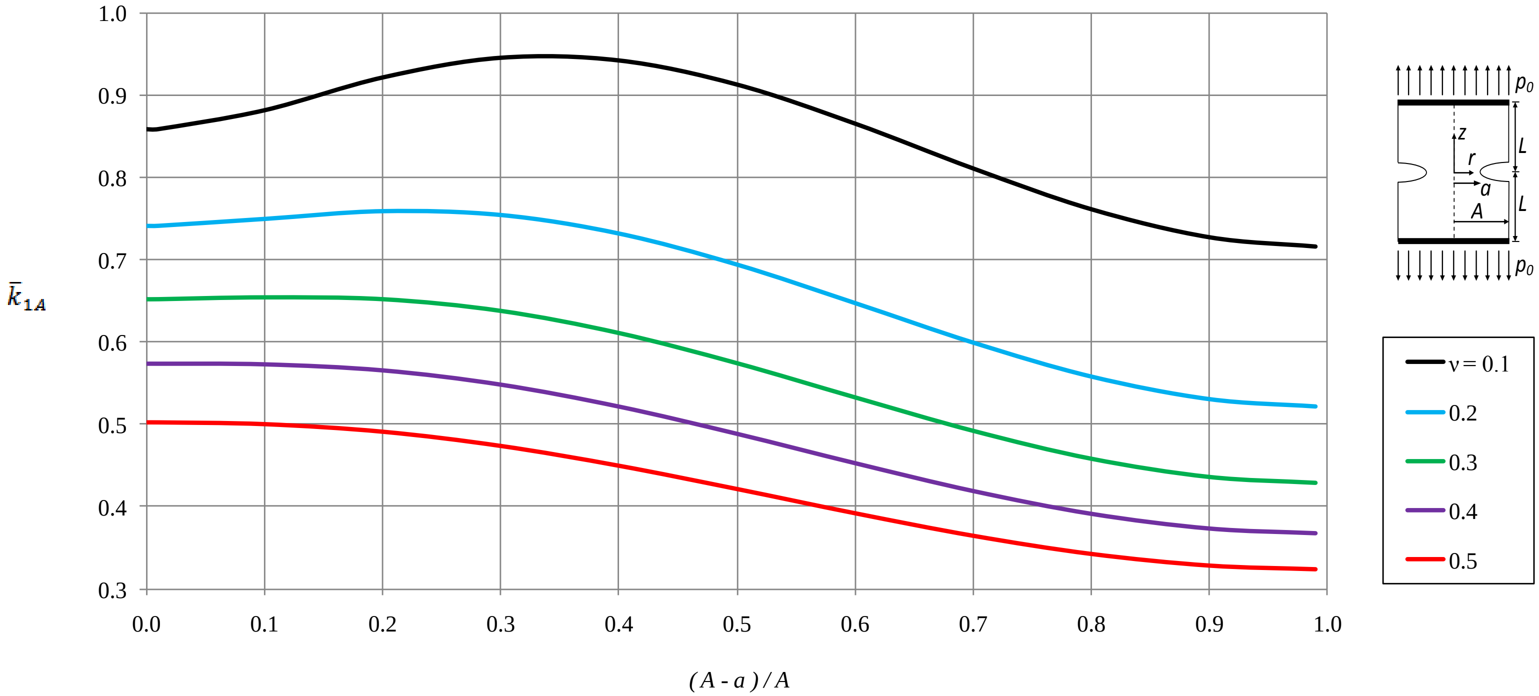

Figure 6.43 Normalized Mode I stress intensity factor $\bar{k}_{1A}$ at the corner of the finite cylinder when $L = A$.

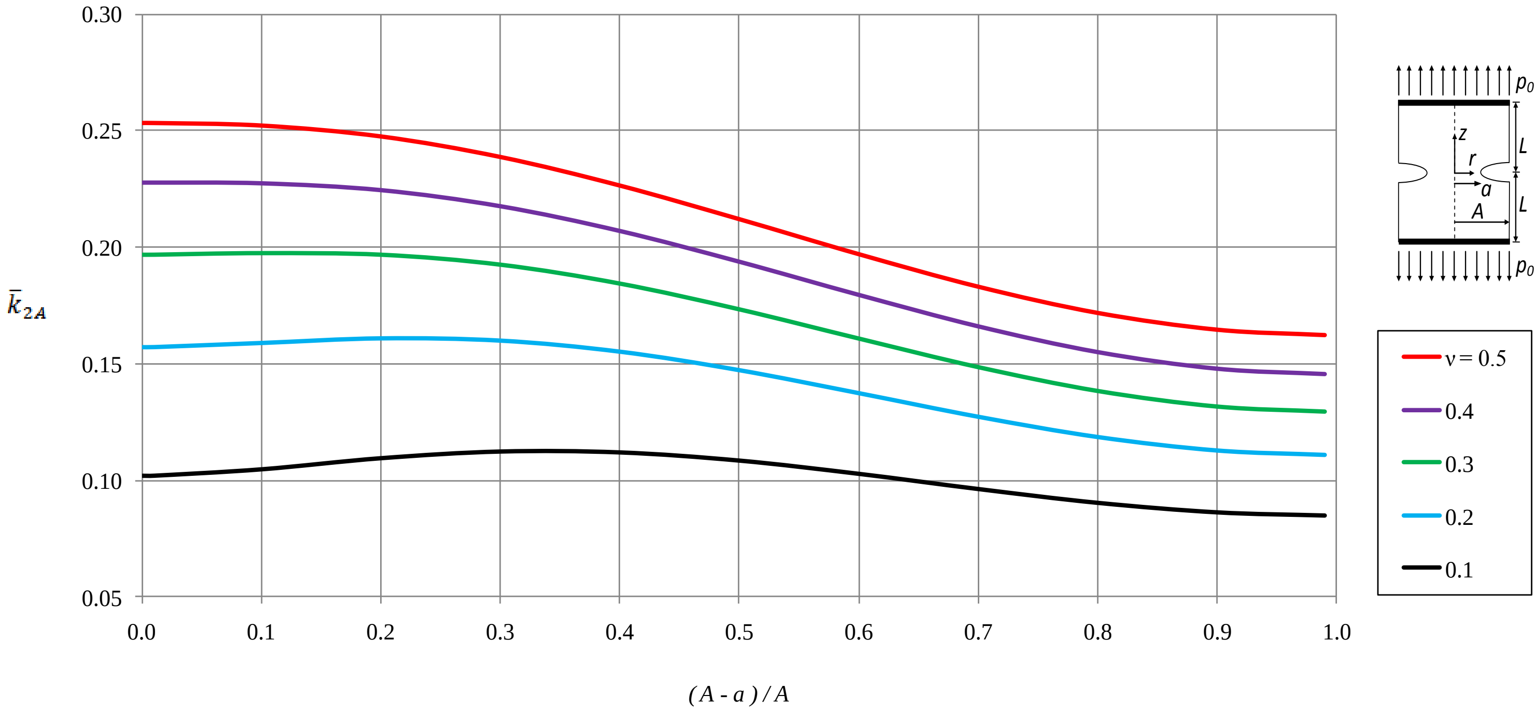

Figure 6.44 Normalized Mode II stress intensity factor $\bar{k}_{2A}$ at the corner of the finite cylinder when $L = A$.

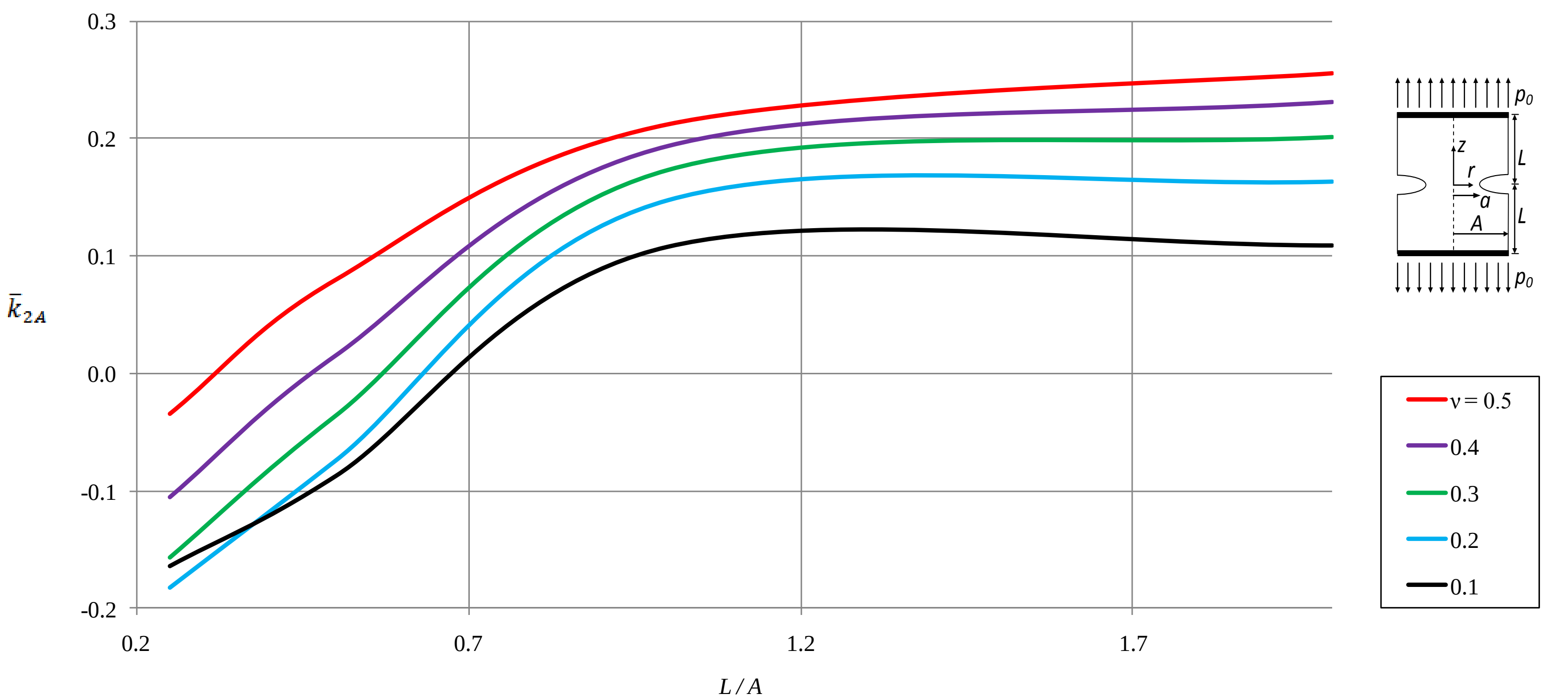

Figure 6.45 Normalized Mode II stress intensity factor $\bar{k}_{2A}$ at the corner of the finite cylinder when $b - a = 0.5A$.

REFERENCES

Abramowitz, M. and Stegun, I.A., Handbook of Mathematical Functions, Dover, 1965.

Artem, H.S.A. and Geçit, M.R., "An Elastic Hollow Cylinder under Axial Tension Containing a Crack and Two Rigid Inclusions of Ring Shape", Computers and Structures, Vol. 80, pp. 2277-2287 (2002).

Chang, S.S., "The General Solution of a Finite Cylinder with a Concentric Penny-Shaped Crack under Torsion", Engineering Fracture Mechanics, Vol. 22, pp. 571-578 (1985).

Cook, T.S. and Erdogan, F., "Stresses in Bonded Materials with a Crack Perpendicular to the Interface", International Journal of Engineering Science, Vol. 10, pp. 677-697 (1972).

Delale, F. and Erdogan, F., "Stress Intensity Factor in a Hollow Cylinder Containing a Radial Crack", International Journal of Fracture, Vol. 20, pp. 251-265 (1982).

Erdoğan, F., "Simultaneous Dual Integral Equations with Trigonometric and Bessel Kernels", Zeitschrift für Angewandte Mathematik und Mechanik, Vol. 48, pp. 217–225 (1968).

Erdogan, F., Gupta, G.D. and Cook, T.S., "Numerical Solution of Singular Integral Equation", Mechanics of Fracture 1, Methods of Analysis and Solutions of Crack Problems, Edited by Sih, G.C., Noordhoff International Publishing Leyden, pp.368-425 (1973).

Erdöl, R. and Erdogan, F., “Thick-Walled Cylinder with an Axisymmetric Internal or Edge Crack”, Journal of Applied Mechanics-Transactions of the ASME, Vol. 45, pp. 281-286 (1978).

Freese, C.E. and Baratta, F.I., “Single Edge-Crack Stress Intensity Factor Solutions”, Engineering Fracture Mechanics, Vol. 73, pp. 616-625 (2006).

Geçit, M.R., “Antiplane Shear in Adhesively Bonded Semi-infinite Media with Transverse Cracks”, International Journal of Fracture, Vol. 24, pp. 163-178 (1984).

Geçit, M.R., “Axisymmetric Contact Problem for a Semi-Infinite Cylinder and a Half Space”, International Journal of Engineering Science, Vol. 24, pp. 1245-1256 (1986).

Geçit, M.R., “Analysis of Tensile Test for a Cracked Adhesive Layer Pulled by Rigid Cylinders”, International Journal of Fracture, Vol. 32, pp. 241-256 (1987).

Geçit, M.R., “Axisymmetric Pull-off Test for a Cracked Adhesive Layer”, Journal of Adhesion Science and Technology, Vol. 2, pp. 349-362 (1988).

Geçit, M.R. and Turgut A., “Extension of a Finite Strip Bonded to a Rigid Support”, Computational Mechanics, Vol. 3, pp. 398-410 (1988).

Gradshteyn, I.S. and Ryzhik, I.M., Table of Integrals, Series and Products, Fifth Edition, Boston: Academic Press, 1994.

Guo, L.-C., Wu, L.-Z. and Zeng, T., “The Dynamic Response of an Edge Crack in a Functionally Graded Orthotropic Strip”, Mechanics Research Communications, Vol. 32, pp. 385-400 (2005).

Gupta, G.D., “An Integral Equation Approach to the Semi-Infinite Strip Problem”, Journal of Applied Mechanics, Transactions of the ASME, Vol. 40, pp. 948-954 (1973).

Gupta, G.D., “The Analysis of the Semi-Infinite Cylinder Problem”, International Journal of Solids and Structures, Vol. 10, pp. 137-148 (1974).

Gupta, G.D., “The Problem of a Finite Strip Compressed between Rough Rigid Stamps”, Journal of Applied Mechanics, Transactions of the ASME, Vol. 42, pp. 81-87 (1975).

Kadioglu, F.S., “Edge Cracks in a Transversely Isotropic Hollow Cylinder”, Engineering Fracture Mechanics, Vol. 72, pp. 2159-2173 (2005).

Kaman, M.O., and Geçit, M.R., “Cracked Semi-Infinite Cylinder and Finite Cylinder Problems”, International Journal of Engineering Science, Vol. 44, pp. 1534–1555 (2006).

Kaman, M.O., and Geçit, M.R., “Axisymmetric Finite Cylinder with One End Clamped and the Other under Uniform Tension Containing a Penny-Shaped Crack”, Engineering Fracture Mechanics, Vol. 75, pp. 3909-3923 (2008).

Krenk, S., “Quadrature Formulae of Closed Type for Solution of Singular Integral Equations”, Journal of the Institute of Mathematics and its Applications, Vol. 22, pp. 99-107 (1978).

Lee, D.S., “A Long Circular Cylinder with a Circumferential Edge Crack Subjected to a Uniform Shearing Stress”, International Journal of Solids and Structures, Vol. 39, pp. 2613-2628 (2002).

Lee, D.S., “Tension of a Long Circular Cylinder Having a Spherical Cavity with a Peripheral Edge Crack”, International Journal of Solids and Structures, Vol. 40, pp. 2659-2671 (2003).

Liang, B. and Zhang, X.S., “The Problem of a Concentric Penny-Shaped Crack of Mode III in a Nonhomogeneous Finite Cylinder”, Engineering Fracture Mechanics, Vol. 42, pp. 79-85 (1992).

McLachlan, N.W., Bessel Functions for Engineers, Oxford at the Clarendon Press, 1934.

Meshii, T. and Watanabe, K., “Stress Intensity Factor for a Circumferential Crack in a Finite-Length Thin to Thick-Walled Cylinder under an Arbitrary Biquadratic Stress Distribution on the Crack Surface”, Engineering Fracture Mechanics, Vol. 68, pp. 975-986 (2001).

Muskhelishvili, N.I. Singular Integral Equations, P.Noordhoff, Gröningen, Holland, 1953.

Nied, H.F. and Erdogan, F., “The Elasticity Problem for a Thick-Walled Cylinder Containing a Circumferential Crack”, International Journal of Fracture, Vol. 22, pp. 277-301 (1983).

Sneddon, I.N. Fourier Transforms, McGraw-Hill Book Company, Inc., 1951.

Toygar, M.E. and Geçit, M.R., “Cracked Infinite Cylinder with Two Rigid Inclusions Under Axisymmetric Tension”, International Journal of Solids and Structures, Vol. 43, pp. 4777–4794 (2006).

Turgut, A. and Geçit, M.R., “A Semi-Infinite Elastic Strip Containing a Transverse Crack”, The Arabian Journal for Science and Engineering, Vol. 13, pp. 71-80 (1988).

Williams, M.L., “Stress Singularities Resulting from Various Boundary Conditions in Angular Corners of Plates in Extension”, Journal of Applied Mechanics, Vol. 19, pp. 526-528 (1952).

Wu, X.F. and Dzenis, Y.A., “Closed-Form Solution for a Mode-III Interfacial Edge Crack between Two Bonded Dissimilar Elastic Strips”, Mechanics Research Communications, Vol. 29, pp. 407-412 (2002).

Yan, X., "Rectangular Tensile Sheet with Single Edge Crack or Edge Half-Circular-Hole Crack", Engineering Failure Analysis, Vol. 14, pp. 1406-1410 (2007).

Yetmez, M. and Geçit, M.R., "Finite Strip with a Central Crack under Tension", International Journal of Engineering Science, Vol. 43, pp. 472-493 (2005).

Zhang, X.S., "Off-Plane Concentric Penny-Shaped Crack in a Finite Cylinder under Arbitrary Torsion", Theoretical and Applied Fracture Mechanics, Vol. 9, pp. 263-270 (1988).

APPENDIX A

DEFINITE INTEGRAL FORMULAS USED IN EQS. (2.48)

Integral formulas, Gradshteyn and Ryzhik (1994), used in deriving the expressions in Eqs. (2.48a,b) are

$$\int_0^\infty J_1(\rho A) J_0(\rho t) d\rho = \frac{1}{A}, \qquad (t < A) \qquad (\mathrm{A.1})$$

$$\int_0^\infty \frac{1}{\alpha^2+\rho^2} J_1(\rho A) J_0(\rho t) d\rho = \frac{1}{A\alpha^2} - \frac{K_1(\alpha A) I_0(\alpha t)}{\alpha}, \qquad (t < A) \qquad (\mathrm{A.2})$$

$$\begin{aligned}\int_0^\infty \frac{1}{(\alpha^2+\rho^2)^2} J_1(\rho A) J_0(\rho t) d\rho \\ &= \frac{1}{A\alpha^4} - \frac{K_1(\alpha A) I_0(\alpha t)}{\alpha^3} \\ &\quad - \frac{1}{2\alpha^2}\left[A K_0(\alpha A) I_0(\alpha t) - t K_1(\alpha A) I_1(\alpha t)\right], \qquad (t < A) \qquad (\mathrm{A.3})\end{aligned}$$

$$\int_0^\infty \frac{\rho}{\alpha^2+\rho^2} J_1(\rho A) J_1(\rho t) d\rho = K_1(\alpha A) I_1(\alpha t), \qquad (t < A) \qquad (\mathrm{A.4})$$

$$\int_0^\infty \frac{\rho}{\alpha^2+\rho^2} J_0(\rho A) J_0(\rho t) d\rho = K_0(\alpha A) I_0(\alpha t), \qquad (t < A) \qquad (\mathrm{A.5})$$

$$\int_0^\infty \frac{\rho}{(\alpha^2+\rho^2)^2} J_1(\rho A) J_1(\rho t) d\rho$$
$$= \frac{1}{2\alpha}\left[A K_0(\alpha A) I_1(\alpha t) + \frac{2}{\alpha} K_1(\alpha A) I_1(\alpha t) \right.$$
$$\left. - t K_1(\alpha A) I_0(\alpha t) \right], \qquad (t < A) \qquad (\mathrm{A}.6)$$

$$\int_0^\infty \frac{\rho}{(\alpha^2+\rho^2)^2} J_0(\rho A) J_0(\rho t) d\rho$$
$$= \frac{1}{2\alpha}\left[A K_1(\alpha A) I_0(\alpha t) - t K_0(\alpha A) I_1(\alpha t) \right], \qquad (t < A) \qquad (\mathrm{A}.7)$$

$$\int_0^\infty \frac{\rho}{(\alpha^2+\rho^2)^2} J_1(\rho A) J_0(\rho t) d\rho$$
$$= \frac{1}{2}\left[A K_0(\alpha A) I_0(\alpha t) - t K_1(\alpha A) I_1(\alpha t) \right], \qquad (t < A) \qquad (\mathrm{A}.8)$$

$$\int_0^\infty \frac{\rho^2}{\alpha^2+\rho^2} J_1(\rho A) J_0(\rho t) d\rho = \alpha K_1(\alpha A) I_0(\alpha t), \qquad (t < A) \qquad (\mathrm{A}.9)$$

$$\int_0^\infty \frac{\rho^2}{\alpha^2+\rho^2} J_0(\rho A) J_1(\rho t) d\rho = -\alpha K_0(\alpha A) I_1(\alpha t), \qquad (t < A) \qquad (\mathrm{A}.10)$$

$$\int_0^\infty \frac{\rho^2}{(\alpha^2+\rho^2)^2} J_0(\rho A) J_1(\rho t) d\rho$$
$$= \frac{1}{2}\left[t K_0(\alpha A) I_0(\alpha t) - A K_1(\alpha A) I_1(\alpha t) \right], \qquad (t < A) \qquad (\mathrm{A}.11)$$

$$\int_0^\infty \frac{\rho^3}{(\alpha^2+\rho^2)^2} J_1(\rho A) J_1(\rho t) d\rho$$
$$= \frac{\alpha}{2}\left[t K_1(\alpha A) I_0(\alpha t) - A K_0(\alpha A) I_1(\alpha t) \right], \qquad (t < A) \qquad (\mathrm{A}.12)$$

where J_0 and J_1 are Bessel functions of the first kind of order zero and one, I_0 and I_1 are modified Bessel functions of the first of order zero and one and K_0 and K_1 are modified Bessel functions of the second kind of order zero and one, respectively.

APPENDIX B

DEFINITE INTEGRAL FORMULAS USED IN EQS. (2.50)

Integrals of products of Bessel functions of the first kind, exponential functions and power functions used in deriving the expressions in Eqs. (2.49), Gradshteyn and Ryzhik (1994):

$$\int_0^\infty e^{-z\rho} J_0(t\rho)J_0(r\rho)d\rho = \frac{2}{\pi\sqrt{q_1}} K\left(2\sqrt{\frac{tr}{q_1}}\right), \tag{B.1}$$

$$\int_0^\infty e^{-z\rho} \rho J_0(t\rho)J_0(r\rho)d\rho = \frac{2z}{\pi\sqrt{q_1}q_2} E\left(2\sqrt{\frac{tr}{q_1}}\right), \tag{B.2}$$

$$\begin{aligned}\int_0^\infty e^{-z\rho} \rho^2 J_0(t\rho)J_0(r\rho)d\rho \\ &= \frac{2z^2}{\pi {q_1}^{3/2} q_2}\left[2E\left(2\sqrt{\frac{tr}{q_1}}\right) - K\left(2\sqrt{\frac{tr}{q_1}}\right)\right] \\ &- \frac{2[(t-r)^2 - z^2]}{\pi\sqrt{q_1}{q_2}^2} E\left(2\sqrt{\frac{tr}{q_1}}\right),\end{aligned} \tag{B.3}$$

$$\int_0^\infty e^{-z\rho} J_1(t\rho)J_1(r\rho)d\rho = \frac{(t^2+r^2+z^2)}{\pi tr\sqrt{q_1}} K\left(2\sqrt{\frac{tr}{q_1}}\right) - \frac{\sqrt{q_1}}{\pi tr} E\left(2\sqrt{\frac{tr}{q_1}}\right), \tag{B.4}$$

$$\int_0^\infty e^{-z\rho}\,\rho J_1(t\rho)J_1(r\rho)d\rho = \frac{z(t^2+r^2+z^2)}{\pi tr\sqrt{q_1}q_2}E\left(2\sqrt{\frac{tr}{q_1}}\right) - \frac{z}{\pi tr\sqrt{q_1}}K\left(2\sqrt{\frac{tr}{q_1}}\right), \quad (\mathrm{B.5})$$

$$\int_0^\infty e^{-z\rho}\,\rho^2 J_1(t\rho)J_1(r\rho)d\rho$$

$$= \frac{z^2(t^2+r^2)+(t^2-r^2)^2}{\pi tr{q_1}^{3/2}q_2}K\left(2\sqrt{\frac{tr}{q_1}}\right)$$

$$+ \frac{4z^2(t^2+r^2+z^2)^2}{\pi tr{q_1}^{3/2}{q_2}^2}E\left(2\sqrt{\frac{tr}{q_1}}\right) - \frac{(t^2+r^2+4z^2)}{\pi tr\sqrt{q_1}q_2}E\left(2\sqrt{\frac{tr}{q_1}}\right), \quad (\mathrm{B.6})$$

$$\int_0^\infty e^{-z\rho}\,\rho J_0(t\rho)J_1(r\rho)d\rho = \frac{1}{\pi r\sqrt{q_1}}K\left(2\sqrt{\frac{tr}{q_1}}\right) + \frac{(r^2-t^2-z^2)}{\pi r\sqrt{q_1}q_2}E\left(2\sqrt{\frac{tr}{q_1}}\right), \quad (\mathrm{B.7})$$

$$\int_0^\infty e^{-z\rho}\,\rho^2 J_0(t\rho)J_1(r\rho)d\rho$$

$$= \frac{z(r^2-t^2-z^2)}{\pi r{q_1}^{3/2}q_2}\left[2E\left(2\sqrt{\frac{tr}{q_1}}\right) - K\left(2\sqrt{\frac{tr}{q_1}}\right)\right]$$

$$+ \frac{z[(t-r)(t-5r)+z^2]}{\pi r\sqrt{q_1}{q_2}^2}E\left(2\sqrt{\frac{tr}{q_1}}\right), \quad (\mathrm{B.8})$$

$$\int_0^\infty e^{-z\rho}\,\rho J_1(t\rho)J_0(r\rho)d\rho = \frac{1}{\pi t\sqrt{q_1}}\,K\left(2\sqrt{\frac{tr}{q_1}}\right) + \frac{(t^2-r^2-z^2)}{\pi t\sqrt{q_1}q_2}\,E\left(2\sqrt{\frac{tr}{q_1}}\right), \quad (\mathrm{B.9})$$

$$\int_0^\infty e^{-z\rho}\,\rho^2 J_1(t\rho)J_0(r\rho)d\rho$$

$$= \frac{z(t^2-r^2-z^2)}{\pi t {q_1}^{3/2} q_2}\left[2E\left(2\sqrt{\frac{tr}{q_1}}\right) - K\left(2\sqrt{\frac{tr}{q_1}}\right)\right]$$

$$+ \frac{z[(t-r)(5t-r)+z^2]}{\pi r\sqrt{q_1}{q_2}^2}E\left(2\sqrt{\frac{tr}{q_1}}\right), \qquad \text{(B.10)}$$

where K and E are the complete elliptic integrals of the first and the second kinds and

$$q_1 = (t+r)^2 + z^2,$$
$$q_2 = (t-r)^2 + z^2. \qquad \text{(B.11a, b)}$$

APPENDIX C

EXPRESSIONS APPEARING IN EQS. (3.3)

The expressions for $T_i(r,t)(i=1-8)$ appearing in Eqs.(3.3) are as follows

$$T_1(r,t) = (\kappa-1)\left[\frac{1}{\pi t\sqrt{y_1}}K\left(2\sqrt{\frac{tr}{y_1}}\right)+\frac{y_5}{\pi t\sqrt{y_1}y_2}E\left(2\sqrt{\frac{tr}{y_1}}\right)\right]$$
$$-\frac{2L^2y_5}{\pi t{y_1}^{3/2}y_2}\left[2E\left(2\sqrt{\frac{tr}{y_1}}\right)-K\left(2\sqrt{\frac{tr}{y_1}}\right)\right]$$
$$-\frac{2L^2[(r-t)(r-5t)+L^2]}{\pi t\sqrt{y_1}{y_2}^2}E\left(2\sqrt{\frac{tr}{y_1}}\right), \qquad (\mathrm{C.}1)$$

$$T_2(r,t) = -\frac{2L(\kappa+1)}{\pi\sqrt{y_1}y_2}E\left(2\sqrt{\frac{tr}{y_1}}\right)-\frac{4L^3y_5}{\pi{y_1}^{3/2}y_2}\left[2E\left(2\sqrt{\frac{tr}{y_1}}\right)-K\left(2\sqrt{\frac{tr}{y_1}}\right)\right]$$
$$+\frac{4L[(t-r)^2-L^2]}{\pi\sqrt{y_1}{y_2}^2}E\left(2\sqrt{\frac{tr}{y_1}}\right), \qquad (\mathrm{C.}2)$$

$$T_3(r,t) = (\kappa-1)\left[\frac{1}{\pi t\sqrt{y_1}}K\left(2\sqrt{\frac{tr}{y_1}}\right) + \frac{y_5}{\pi t\sqrt{y_1}y_2}E\left(2\sqrt{\frac{tr}{y_1}}\right)\right]$$

$$-\frac{2L^2 y_5}{\pi t {y_1}^{3/2} y_2}\left[2E\left(2\sqrt{\frac{tr}{y_1}}\right) - K\left(2\sqrt{\frac{tr}{y_1}}\right)\right]$$

$$-\frac{2L^2[(r-t)(r-5t)+L^2]}{\pi t\sqrt{y_1}{y_2}^2}E\left(2\sqrt{\frac{tr}{y_1}}\right), \qquad (\mathrm{C}.3)$$

$$T_4(r,t) = \frac{4L^2(t^2-r^2-4L^2)}{\pi t {y_3}^{3/2} y_4}\left[2E\left(2\sqrt{\frac{tr}{y_3}}\right) - K\left(2\sqrt{\frac{tr}{y_3}}\right)\right]$$

$$+\frac{4L^2[(r-t)(r-5t)+4L^2]}{\pi t\sqrt{y_3}{y_4}^2}E\left(2\sqrt{\frac{tr}{y_3}}\right)$$

$$-2L^2\kappa\left[\frac{1}{\pi t\sqrt{y_3}}K\left(2\sqrt{\frac{tr}{y_3}}\right) + \frac{t^2-r^2-4L^2}{\pi t\sqrt{y_3}y_4}E\left(2\sqrt{\frac{tr}{y_3}}\right)\right], \qquad (\mathrm{C}.4)$$

$$T_5(r,t) = \frac{16L^3}{\pi {y_3}^{3/2} y_4}\left[2E\left(2\sqrt{\frac{tr}{y_3}}\right) - K\left(2\sqrt{\frac{tr}{y_3}}\right)\right]$$

$$-\frac{4L^2[(t-r)^2-4L^2]}{\pi\sqrt{y_3}{y_4}^2}E\left(2\sqrt{\frac{tr}{y_3}}\right), \qquad (\mathrm{C}.5)$$

$$T_6(r,t) = (\kappa+1)\left[\frac{L(t^2+r^2+L^2)}{\pi tr\sqrt{y_1}y_2}E\left(2\sqrt{\frac{tr}{y_1}}\right) + \frac{L}{\pi tr\sqrt{y_1}}K\left(2\sqrt{\frac{tr}{y_1}}\right)\right]$$

$$+2L\left[\frac{L^2(t^2+r^2)+(t^2-r^2)^2}{\pi tr {y_1}^{3/2} y_2}K\left(2\sqrt{\frac{tr}{y_1}}\right)\right.$$

$$\left.+\frac{4L^2(t^2+r^2+L^2)^2}{\pi tr {y_1}^{3/2} {y_2}^2}E\left(2\sqrt{\frac{tr}{y_1}}\right) - \frac{t^2+r^2+4L^2}{\pi tr\sqrt{y_1}y_2}E\left(2\sqrt{\frac{tr}{y_1}}\right)\right], \qquad (\mathrm{C}.6)$$

$$T_7(r,t) = -2L\left[\frac{4L^2(t^2+r^2)+(t^2-r^2)^2}{\pi tr{y_3}^{3/2}y_4}K\left(2\sqrt{\frac{tr}{y_3}}\right)\right.$$

$$+\frac{16L^2(t^2+r^2+4L^2)^2}{\pi tr{y_3}^{3/2}{y_4}^2}E\left(2\sqrt{\frac{tr}{y_3}}\right)$$

$$\left.-\frac{t^2+r^2+16L^2}{\pi tr\sqrt{y_3}y_4}E\left(2\sqrt{\frac{tr}{y_3}}\right)\right], \qquad \text{(C.7)}$$

$$T_8(r,t) = -\kappa\left[\frac{1}{\pi r\sqrt{y_3}}K\left(2\sqrt{\frac{tr}{y_3}}\right)+\frac{r^2-t^2-4L^2}{\pi r\sqrt{y_3}y_4}E\left(2\sqrt{\frac{tr}{y_3}}\right)\right]$$

$$-\frac{4L^2(r^2-t^2-4L^2)}{\pi r{y_3}^{3/2}y_4}\left[2E\left(2\sqrt{\frac{tr}{y_3}}\right)-K\left(2\sqrt{\frac{tr}{y_3}}\right)\right]$$

$$-\frac{4L^2[(t-r)(t-5r)+4L^2]}{\pi r\sqrt{y_3}{y_4}^2}E\left(2\sqrt{\frac{tr}{y_3}}\right). \qquad \text{(C.8)}$$

.

where

$$y_1 = (t+r)^2 + L^2,$$

$$y_2 = (t-r)^2 + L^2,$$

$$y_3 = (t+r)^2 + 4L^2,$$

$$y_4 = (t-r)^2 + 4L^2,$$

$$y_5 = t^2 - r^2 - L^2. \qquad \text{(C.9a – e)}$$

APPENDIX D

KERNELS OF EQS. (3.10)

The expressions for the integrands $L_{ij}(r,t,\alpha)(i,j=1-3)$ appearing in Eqs.(3.10) are as follows

$$L_{11}(r,t,\alpha)=\frac{1}{d_0}\{[4\alpha t(4-d_2-d_1d_3)\alpha AI_0(\alpha t)$$
$$+(4d_1-8d_2-8d_1d_3)\alpha AI_1(\alpha t)]\alpha I_0(\alpha r)$$
$$+[4\alpha^2 AtI_0(\alpha t)-2(d_2+d_1d_3)\alpha AI_1(\alpha t)]2\alpha^2 rI_1(\alpha r)\}, \qquad \text{(D. 1)}$$

$$L_{12}(r,t,\alpha)=\frac{1}{d_0}\Big\{\{2\alpha t(-4+d_2+d_1d_3)\alpha AI_0(\alpha t)$$
$$-[2d_1-4(\kappa+1)+(\kappa-3)(d_2+d_1d_3)]\alpha AI_1(\alpha t)\}\alpha I_0(\alpha r)$$
$$+\{-2\alpha^2 AtI_0(\alpha t)$$
$$+(1+\kappa+d_2+d_1d_3)\alpha AI_1(\alpha t)\}2\alpha^2 rI_1(\alpha r)\Big\}\cos\alpha L, \qquad \text{(D. 2)}$$

$$L_{13}(r,t,\alpha)=\frac{1}{d_0}\Big\{\{[2d_1+4(\kappa+1)-(\kappa+5)(d_2+d_1d_3)]\alpha AI_0(\alpha t)$$
$$+2\alpha t(4-d_2-d_1d_3)\alpha AI_1(\alpha t)\}\alpha I_0(\alpha r)$$
$$+[(1+\kappa-d_2-d_1d_3)\alpha AI_0(\alpha t)$$
$$+2\alpha^2 AtI_1(\alpha t)]2\alpha^2 rI_1(\alpha r)\Big\}\sin\alpha L, \qquad \text{(D. 3)}$$

$$
\begin{aligned}
L_{21}(r,t,\alpha) = \frac{1}{d_0}\Big\{&\{2\alpha t(1+\kappa+d_2+d_1d_3)\alpha A I_0(\alpha t)\\
&-[2d_1+(\kappa+1)(d_2+d_1d_3)]\alpha A I_1(\alpha t)\}\alpha I_0(\alpha r)\\
&-4[2\alpha^2 At I_0(\alpha t)-(d_2+d_1d_3)\alpha A I_1(\alpha t)]\alpha I_0(\alpha r)\\
&-2[2\alpha^2 At I_0(\alpha t)-(d_2+d_1d_3)\alpha A I_1(\alpha t)]\alpha^2 r I_1(\alpha r)\Big\}\cos\alpha L, \qquad \text{(D. 4)}
\end{aligned}
$$

$$
\begin{aligned}
L_{22}(r,t,\alpha) = \frac{1}{d_0}\Big\{&\{-2\alpha t(1+\kappa+d_2+d_1d_3)\alpha A I_0(\alpha t)\\
&+[2d_1+(\kappa+1)^2+2(\kappa+1)(d_2+d_1d_3)]\alpha A I_1(\alpha t)\}\alpha I_0(\alpha r)\\
&+4[2\alpha^2 At I_0(\alpha t)-(1+\kappa+d_2+d_1d_3)\alpha A I_1(\alpha t)]\alpha I_0(\alpha r)\\
&+2[2\alpha^2 At I_0(\alpha t)\\
&-(1+\kappa+d_2+d_1d_3)\alpha A I_1(\alpha t)]\alpha^2 r I_1(\alpha r)\Big\}\cos^2\alpha L, \qquad \text{(D. 5)}
\end{aligned}
$$

$$
\begin{aligned}
L_{23}(r,t,\alpha) = \frac{1}{d_0}\Big\{&\{[(\kappa+1)^2-2d_1]\alpha A I_0(\alpha t)\\
&+2\alpha t(1+\kappa+d_2+d_1d_3)\alpha A I_1(\alpha t)\}\alpha I_0(\alpha r)\\
&+[-4(1+\kappa-d_2-d_1d_3)\alpha A I_0(\alpha t)-8\alpha^2 At I_1(\alpha t)]\alpha I_0(\alpha r)\\
&+[-2(1+\kappa-d_2-d_1d_3)\alpha A I_0(\alpha t)\\
&-4\alpha^2 At I_1(\alpha t)]\alpha^2 r I_1(\alpha r)\Big\}\sin\mathrm{\alpha L}\cos\mathrm{\alpha L}, \qquad \text{(D. 6)}
\end{aligned}
$$

$$
\begin{aligned}
L_{31}(r,t,\alpha) = \frac{1}{d_0}\Big\{&\{2\alpha t(1+\kappa-d_2-d_1d_3)\alpha^2 A I_0(\alpha t)\\
&+[2d_1-(\kappa+1)(d_2+d_1d_3)]\alpha^2 A I_1(\alpha t)\}I_1(\alpha r)\\
&+[4\alpha^2 At I_0(\alpha t)-2(d_2+d_1d_3)\alpha A I_1(\alpha t)]\alpha^2 r I_0(\alpha r)\Big\}\sin\mathrm{\alpha L}, \qquad \text{(D. 7)}
\end{aligned}
$$

$$
\begin{aligned}
L_{32}(r,t,\alpha) = \frac{1}{d_0}\Big\{&\{-2\alpha t(1+\kappa-d_2-d_1d_3)\alpha A I_0(\alpha t)\\
&+[-2d_1+(\kappa+1)^2]\alpha A I_1(\alpha t)\}\alpha I_1(\alpha r)\\
&+[-4\alpha^2 At I_0(\alpha t)\\
&+2(1+\kappa+d_2+d_1d_3)\alpha A I_1(\alpha t)]\alpha^2 r I_0(\alpha r)\Big\}\cos\mathrm{\alpha L}\sin\mathrm{\alpha L}, \qquad \text{(D. 8)}
\end{aligned}
$$

$$
\begin{aligned}
L_{33}(r,t,\alpha) = \frac{1}{d_0}\Big\{&\{[2d_1 + (\kappa+1)^2 - 2(\kappa+1)(d_2 + d_1 d_3)]\alpha A I_0(\alpha t) \\
&+ 2\alpha t(1 + \kappa - d_2 - d_1 d_3)\alpha A I_1(\alpha t)\}\alpha I_1(\alpha r) \\
&+ [2(1 + \kappa + d_2 + d_1 d_3)\alpha A I_0(\alpha t) \\
&+ 4\alpha^2 A t I_1(\alpha t)]\alpha^2 r I_0(\alpha r)\Big\} \sin^2 \alpha L. \qquad \text{(D.9)}
\end{aligned}
$$

where d_i $(i = 0 - 3)$ are given in Eqs.(2.50).

APPENDIX E

DEFINITIONS APPEARING IN EQS. (4.18)

The expressions for $L_{ij\infty 0}(t,\alpha) = \lim_{\alpha\to\infty} L_{ij}(0,t,\alpha)$ $(i = 2,, j = 1-3)$ appearing in Eqs.(4.18) are as follows

$$L_{21\infty 0}(t,\alpha) = \cos\alpha L\, e^{-\alpha(2A-t)}\sqrt{\frac{\pi\alpha}{2t}}\Big[4A(A-t)\alpha^2 + (-8A + 2A\kappa + 6t - 2\kappa t)\alpha + \frac{15}{4}\Big], \tag{E.1}$$

$$L_{22\infty 0}(t,\alpha) = \cos^2\alpha L\, e^{-\alpha(2A-t)}\sqrt{\frac{\pi\alpha}{2t}}\Big[4A(-A+t)\alpha^2 + (10A - 4A\kappa - 6t + 2\kappa t)\alpha + \frac{\kappa}{4}(11-4\kappa)\Big], \tag{E.2}$$

$$L_{23\infty 0}(t,\alpha) = \cos\alpha L \sin\alpha L\, e^{-\alpha(2A-t)}\sqrt{\frac{\pi\alpha}{2t}}\Big[4A(A-t)\alpha^2 + (-6A + 6t - 2\kappa t)\alpha + \Big(\frac{19}{4}\kappa + 1\Big)\Big], \tag{E.3}$$

APPENDIX F

DEFINITIONS APPEARING IN EQS. (4.18)

The expressions for the integrands $N_{ijs0}(t)(i=2,,j=1-3)$ appearing in Eq.(4.18) are in the form

$$N_{21s0}(t)=\frac{\pi}{\sqrt{2t}}\left[\frac{15A(A-t)}{2}\frac{\cos\left(\frac{7}{2}s_2\right)}{s_4^{7/4}}+\frac{3(-8A+2A\kappa+6t-2\kappa t)}{4}\frac{\cos\left(\frac{5}{2}s_2\right)}{s_4^{5/4}}\right.$$
$$\left.+\frac{15}{8}\frac{\cos\left(\frac{3}{2}s_2\right)}{s_4^{3/4}}\right] \qquad (\mathrm{F}.1)$$

$$N_{22s0}(t)=\frac{\pi}{\sqrt{2t}}\left\{\frac{15A(-A+t)}{4s_1^{7/2}}\left[1+\frac{\cos\left(\frac{7}{2}s_3\right)}{s_6^{7/4}}\right]\right.$$
$$+\frac{3(3A-2A\kappa-3t+\kappa t)}{4s_1^{5/2}}\left[1+\frac{\cos\left(\frac{5}{2}s_3\right)}{s_6^{5/4}}\right]$$
$$\left.+\frac{\frac{\kappa}{8}(11-4\kappa)}{2s_1^{3/2}}\left[1+\frac{\cos\left(\frac{3}{2}s_3\right)}{s_6^{3/4}}\right]\right\} \qquad (\mathrm{F}.2)$$

$$N_{23s0}(t) = \frac{\pi}{\sqrt{2t}}\left[\frac{15A(A-t)}{4}\frac{\sin\left(\frac{7}{2}s_3\right)}{s_5^{7/4}} + \frac{3(-3A+3t-\kappa t)}{4}\frac{\sin\left(\frac{5}{2}s_3\right)}{s_5^{5/4}}\right.$$
$$\left. + \frac{\left(\frac{19\kappa}{8}-1\right)}{2}\frac{\sin\left(\frac{3}{2}s_3\right)}{s_5^{3/4}}\right] \qquad (\mathrm{F.3})$$

where

$$s_1 = 2A - t,$$

$$s_2 = Arc\tan\left(\frac{L}{s_1}\right),$$

$$s_3 = Arc\tan\left(\frac{2L}{s_1}\right),$$

$$s_4 = L^2 + s_1^2,$$

$$s_5 = (2L)^2 + s_1^2,$$

$$s_6 = 1 + \left(\frac{2L}{s_1}\right)^2. \qquad (\mathrm{F.4a-f})$$

APPENDIX G

LIMITS OF CERTAIN INTEGRALS

Limits of certain integralsa are calculated from Erdogan (1968): f (t) is taken to be continuous and satisfying Hölder condition in the related interval, consequently

$$\lim_{L-z\to 0}\int_0^\infty f(t)\left(\frac{L-z}{(L-z)^2+(t-r)^2}\pm\frac{L-z}{(L-z)^2+(t+r)^2}\right)dt$$
$$=\lim_{L-z\to 0}\int_{r-\varepsilon}^{r+\varepsilon}(L-z)f(t)\left(\frac{1}{(L-z)^2+(t-r)^2}\pm\frac{1}{(L-z)^2+(t+r)^2}\right)dt$$
$$=\lim_{L-z\to 0}\int_{r-\varepsilon}^{r+\varepsilon}f(t)\left(\frac{L-z}{(L-z)^2+(t-r)^2}\right)dt=\pi f(x). \qquad (\mathrm{G}.1)$$

$$\lim_{L-z\to 0}\int_0^\infty f(t)\left\langle\frac{(L-z)^3-(L-z)(t-r)^2}{[(L-z)^2+(t-r)^2]^2}\pm\frac{(L-z)^3-(L-z)(t+r)^2}{[(L-z)^2+(t+r)^2]^2}\right\rangle dt$$
$$=\lim_{L-z\to 0}\int_{r-\varepsilon}^{r+\varepsilon}f(t)\frac{(L-z)^3-(L-z)(t-r)^2}{[(L-z)^2+(t-r)^2]^2}\ dt,$$
$$=f(x)\left\{\frac{\pi}{2}-\frac{\pi}{2}\right\}=0 \qquad (\mathrm{G}.2)$$

$$\lim_{L-z\to 0}\int_0^\infty f(t)\,\langle\frac{(L-z)^2(t+r)}{[(L-z)^2+(t+r)^2]^2}-\frac{(L-z)^2(t-r)}{[(L-z)^2+(t-r)^2]^2}\rangle\,dt$$

$$=\lim_{L-z\to 0}\int_{r-\varepsilon}^{r+\varepsilon} f(t)\,\frac{-(L-z)^2(t-r)}{[(L-z)^2+(t-r)^2]^2}\;\;dt,$$

$$=-\lim_{L-z\to 0}\int_{-\varepsilon}^{\varepsilon} f(r+\alpha)\,\frac{(L-z)^2\alpha}{[(L-z)^2+\alpha^2]^2}\;\;d\alpha \tag{G.3}$$

APPENDIX H

DEFINITIONS APPEARING IN EQS. (5.24)

The expressions for $L_{52}(r,t,\alpha)$ and $L_{63}(r,t,\alpha)$ appearing in Eqs.(5.24) are in the form

$$\begin{aligned} L_{52}(r,t,\alpha) = \frac{1}{d_0}\Big\{ & \{4\alpha t(-4+d_2+d_1d_3)\alpha A I_0(\alpha t) \\ & -2[2d_1-4(\kappa+1)+(\kappa-3)(d_2+d_1d_3)]\alpha A I_1(\alpha t)\}\alpha I_0(\alpha r) \\ & +2[-2\alpha^2 A t I_0(\alpha t) \\ & +(1+\kappa+d_2+d_1d_3)\alpha A I_1(\alpha t)]2\alpha^2 r I_1(\alpha r)\Big\}\cos\alpha L, \end{aligned} \tag{H.1}$$

$$\begin{aligned} L_{63}(r,t,\alpha) = \frac{1}{d_0}\Big\{ & \{[2(\kappa+1)(d_2+d_1d_3)-4d_1]\alpha A I_0(\alpha t) \\ & +4\alpha t(d_2+d_1d_3)\alpha A I_1(\alpha t)\}\alpha I_1(\alpha r) \\ & +[-4\alpha(1+\kappa-d_2-d_1d_3)\alpha A I_0(\alpha t) \\ & -8\alpha^3 A t I_1(\alpha t)]\alpha r I_0(\alpha r)\Big\}\sin\alpha L\sin\alpha z, \end{aligned} \tag{H.2}$$

where d_i $(i=0-3)$ are given in Eqs.(2.50).

The expressions for $L_{ij\infty}(t,\alpha)=\lim_{\alpha\to\infty} L_{ij}(r,t,\alpha)$ $(i=2,\ j=1-3)$ are as follows

$$\begin{aligned} L_{52\infty}(r,t,\alpha) = \cos^2\alpha L\, e^{-\alpha(2A-r-t)}\frac{1}{\sqrt{rt}} & [4(A-t)(A-t)\alpha^2 \\ & +(-6A+2A\kappa+6t-2\kappa r)\alpha+(1-3\kappa)], \end{aligned} \tag{H.3}$$

$$L_{63\infty}(r,t,\alpha) = \sin^2\alpha L\, e^{-\alpha(2A-r-t)}\frac{1}{\sqrt{rt}}[-4(A-t)(A-t)\alpha^2 + (2A+2A\kappa-2t-2\kappa r)\alpha-(\kappa+1)], \qquad (\mathrm{H.4})$$

The singular parts of kernels, $N_{52s}(t) = \int_0^\infty L_{52\infty}(r,t,\alpha)d\alpha$ and $N_{63s}(r,t) = \int_0^\infty L_{63\infty}(t,\alpha)d\alpha$ are calculated to be

$$N_{52s}(r,t) = \frac{2}{\sqrt{tr}}\left\{\left[2(A-r)^2\frac{\partial^2}{\partial r^2}-(\kappa+7)(A-r)\frac{\partial}{\partial r}+\frac{1}{2}(3\kappa+5)\right]\left[\frac{1}{t+r-2A}+\frac{1}{t-r+2A}\right] + \left[2(A+r)^2\frac{\partial^2}{\partial r^2}+(\kappa+7)(A+r)\frac{\partial}{\partial r}+\frac{1}{2}(3\kappa+5)\right]\left[\frac{1}{t-r-2A}+\frac{1}{t+r+2A}\right]\right\}, \qquad (\mathrm{H.5})$$

$$N_{63s}(r,t) = \frac{2}{\sqrt{tr}}\left\{\left[-2(A-r)^2\frac{\partial^2}{\partial r^2}-(\kappa-5)(A-r)\frac{\partial}{\partial r}+\frac{1}{2}(\kappa-1)\right]\left[\frac{1}{t+r-2A}+\frac{1}{t-r+2A}\right] + \left[-2(A+r)^2\frac{\partial^2}{\partial r^2}+(\kappa-5)(A+r)\frac{\partial}{\partial r}+\frac{1}{2}(\kappa-1)\right]\left[\frac{1}{t-r-2A}+\frac{1}{t+r+2A}\right]\right\}. \qquad (\mathrm{H.6})$$